UNIVERSITY OF BIRMINGHAM

Utility of Small Extracellular Vesicles in Informing Biological Responses to Exercise and Ageing

By

Hannah-Jade Parker

A thesis submitted to the University of Birmingham for the degree of

DOCTOR OF PHILOSOPHY

School of Sport, Exercise and Rehabilitation Sciences

College of Life and Environmental Sciences

University of Birmingham

January 2024

Abstract

Small extracellular vesicles (sEVs) are nano-sized particles containing proteins, metabolites, lipids, and RNA that can be transferred between cells. SEVs have been implicated in various biological processes. These include exercise, ageing, and cellular senescence. Understanding how sEVs are impacted by these processes may be informative of how these processes work. Additionally, due to the significant release of sEVs that has been reported as part of the senescence-associated secretory phenotype (SASP), and the relative clinical accessibility of circulating sEVs, it may be possible to identify candidate biomarkers of senescence. This thesis investigated the impact that exercise (both acute and chronic), ageing and senescence have on the sEV count and proteome, with an overarching aim to determine the utility of studying sEVs in these wider contexts. **Chapter 2** aimed to determine whether there were significant differences in circulating sEV number after a bout of high intensity cardio-based exercise. This was done by using single EV particle analysis to count circulating sEVs in response to high intensity interval exercise. It was found that there was a statistically significant release of sEVs positive for the CD9, CD63, CD81 and CD41a tetraspanins. **Chapter 3** aimed to further investigate the proteome of sEVs released found within sEVs released during senescence, and whether any of these could have been candidate biomarkers. Using three different methods of inducing senescence, we tested senescence-derived sEVs using nano ultra-high performance liquid chromatography-tandem mass spectrometry (nano UHPLC-MS/MS). Experimentally induced senescence effected a large change in the sEV proteome with NIT2, CARS, EEF1A2, GSTO1, PGAM 1, PGAM 2 and NAMPT identified as candidate biomarkers of senescence.

Finally, **Chapter 4** aimed to identify whether there were any significant quantitative or proteomic differences in circulating sEVs in response to ageing or chronic exercise. This was achieved by examining the impact of ageing and chronic exercise on sEVs in vivo, via single EV particle analysis on young plasma, older adult plasma, and Masters athlete plasma. Although there were significantly fewer CD9 positive sEVs in older adults than in the young cohort, and significantly less CD9 protein expression in Masters athletes compared to the young cohort, there was no large difference in number of circulating sEVs between cohort considering age or chronic exercise. In addition to no major differences in sEV count, nano UHPLC-MS/MS revealed only minor differences in the circulating sEV proteome, including no difference in the candidate markers of senescence. These works indicate that although sEVs are released in response to acute exercise and senescence, there are limited differences in sEV count and protein cargo between young, old and Masters athletes implying a broad look at sEVs does not inform the ageing process nor the impact of lifelong exercise.

Acknowledgements

Firstly, I would like to express my deepest appreciation to my supervisor Dr. Martin Whitham. I wouldn't have gotten here without your dedication, help and support. I hope one day that I will be even a fraction of the scientist you are. I would also like to thank the University of Birmingham and the MRC-Versus Arthritis for jointly funding this project via the Centre for Musculoskeletal Ageing Research.

I would like to thank the Lucas lab, the Breen lab, the University of Sydney's Mass Spectrometry team, and the Whitham group of the past for their help and support with conducting exercise protocols, blood collection, proteomics, and everything in between. A special shout out goes to Dr. Joshua Price for sharing his ExoView expertise and to both Dr. Luke McIlvenna and Dr. Alex Seabright for their support.

Thank you to Dr. Mathewson, Dr. Zoob-Carter, and Dr. Podesta for the wonderful combination of support, dinners, and coffee runs. It was a pleasure to meet you all on my first day of my PhD back in 2019 - Long live the original G06 office. I would also not be where I am without the support of my mum, my sisters Paige and Kayla-Sharn, my brother Daniel, and my closest friends Harry and Hannah. Although you may not always have understood my work, you have always fully supported my career. You have all made me the person I am today, so thank you. And finally, to my wonderful fiancé Shoham. I couldn't ask for a more supportive life partner, and I feel blessed every day that you are here with me. I would also like to thank the work of Café Shoham for providing unlimited peppermint tea and snacks. Thank you.

"Every New Discovery is Just a Reminder –"
"We're All Small and Stupid."
- Everything Everywhere All at Once, 2022

Journal articles arising from the present thesis:

McIlvenna, L.C.*, **Parker, H-J**.*, Seabright, A.P., Sale, B., Anghileri, G., Weaver, S.R.C., Lucas, S.J.E. and Whitham, M. (2023), Single vesicle analysis reveals the release of tetraspanin positive extracellular vesicles into circulation with high intensity intermittent exercise. The Journal of Physiology, 601:5093-5106. https://doi.org/10.1113/JP284047

McIlvenna, L.C *, **Parker, H-J**.*, Sullivan, J., Chen, YY., Lord, J. and Whitham, M. (2024), In depth characterization of the small extracellular vesicle proteome in the context of cellular senescence (Manuscript in preparation).

** Denotes that the authors equally contributed to this work.*

Author Declarations and Candidate Contributions

I declare that the work outlined within this thesis is my own, as described in detail, with the following exceptions:

Chapter 2 –

- Dr. Sam Lucas and Dr. Sam Weaver (University of Birmingham, School of Sport, Exercise & Rehabilitation Sciences) kindly provided collected blood and any corresponding participant data. I completed all Single Particle EV analysis and data analysis.

Chapter 3 –

- Dr. Jack Sullivan of the Janet Lord Group (University of Birmingham Institute of Inflammation & Ageing) experimentally induced senescence in the 40HT model and collected the conditioned media and lysates.
- Dr. Luke McIlvenna (Tissue Cross Talk Lab (Whitham)) assisted with the antimycin and H_2O_2 models of senescence and Dr. Martin Whitham aided in the preparation of sEVs for proteomic analysis.
- Mass spectrometry analysis was facilitated by access to the University of Sydney's Mass Spectrometry Core Facility.
- I completed all other *in vitro* experiments and data analysis.

Chapter 4 –

- Dr. Martin Whitham aided in the preparation of sEVs for proteomic analysis. Plasma samples were kindly provided by Dr. Leigh Breen and Dr. James McKendry (University of Birmingham, School of Sport, Exercise & Rehabilitation Sciences.)

- Mass spectrometry was facilitated by access to the University of Sydney's Mass Spectrometry Core Facility.
- I completed all *in vitro* experiments and data analysis.

Table of Contents

Table of Figures

Table of Tables

Abbreviations

4OHT	4-hydroxytamoxifen
AD	Alzheimer's disease
CARS	Cysteinyl-tRNA synthetase 1
CDCs	Cardiosphere-derived cell
CPC	cardiac progenitor cell
DDA	1,12-Dodecanedioic acid
DG	Density Gradients
DTT	Dithiothreitol
eNAMPT	Extracellular nicotinamide phosphoribosyltransferase
ESCRT	Endosomal Sorting Complex Required for Transport
EV	Extracellular Vesicles
EV-TERA-P	Extracellular Vesicle-Tetraspanin-Plasma
FDR	False Discovery Rate
FTD	Frontotemporal dementia
GST	Glutathione S-transferases
H_2O_2	Hydrogen Peroxide
HIIE	High intensity interval exercise

HPLC-ESI-MS/MS	High-performance liquid chromatography-electrospray ionisation tandem mass spectrometry
IAA	Indole-3-acetic acid
ILVs	Intraluminal vesicles
IR	Ionizing radiation
iRAS	Inducible RAS
ISEV	International Society for Extracellular Vesicles
LDL	low-density lipoprotein
MA	Masters athletes
MiDaS	Mitochondrial dysfunction-associated senescence
MS	Mass Spectrometry
MSC	Mesenchymal stem cells
MVBs	Multivesicular bodies
NAD+	Nicotinamide adenine dinucleotide
NAMPT	Nicotinamide Phosphoribosyltransferase
NaN	Non-Assigned Number
NTA	Nanoparticle Tracking Analysis
nUHPLC-MS/MS	nano ultra-high pressure liquid chromatography tandem mass spectrometry
O	Older participants

OIS	oncogene-induced senescence
OSIS	oxidative stress-induced senescence
PBP	Polymer-based precipitation
PFP	Platelet free plasma
PGAM1	Phosphoglycerate mutase 1
PGAM2	Phosphoglycerate mutase 2
PPP	Platelet poor plasma
PRIDE Archive	PRoteomics IDEntifications Database
ROS	Reactive oxygen species
SASP	Senescence-associated secretory phenotype
SA-β-gal	Senescence-associated β Galactosidase Activity.
SEC	Size Exclusion Chromatography
sEV	Small Extracellular Vesicles
SILAC	Stable isotope labelling by amino acids in cell culture
SP-IRIS	Single Particle Interferometric Reflectance Imaging Sensor
TEM	Transmission electron microscope
TEMs	Tetraspanin-enriched microdomains
TSG101	tumour susceptibility gene 101
UC	Ultracentrifugation
UF	Ultrafiltration

WB	Western Blot
Y	Young participants
γ-H2AX	Phosphorylated H2A histone family member X

Chapter 1

General Introduction

1.1. Introduction

Extracellular vesicles are small, membrane-bound particles which are released by and taken up by cells. They have been implicated in a multitude of biological processes and adaptations, including exercise, ageing and senescence which will be the main theme of this thesis. Interestingly, some extracellular vesicles are selectively released and taken up by cells (Berumen Sánchez et al., 2021).This general introduction will therefore explain what extracellular vesicles are and any responsibility they may play within cellular processes associated with exercise, ageing, and senescence. There is difficulty studying sEVs due to the lack of gold standard for their isolation and analysis, which will be further detailed.

1.2.1. Extracellular Vesicles

The existence of extracellular vesicles (EVs) has been known since 1967, with Wolf first describing platelet derived EVs when he coined the term “platelet dust” (Wolf, 1967). In recent years, the interest in extracellular vesicles has rapidly increased, and with it a more in depth understanding of their biological importance. EVs are ubiquitous, being released from almost every cell type across every kingdom of life including prokaryotes and archaea (Gill et al., 2019).

EVs are composed of lipid bilayers which allow them to carry a large variety of cargo including nucleic acids, proteins, metabolites, and lipids (Yokoi and Ochiya, 2021). Extracellular vesicles have been implicated in many necessary processes within the human body, including but not limited to cellular metabolism (Kobayashi et al., 2021), shuttling of cargo (Cai et al., 2021), immunity (Yang et al., 2021) and clearance of RNA

and proteins (O'Brien et al., 2020). EVs have also been implicated in the malfunction of these processes and have been linked to diseases such as cancers (Riches et al., 2014), sarcopenia (Wang et al., 2023) and rheumatoid arthritis (Schioppo et al., 2021).

In blood, there are three main types of identified extracellular vesicles: exosomes, microvesicles and apoptotic bodies. Exosomes are released during the fusion of multivesicular bodies with the plasma membrane and have a diameter of 40-150nm. Microvesicles bud directly from the plasma membrane and can be between ~50nm to 1μM (Sidhom et al., 2020). Finally, there are apoptotic bodies which are often released from dying cells and can be between 50nm - 2μM (Zaborowski et al., 2015).

1.2.2. Biogenesis of Extracellular Vesicles

As well as having different sizes, each subpopulation of extracellular vesicles have different methods of biogenesis. Microvesicles originate through the aggregation of contents around the inner membrane of the cell they are released from. These become encased in a lipid bilayer before detaching from the cell through a pinching process, which is often referred to as blebbing (Tricarico et al., 2017).

The formation of exosomes is an extremely complex process, with much to still be learned about the various mechanisms involved. Exosomes are formed through the inward budding of the plasma membrane to create multivesicular bodies (MVBs), in a process known as invagination. This results in the formation of intraluminal vesicles (ILVs) inside MVBs (Perrin et al., 2021). It is these ILVs which will eventually become exosomes. During the formation of ILVs, EV molecular cargo are selectively sorted and

incorporated into vesicles. This selection of cargo is what makes exosomes of interest to biologists, as it implies that their release is an intended highly regulated process (Kalluri and LeBleu, 2020). This can be achieved via multiple mechanisms, including the Endosomal Sorting Complex Required for Transport (ESCRT) dependent mechanism or the ESCRT-independent pathway (Perrin et al., 2021).

1.2.3. ESCRT-Dependent Pathway

The ESCRT machinery consists of multiple protein complexes (ESCRT-0, ESCRT-I, ESCRT-II, and ESCRT-III) that are involved in cargo recognition, membrane deformation, and vesicle scission. The ESCRT-0 complex recognises and binds to the relevant cargo (Babst et al., 2011). This is followed by the recruitment of the endosomal membrane, using ESCRT-I and ESCRT-II. ESCRT-III then triggers the invagination of the endosomal membrane, driving membrane budding and leading to the direct formation of the ILVs (Babst et al., 2011). Other proteins such as syntenin-1, tumour susceptibility gene 101 (TSG101) and apoptosis-linked gene 2 interacting protein X (ALIX) are also involved in this process (Larios et al., 2020). Due to this, these proteins are often proposed as markers of extracellular vesicles.

1.2.4. ESCRT-Independent Pathway

The ESCRT-independent Pathway has several mechanisms of sorting and packaging cargo into ILVs. One such mechanism is through lipid-dependent pathways, such as by using ceramide-rich membrane domains. Ceramides initiate membrane invagination, allowing for the formation of MVBs, in a spontaneous way due to their singular cone-shaped structure (Horbay et al., 2022). These ceramides may also trigger lipid rafts,

which then lead to vesicle budding (Sapoń et al., 2023). Tetraspanins are a protein superfamily which are able to associate with each other and with other membrane proteins, forming specialized microdomains on the cell surface known as tetraspanin-enriched microdomains (TEMs) (Termini and Gillette, 2017). The tetraspanins play a fundamental role in ESCRT-independent pathways (van Niel et al., 2011). In particular, the tetraspanins CD9, CD63 and CD81 are frequently associated with the organization of MVB membranes, and the sorting of cargo into ILVs (Larios et al., 2020). Due to this, they are often found in high abundances within extracellular vesicles and are thus frequently used as proteins markers of EVs (Andreu and Yáñez-Mó, 2014).

1.2.5. Release and Uptake of sEVs

After the formation of MVBs with ILVs, they are fused with the cellular membrane. This leads to the release of exosomes into the extracellular matrix via exocytosis. Once within the extracellular matrix, the exosomes can be taken by other cells, allowing for the transfer of their cargo, impacting the biogenesis of the recipient cell (Krylova and Feng, 2023). This uptake process is dependent on a plethora of mechanisms and binding complexes. Interestingly, the ESCRT-dependent and ESCRT-independent pathways are not mutually exclusive, meaning they may occur concurrently within the same cells (Han et al., 2022). As there is currently no clear way of completely separating exosomes and microvesicles during isolation from biofluids (Théry et al., 2018), or demonstrating with high confidence the route of biogenesis of the isolated vesicle, the umbrella term ‘small extracellular vesicles’, or sEVs, will be used throughout this thesis. Intercellular communication via sEVs is depicted in **Figure 1.1.**

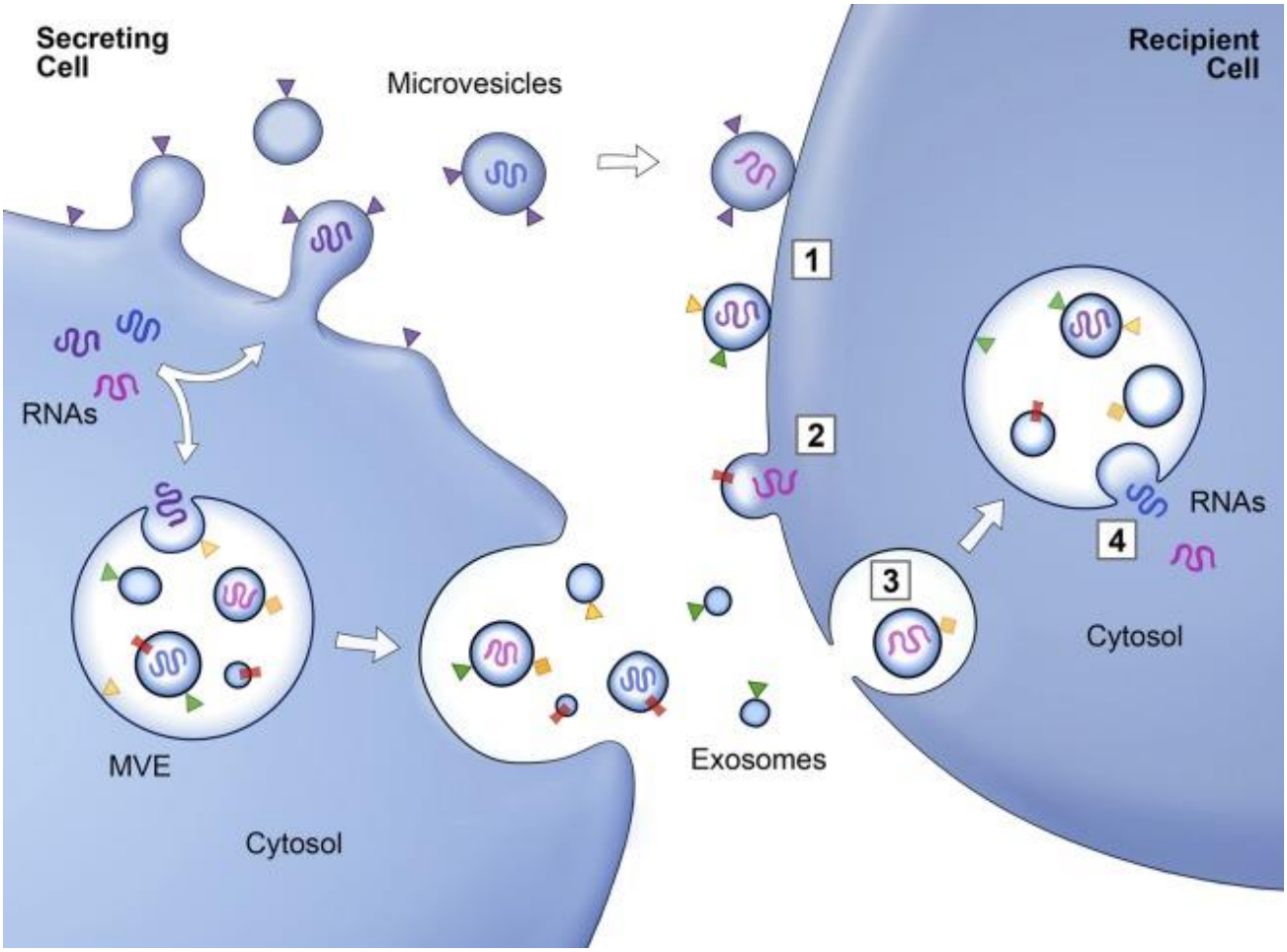

Figure 1.1 | *An example of protein and RNA transfer by EVs. Microvesicles and exosomes dock at the plasma membrane (1). Vesicles may be fused with the plasma membrane (2) or undergo endocytosis (3). Endocytosed vesicles may fuse within the endocytic compartment (*4). The vesicles are then able to deliver proteins and RNA into the cellular cytosol or membrane (Raposo and Stoorvogel, 2013)

1.3.1. Role of sEVs in Cellular Communication

The bioactive cargo of sEVs may include proteins (signalling proteins, surface receptors, enzymes), lipids (phospholipids, sterols, sphingolipids), metabolites (TCA cycle intermediates, amino acids, steroid hormones) and nucleic acids (DNA fragments,

mRNAs, microRNAs) (Malkin and Bratman, 2020). This bioactive cargo may participate in signalling pathways, modulate gene expression, and affect membrane composition. They can also lead to changes in cellular processes such as proliferation, differentiation, migration, and immune responses (Kalluri and LeBleu, 2020). This transfer of information through sEV-mediated crosstalk also contributes to the regulation of tissue homeostasis, coordinating responses to environmental cues, maintain tissue function and participate in tissue repair and regeneration. Additionally, sEVs have been shown to possess cell-specific homing capabilities (Berumen Sánchez et al., 2021). Rather than just being taken up by any cells, sEVs can be selectively taken up by cells, allowing them to direct the molecular cargo they carry and trigger phenotypic changes in specific receptor cells. Indeed, although sEVs are ubiquitous, it has been shown that sEVs from different sources are likely to have preferential interactions with specific cell types (Jurgielewicz et al., 2020), for example vesicles released from liver cancer have a more than fourfold increase in preferentially localisation to the liver (Hoshino et al., 2015). This allows them to be useful in cellular communication, beyond just shuttling cargo haphazardly between random cells.

The tetraspanins found on the membrane of sEVs are partially responsible for this uptake into recipient cells – particularly CD63 (Ginini et al., 2022) and CD9 which play a role in exosomal docking (Matsuzaka and Yashiro, 2022). Interestingly, a recipient cell can also be the cell responsible for producing the sEV, allowing cells to generate autocrine responses with sEVs (Yoon et al., 2020).

1.3.2. Tissue Homeostasis and Repair

Initially, there was a belief that sEVs primarily served to process cellular waste. Although we now recognise that sEVs have a more extensive and significant purpose, we also know that indeed sEVs play a valuable role in clearing cellular waste. They serve as a quality control system to determine whether membrane molecules can be reused or recycled (Vidal, 2019). sEVs can also secrete misfolded proteins, aiding in extracellular proteostasis and keeping cells healthy.

sEVs contribute to biologically preserving regular cardiac function and structure (Wu et al., 2023) with cardiosphere-derived cell (CDC) derived sEVs promoting angiogenesis, proliferation, and cardiomyocyte survival (Ibrahim et al., 2014). Another mechanism of preservation that sEVs are involved in is through management of apoptosis, as preserving cellular survival is crucial in the tissue repair process and the maintenance of tissue and organ homeostasis. sEV-associated proteins have been identified as effective preventers of cell apoptosis in various tissues, including in the cardiovascular system (Liu et al., 2020), in bone regeneration (Liu et al., 2018), and in nephrotic repair in the kidneys (Bussolati and Camussi, 2017). An example of this ability to aid in tissue repair can be seen in cases of myocardial injury, where the administration of mesenchymal stem cell (MSC) derived sEVs and cardiac progenitor cell (CPC) derived sEVs were shown to reduce scar size and enhance cardiac function (Barile et al., 2018). sEVs also inhibit the death of cardiomyocytes by reducing apoptosis (Xuan et al., 2022).

A further strategy employed by sEVs in mediating tissue protection during ischemia involves delivering antioxidation enzymes to mitigate oxidative stress caused by an imbalance in reactive oxygen species (ROS) (Yao et al., 2019).

1.3.3. Immune System Modulation

Due to their ubiquitous nature, sEVs are also released from immune cells such as macrophages and T-cells. One example of the use of sEV in immune system modulation is through the modulation of inflammatory responses by inducing differentiation of M2 macrophages and suppressing M1 macrophages (Roefs et al., 2020). sEVs are also responsible for inhibiting NK cell proliferation (Zhao et al., 2019) and impairing dendritic cell maturation (Grange et al., 2015), and thus reducing inflammation. Another example of the use of sEVs within immune system modulation is through pro-inflammatory responses. sEVs with HSP70 on their surface lead to an activated immune response by promoting a proinflammatory mesenchymal stromal cell phenotype (Li et al., 2016, Zheng et al., 2018). This highlights how the molecular composition and cargo of sEVs are key in our understanding of them.

1.4.1 sEVs are an insight into pathological conditions

Just as sEVs can be useful in providing information about healthy biological processes, they can also provide data about pathological conditions such as cancers, cardiovascular disease, and, in focus in this thesis, ageing. One example of this is within the tumour microenvironment, where acidosis, increased pressure and hypoxia allow for the progression of and metastasis of cancer cells (Baghban et al., 2020, Anderson and Simon, 2020, de Visser and Joyce, 2023). sEVs are secreted in much larger numbers from tumour cells than their healthy counterparts (Riches et al., 2014),

with cancer patients showing significantly higher levels of circulating sEVs compared to healthy individuals (Melo et al., 2015). sEVs released from highly metastatic cancer cells have been shown to induce migration, invasion and metastasis of cancer cells which are less aggressive (Qiao et al., 2019). Interestingly, studies seem to only indicate more aggressive cancers passing sEVs to less aggressive cancers, which may reflect the unique properties of tumour cells reflecting their produced sEVs (Fares et al., 2020, Faubert et al., 2020, Novais et al., 2023).

Another example is in Alzheimer's disease. sEVs isolated from human brain tissue of sufferers of Alzheimer's Disease (AD), frontotemporal dementia (FTD) and so called 'healthy' donors who died of natural causes were injected into wild type and tau mouse models. They showed that both AD-sEVs and FTD-sEVs triggered changes in protein composition, which are associated with synapse regulation and transmission in dementia (Bodart-Santos et al., 2023). Additionally, there was a significant decrease in memory noted but only in the tau-positive murine model. This indicates that sEVs released from dementia-associated cells are able to make phenotypical changes within the brain, and these changes can work in association with the presence of tau. Furthermore, sEVs are reported to be present in all stages of atherosclerosis development, from intimal lesions to advance plaques, suggesting they participate in all stages of plaque formation (Charla et al., 2020). Platelet-derived sEVs containing miRNA-223, mi-RNA-21, miRNA-320, miRNA-191 and miRNA-339 are linked to the aggregation of platelets, a key stage in the development of atherosclerosis (Lu et al.,

2018). sEVs from atherosclerotic plaques can promote atherogenesis, mimicking mechanisms used in cancer metastasis in the blood (Coly and Boulanger, 2022).

1.4.2. sEVs as an insight into biological phenotype

Such is the complexity of biomolecules carried in circulation in sEVs, there is a growing appreciation of their role in fundamental biological process, such that an examination of quantitative differences and differences in their cargo or membrane composition might improve understanding of the regulation of human function in health and disease. Progress in this endeavour, however, is challenged by a wide variety of analytical approaches, none of which are considered gold standard.

1.5. Methods of Isolating Extracellular Vesicles

There are multiple methods for isolating sEVs, with each method having a number of benefits to its use. Differences in isolation method may impact things such as EV number, protein content and purity of samples. Due to this, the International Society for Extracellular Vesicles (ISEV) have published a list of considerations and details that must be included when presenting sEV data (Théry et al., 2018). Although there are several methods of isolation available, selection of a specific approach leads to a trade-off between recovery (yield) and specificity (purity), (Cocozza et al., 2020). Contemporary methods of isolation will now be described and discussed in order of ascending specificity.

1.5.1 Polymer-based Precipitation

Polymer-based precipitation (PBP) is a form of sEV isolation, which usually comes in the form of commercially available isolation kits. Samples are added to the precipitant

and incubated for between 30 minutes to an hour, depending on the specific kit. Following this incubation, the sample is then pelleted by centrifugation at a low speed (1500 x g), which allows the sEVs to be resuspending in whatever diluent is most appropriate. PBP isolation requires low amounts of sample, simple setup and low equipment demands, making it convenient to use (Chung et al., 2020). It can also be rapid, with some kits requiring only 30 minutes in the precipitant (Brown and Yin, 2017). As with most isolation methods that produce a high yield of sEVs, PBP isolated samples have low purity. This is due to contaminant from residuary polymers or due to co-purification of protein aggregates (Kim et al., 2020). Low purity means that it is impossible to determine whether only sEVs are being considered in terms of any data collected.

1.5.2. Ultrafiltration

Ultrafiltration is the process of removing sEVs from biofluid or cell media by passing the sample through a porous membrane, which will allow sEVs of the relevant size to pass. These membranes are most commonly made from cellulose but can also be made from hydrogenated salts and polyethersulfone. When isolating sEVs, membranes with a molecular weight cut off ranging from 10-100kDa are often used (Liangsupree et al., 2021). sEV samples purified using UF appeared to show significantly higher yields compared to ultracentrifugation and polymer-based precipitation (Wang et al., 2021). Furthermore, recovery rates of particles smaller than 100nm are higher from ultrafiltration than from alternate methods of isolation (Zeng et al., 2022). Ultrafiltration is also an extremely easy procedure, which allows for concurrent processing of many samples. There is also no limitation of the sample volume which

can be processed, making it extremely convenient when attempting to run large samples. In addition to ultrafiltration being simple to complete, there is no need for additional expensive equipment, making it more affordable than other methods of isolation. Ultrafiltration also has a relatively quick isolation time (Park et al., 2020). The key concern when using ultrafiltration is the possibility of filter plugging effecting reliability. This occurs when particles get stuck when attempting to pass through the membrane, and consequently create blockages in the filter, preventing other particles from passing through. This can cause a loss of sample and deformation of vesicles (Liangsupree et al., 2021). Oeyen (2018) also reported that contamination of ultrafiltration samples is high, with uromodulin still present within sEV samples isolated from urine. It was also noted that although overall protein content of ultrafiltration samples was higher than UC or polymer-based precipitation, CD63, a common sEV marker, was not found within samples, suggesting that sEVs are lost during the isolation process (Oeyen, 2018). Due to this lack of specificity, Ultrafiltration is often used in conjunction with other isolation methods, allowing for purer samples than one would receive from using a single method of isolation.

1.5.3. Ultracentrifugation

Ultracentrifugation (UC) is widely accepted as a cost-efficient way to isolate sEVs (Gardiner et al., 2016). UC is conducted with several centrifugation steps with increased centrifugal force intended to produce sequential pellets of cells and cell-debris (300-1000g), microvesicles (10,000-20,000g) and small extracellular vesicles (100,000g). This method means large volume samples can be isolated as one, and no additional

chemicals are required for purification. As well as being cost effective, UC is widely used due to how well it couples with other methods such as ultrafiltration to provide samples which are low in contaminants. Contrary to this, UC has more contamination than more specific methods of isolation due to an increase in copurification of non-EV associated proteins and microvesicles (Torres Crigna et al., 2021). Using UC independently leads to higher amounts of lipoprotein contaminants than using combination methods. (2020)

A key thing to note with ultracentrifugation is factors such as relative centrifugal force, temperature, type of rotor used and duration of spin may lead to different sEV and protein yields (Cvjetkovic et al., 2014). There is currently no golden standard for how to conduct UC, which could explain some inconsistencies in reported results. Additionally, it is important to note that EV surface disruption occurs after 70 minutes of UC at 120,000g (Nordin et al., 2015), meaning that it is important to know whether these high UC speeds have been used when considering results. A practical consideration of using UC is the limited number of samples which can be prepared at one time, and the time associated with wanting to purify more samples than there is space for in the ultracentrifuge.

1.5.4. Size Exclusion Chromatography (SEC)

Size Exclusion Chromatography (SEC) works by running samples through a porous polymer gel filtration matrix. This allows particles of assorted sizes to be eluted into different fractions dependent on their size, with smaller particles travelling through the columns quicker, and thus eluting first. sEVs are typically found within the first few

fractions (Takov et al., 2019). As with other methods of isolating sEVs, there are many advantages and disadvantages to the use of SEC. sEVs purified by SEC are subjected to reduced aggregation during the isolation procedure than other methods such as a UC. This helps to produce pure, intact, and biologically undisrupted sEVs (Arntz et al., 2020), making them particularly useful for research focusing on their membrane morphology or bioengineering (Rhim et al., 2023). The SEC isolation method is relatively fast, inexpensive and has the potential to be automated. There is debate about the level of purity of samples that can be achieved by SEC. Despite the potential for less contaminants within the sample because of the different particle sizes, some contaminants such as microvesicles, and lipoproteins such as chylomicrons (75-1200nm), LDL (25nm) or VLDL (30-80nm) which are the same size as sEVs may filter at the same rate (Monguió-Tortajada et al., 2019, Torres Crigna et al., 2021). Brennan *et al*., (2020) acknowledged that although SEC had the ability to collect high yields of sEVs, they had a higher rate of contaminants than methods such as UC. For this reason, it is advised that SEC is used in combination with other methods. Another consideration is that SEC requires sEVs to be collected in fractions in solution. This may interfere with downstream analyses where sample volume needs to be low.

1.5.5. Density Gradients

By using different buffers, sEVs can be separated according to density. When particles are denser than the buffer they are suspended in, they will sink; those which are less dense will rise in the buffer. This allows different sized EVs to be separated. Two popular types of media used for density gradient (DG) are sucrose gradient and

iodixanol gradient. DG is particularly beneficial to overcome the co-purification concerns that are found when using other methods (Zhang et al., 2019). Furthermore, viral particle contamination, which may be a concern with other isolation methods, is completely negated by using iodixanol gradient centrifugation, where no viral contaminants are detected within the EV fraction (Gias et al., 2008). Despite the benefits to DG, it is a complex and lengthy isolation method, making it impractical when many samples are needed to be isolated quickly. It also requires a much higher starting concentration than many other methods (Zhang et al., 2019), as the final yield is relatively low. Additionally, much like other methods, DG does not provide a completely pure sEV sample free from contaminant proteins.

1.5.6. Immunoaffinity

Immunoaffinity methods of isolating sEVs usually comprise of antibody-coated latex beads which are magnetic. The sample is placed into a tube with the immunoaffinity beads. Frequently, these are conjugated with different tetraspanins such as CD9, CD63 and CD81, described earlier as key mediators of ESCRT independent vesicle biogenesis. sEVs which are positive for the membrane proteins are then bound to the antibody-coated beads, allowing them to be separated from the solution (Lo et al., 2020). They can then be eluted into the desired dilutant. The immunoaffinity method of isolation is highly specific due to its use of antibodies. This specificity allows for a specific sub-population of sEVs to be isolated, for example if the researcher chooses to study sEVs with a specific marker on the surface. It is worth noting that there are no markers which are currently able to separate exosomes and microvesicles (Doyle and

Wang, 2019). This specificity also allows for the samples to be highly pure, with little to no contaminants. Immunoaffinity is most appropriate when isolating small amounts of sEVs, as it is not compatible with large-volume samples. The immunoaffinity approach has been combined with immunofluorescent imaging in specific instruments to facilitate accurate quantitation of sEVs. These techniques will be tested in **Chapter 2**.

Table 1.1 | *Summary of the advantages and disadvantages of methods of sEV isolation.*

	SUMMARY OF METHOD	ADVANTAGES	DISADVANTAGES
POLYMER-BASED PRECIPITATION	Polymer-based precipitation (PBP) usually comes in the form of commercially available isolation kits. Samples are added to the precipitant. The sample is then pelleted by centrifugation at 1500 x g.	High yield. Low amounts of sample. Simple set up and low equipment demands. Rapid depending on selected kit. Reduced centrifugal force required. Biologically undisrupted.	Low purity, contamination risk from residuary polymers or co-purification of protein aggregates. Can be time consuming depending on the selected kit.
ULTRAFILTRATION	Ultrafiltration is the process of removing sEVs from biofluid or cell media by passing the sample through a porous membrane, which will allow sEVs of the relevant size to pass.	Frequently used in conjunction with other isolation methods. Higher protein levels than some other isolation methods. Increased recovery rates of EVs below 100nm. Easy procedure. Ability to run large samples. Affordable and quick.	Filter plugging can cause a loss of sample and deformation of vesicles. Contamination with similarly sized particles. sEVs lost during isolation process.

ULTRACENTRIFUGATION	Ultracentrifuge comprises of several centrifugation steps with increased centrifugal force to produce sequential pellets of cells and cell-debris (300-1000g), microvesicles (10,000-20,000g) and exosomes (100,000g).	Large volume samples can be isolated as one. No additional chemicals required. Cost effective once initial equipment is purchased. Couples well with other methods such as UF. Low lipoprotein contamination.	Risk of copurification of non-EV associated protein. Lipoprotein contaminants. Things such as relative centrifugal force, temperature, rotor and duration of spin need to be considered. No global standard for use. EV surface disruption risk. Limited number of samples prepared at one time. Time association. High start-up cost.
SIZE EXCLUSION CHROMATOGRAPHY	Samples are run through a porous polymer gel filtration matrix, with EVs eluted in accordance with their size.	High yield. Reduced aggregation during isolation compared to other isolation procedures. Biologically undisrupted EVs. Relatively fast and inexpensive. Potential to be isolated. EVs can change dilutant with little disruption. Lack of pellet.	Potential for contaminants of similar size to EVs or due to complexes. Higher rate of contamination than other methods. Lack of pellet.

DENSITY GRADIENTS	Using different buffers, EVs can be separated according to density. Two popular types of density gradient buffer are sucrose gradient and iodixanol gradient.	Reduced risk of co-purification compared to UC. High purity. High protein concentration. Reduced risk of viral particle contamination if using iodixanol gradient centrifugation.	Complex and time consuming. High starting concentration of EVs required. Low yield. Risk of contamination from plasma derived lipoproteins, albumin in urine and from viral particles if using sucrose density gradient.
IMMUNOAFFINITY	Magnetic antibody-coated latex beads are mixed with the biological sample and the relevant antibodies. The EVs bind to these antibody-coated beads, allowing for them to be separated from the solution.	Highly specific to the point subpopulations can be isolated. High purity with little to no contaminants. Higher EV yields than methods like DG. EVs are not pelleted and can be eluted into desired dilutant.	Not compatible with large-volume samples. May require concentration of samples. Additional purification steps may be required. Low yield compared to other methods such as UC or SEC. Time consuming and requires hands on time, especially if additional purification is needed. Evidence small changes to EV size and their surface structure may occur.

1.6.1. Methods of studying sEVs

As with isolation methods, there are different approaches to studying sEVs which differ on their appropriateness according to the needs of the researcher and the available/selected isolation method. Due to the small size of sEVs, traditional quantification methods may be inaccurate, so alternative approaches are used. Some of these approaches are quantitative, providing counts of individual sEVs or their associated markers. Others are qualitative, providing information on their phenotype. Additionally, there are differences associated with whether the researcher wants to investigate the molecules found on the surface of the sEVs compared to the cargo contained inside.

1.6.2. Nanoparticle Tracking Analysis (NTA)

One of the most popular methods used to study sEVs is Nanoparticle Tracking Analysis (NTA), which is able to determine size distribution and concentration of nano-sized particles within suspension using Brownian motion calculations (Filipe et al., 2010) associated with light scattering using a light microscope. A key benefit of this method is that it allows for the measurement of different-sized particles within the same solution simultaneously (Dragovic et al., 2011). The main problem with NTA is that sEVs are assessed by their size. This is particularly an issue regarding particles which are the same size as sEVs such as microvesicles and lipoproteins can be registered as sEVs so thus incorrectly measured. Even once sEVs are isolated, a high-fat meal prior to blood collection was found to have a significant effect on particle numbers estimated by

NTA (Brahmer et al., 2019), indicating that lipoproteins were being counted by NTA. The accuracy of this is tied in with the complexity of the starting sample. That is, complex samples such as plasma or serum are more likely to contain contaminants than simple samples such as conditioned media (Takov et al., 2019). Another key issue with NTA is how variable sample recording is. Intra-assays and inter-assays, taken across different days and within different laboratories, using the same settings and operator found differences in EV counts between 2%-25% for the same samples (Vestad et al., 2017). Although this can be reduced by using the same machine and completing all samples on the same day, these changes are still something that need to be accounted for. Additionally, it has been identified that NTA may overestimate particle counts below 0.9×10^8/ml and underestimate particle count above 29.0×10^8/ml (Maas et al., 2015), bringing into question how accurate NTA is. These limitations are why NTA is now frequently used merely as a confirmatory method to show that sEVs are isolated rather than a quantitative method.

1.6.3. Western Blot

Western blots are perhaps the most used protein-analytical technique. Proteins are separated by molecular weight onto a membrane. Antibodies are placed onto the membranes, and these bind to their corresponding proteins. Once imaged, the bound antibody will display chemiluminescence, allowing the researcher to determine whether the specific protein is present. Western blots are widely used to study the presence of proteins because they can be both highly sensitive and highly specific, protein and corresponding antibody dependent. As proteins are separated by size, the combination of antibody specificity and the location of the band lining up with the ladder, it is also

possible to identify whether the correct protein is florescent. This increases the specificity. There is, however, a chance of non-specific binding, leading to misidentification of proteins (Haytural et al., 2019).

With regard to studying sEVs, a disadvantage of using western blots is that although some proteins may be detected with as little as 0.1ng of protein (Bass et al., 2017), it is recommended that 2-30µg of protein lysates or 1µg of purified protein are used (Bass et al., 2017). This means the balance between purity of sample and concentration of sample needs to be considered when deciding isolation method. Western blots also require high technical demand, with little ability for affordable automation. This makes them time consuming. They are also prone to false or subjective results, due to their semi-quantitative nature. Bands may be misread or misidentified due to this subjectivity. Additionally, this can be highly antibody specific, meaning that frequently it requires several attempts to validate or confirm whether an antibody is suitable. When considering western blots, it is only possible to analyse a handful of proteins. This may reflect a limitation as sEVs are known to carry over 5000 proteins (Whitham et al., 2018).

1.6.4. Flow Cytometry

Flow cytometry can count particles of a size larger than 500nm, so can count microvesicles and apoptotic bodies. If the researcher wants to study sEVs, beads need to be conjugated with specific antibodies against the antigens found on the vesicle surface. Beads are then bound to secondary fluorophore-conjugated antibodies and are suspended in fluid. This fluid is passed through a detection cell and the fluorophores

bound to the beads will fluoresce. The fluorescence detector will measure the fluorescence intensity and number of emission ‘events’ to count the number of beads and thus the number of sEVs present in the sample (An et al., 2018). Being able to choose which antibodies are used means that cargo and specific molecules on the surface of sEVs can be used. When done correctly, flow cytometry provides both accurate particle counting, and rapid particle counting – with thousands of sEVs being counted a second (Austin-Suthanthiraraj and Graves, 2013).

Although flow cytometry may be quick and convenient for researchers who have the equipment readily available, there are limitations which occur specifically when studying sEVs. One example is that immune complexes in the sample can have similar biophysical characteristics to extracellular vesicles and this can disrupt the scattered light intensities, providing inaccurate counts and errors with the gating strategies sample (An et al., 2018). Commonly used membrane dyes may fail in labelling all sEVs within a sample, or may stain these complexes with similar biophysical characteristics, meaning non-EV samples are incorrectly identified as sEVs (de Rond et al., 2018). Another concern is the swarm effect. The swarm effect occurs when high particle concentrations cause swarms of small particles to only be registered as one event, usually due to the fluorescent signal exceeding the detection limit. This means that the sample must be suitably diluted, meaning a method such as NTA may be required to get initial counts to accurately dilute the samples (Libregts et al., 2018). Additionally, the use of flow cytometry to study sEVs requires the researcher to be high skilled and consistent, with validation and gating for sEV samples requiring more expertise, with errors changing the recorded results (Morales-Kastresana and Jones, 2017).

1.6.5. Transmission Electron Microscope

Transmission electron microscope (TEM) uses a tungsten filament to create an electron beam to capture images of samples which have previously been fixed and dehydrated. The use of electrons allows for images of individual sEVs to be collected (Chuo et al., 2018). Additionally, sEVs can be labelled with immunogold, combining both TEM and immunofluorescence analysis to identify specific sEV cargo which may be present (Burbidge et al., 2020).

Although TEM can be used to count sEVs, this process is often time consuming, tedious, and inefficient. The quantitative data produced from TEM readings often under-represents both the number of sEVs present, and any quantitative values for the cargo content of the sEVs (Doyle and Wang, 2019). This is most likely due to the loss of vesicles during sample preparation. This sample preparation and drying process can also lead to changes in the morphology of the sEVs, often leading to them appearing to be cup-shaped (Burbidge et al., 2020). This needs to be considered when taking images of sEVs. Due to these limitations, TEM is now often used to check the quality of sEV isolation and to ensure vesicles are undamaged after undergoing the isolation process, rather than as a quantitative method.

1.6.6. Mass Spectrometry

Mass spectrometry is used to identify unknown compounds, a property which is particularly useful when studying unexpected cargo within sEVs. The samples are vaporised, ionised, and accelerated through the mass spectrometer. These ions are

then fragmented with the resulting mass equating directly to primary amino acid sequence of the proteins detected within the sample (Neagu et al., 2022). A key benefit of the use of mass spectrometry is the many possible ways that equipment can be combined to match the needs of the researcher. For the study of extracellular vesicles, the use of mass spectrometry may be favoured as it allows for the identification of proteins in a non-biased way, accelerating discovery regarding the protein cargo of sEVs in various biological contexts. Mass spectrometry can be highly specific and highly sensitive. There is potential for the use of mass spectrometry to be used as a diagnostic tool by characterising biomarkers found within sEVs (Mallia et al., 2020) due to these properties.

Despite the ability to automate some parts of the mass spectrometry process, there is still manual work required. sEVs must be purified, which may cause disruption to any proteins which may be present (Bandu et al., 2019). Mass spectrometry analysis may also miss any proteins which are present due coelution or varied ionisation efficiency, which can lead to limited reproducibility (Li et al., 2019). Mass spectrometry is also expensive and requires high start-up costs.

In summary the choice of isolation method and the analytical method which follows need consideration and careful interpretation.

Table 1.2 | *Summary of the advantages and disadvantages of methods of studying sEVs.*

	SUMMARY OF METHOD	ADVANTAGES	DISADVANTAGES
NANOPARTICLE TRACKING ANALYSIS (NTA)	Size, distribution, and concentration of EVs are measured in suspension using Brownian motion calculations.	Quantitative. Can phenotype and measure size of individual vesicles. Less bias than some other methods. High accuracy. Can detect smaller particles than other methods.	Similarly sized particles can be registered as EVs e.g. lipoproteins. Differences according to users. Particle counts may be overestimated in high and low concentration samples.
WESTERN BLOT	Proteins are separated by molecular weight onto a membrane. Antibodies are placed onto the membranes, and these bind to their corresponding proteins. Once imaged, the bound antibody will fluoresce, allowing the researcher to determine whether the specific protein is present.	Useful for phenotyping. Highly sensitive, requiring lower amounts of proteins than other methods. Highly specific. Well established. Vast availability of antibodies to test. Low start-up cost.	Purification required. Purification/concentration of samples needs to be considered prior to completion. Same amount of total protein loaded for all samples. High technical demands. Prone to false or subjective results.

		Semi-quantitative.	Cost of antibodies. Semi-quantitative.
FLOW CYTOMETRY	The number of EVs present in a sample are counted using a combination of fluorescence intensity and the number of emission events to calculate the number of beads found within a sample which are bound to an EV.	Possibility of choosing antibodies, allowing for specific cargo to be counted. Accurate particle counting. Rapid particle counting. Can count particles larger than 500nm, allowing microvesicles and apoptotic bodies to be studied.	Need for conjugation. Immune complexes may have similar biophysical characteristics to EVs and be counted. Labelling may fail or incorrectly label non-EV particles. Swarm effect. Other method may be needed to suitably dilute. High level of training required.
TRANSMISSION ELECTRON MICROSCOPE (TEM)	Transmission electron microscope (TEM) uses a tungsten filament to create an electron beam to capture images of samples which have previously been fixed and dehydrated.	Images of individual sEVs. Can be used to count EVs. Check quality of EVs and the isolation process. Can be used to identify specific cargo.	Time consuming, tedious, and inefficient if using for counts. Quantitative data collected often underrepresents data. Loss of vesicles during sample preparation. Changes in EV morphology.

MASS SPECTROMETRY	Mass spectrometry is used to identify unknown compounds. The samples are vaporised, ionised, and accelerated through the mass spectrometer. These ions are then deflected and then the present proteins within the samples are identified.	Combination of different MS methods can increase specificity. These combinations can be used to match need of researchers. Identification of proteins in a less biased way. Highly specific. Highly sensitive. Automation is possible. High throughput. Possible to study the presence of unknown cargo.	Manual work required despite possible automation. Damage to sEVs and present proteins possible. May miss proteins which are present. Limited reproducibility. Expensive and requires high start-up costs.

1.7. sEVs may provide information about biological adaptations

Notwithstanding the challenges of sEV research, sEVs have recently been shown to alter in the context of acute exercise and ageing. This suggests that they may contain information about adaptations to exercise and the ageing process.

1.7.1. sEVs in Exercise

The first indication that sEVs could be released during exercise came from Fruhbeis (et al.,) in 2015. Plasma was collected pre and post both a treadmill running and a cycling ergometer incremental test to exhaustion, sEVs were purified using a 0.2μm filter, followed by ultracentrifugation. NTA was used to determine sEV counts, and western blots were used to detect sEV markers. There was an increase in NTA particle count post-exercise in the cycle and treadmill studies by ~2.7 fold and ~1.5 fold respectively. They also showed a significant increase, via western blot, in the expression of Flot1, HSP and Integrin- αIIb (CD41), which were assumed relevant sEV markers (Frühbeis et al., 2015). Taken together, this was the first indication that sEVs may be released during physical activity.

Since then, there have been multiple studies focusing on the number of sEVs released during exercise with multiple studies focusing on the miRNA content (Guescini et al., 2015, D'Souza et al., 2018, Lovett et al., 2018, Just et al., 2020, Rigamonti et al., 2020) and protein cargo of sEVs released during exercise (Whitham et al., 2018, Kobayashi et al., 2021, Vanderboom et al., 2021). The vast majority of these interpreted that there were significant increases in sEVs and that their miRNA or protein cargo differ

compared to resting state. Two studies found no statistical increase in overall EV count between pre and post exercise condition, when analysing counts with NTA (Lovett et al., 2018, Brahmer et al., 2019). They did, however, show a significant increase in the sEV markers CD9, CD63 and CD81 when analysing vesicles with flow cytometry (Brahmer et al., 2019). Rigamonti (et al., 2020) isolated sEVs via centrifugation and using a 10 µm filter. NTA and flow cytometry were then used to analyse sEVs pre and post exercise in both healthy and obese participants. They showed a decrease in sEVs in both healthy and obese participants during exercise.

In light of previous commentary on the impact of analytical approach on sEVs, the majority of studies would support the hypothesis that sEVs are released during exercise [**Table 1.3**]. However, these are potentially subject to various sources of bias.

1.7.2. The impact analysis method has on sEV quantification

Some of the studies looking at the sEV response to exercise are summarised [**Table 1.3].** The use of different methods of isolation and analysis of each may be a source of bias or contamination, as discussed in **Chapter 1.5** – **Chapter 1.6**. Platelet poor plasma (PPP) was used by the vast majority of these studies, with only Whitham (et al., 2018); Brahmer (et al., 2019) and Vanderboom (et al., 2021) using platelet free plasma (PFP). Platelet-derived sEVs, such as those from remnant platelets, support factor XII-dependent thrombin, which triggers the release of more platelets (Tripisciano et al., 2017). This suggests that the use of PPP may induce further bias and impact any quantitative results.

Table 1.3. | *A summary of human based studies into the impact of acute exercise on the number and molecular profile of circulating sEVs.*

	PPP OR PFP?	EXERCISE TYPE	ISOLATION METHOD	METHOD OF STUDY	SUMMARY OF RESULTS
FRUHBEIS *ET AL*., 2015	PPP	Cycling bout: Starting at 50W and increasing power by 50 W every 3 minutes until exhaustion. Treadmill bout: Starting speed at 6 km/h and increasing velocity by 2km/h every 3 minutes until exhaustion.	Samples were filtered through a 0.2µm syringe filter, before undergoing ultracentrifugation at either 10,000 or 100,000 x g for 2 hours.	Nanoparticle Tracking Analysis. Western blot.	Increase in NTA particle count post-exercise in the cycle and treadmill studies by ~2.7 fold and ~1.5 fold respectively. Western blots on both the 10,000 x g samples and the 100,000 x g samples were tested against the sEV biomarkers Flot1, HSP/Hsc70 and Integrin aIIb. No significant correlation with physical activity was observed in the 10,000 x g sample. This suggests sEVs are significantly released during exercise.
GUESCINI *ET AL.,* 2015	PPP	Treadmill bout: Progressive increase in speed until 80% of the VO_2 max was reached.	Samples were filtered through a 0.2µm syringe filter, before undergoing ultracentrifugation at	Flow cytometry. Western blots.	sEVs significantly up regulated an hour after acute exercise, using

			110,000 x g for 70 minutes. Followed by Density Gradient Isolation and Immunoaffinity capture beads to isolate for Streptavidin positive sEVs.	MicroRNA probe array.	Tsg101 as a marker for sEVs. miRNA tested with miRNA probe array.
HELMIG *ET AL*., 2015	PPP	Cycling bout: Starting at 50W and increasing power by 50 W every 3 minutes until exhaustion.	Samples were filtered through a 0.2µm syringe filter, before undergoing ultracentrifugation at 100,000 x g for 2 hours.	Nanoparticle Tracking Analysis.	NTA was used to determine EV counts. EVs (100 – 130nm) were significantly increased immediately after cycling exercise and declined again after 90 minutes of rest. Most of these EVs were released in an early phase of exercise, prior to the participants reaching their anaerobic threshold.
D'SOUZA *ET AL.*, 2018	PPP	10 x 60 second intervals of cycling at peak power output, with 75 second rests between intervals.	Size Exclusion Chromatography.	Immunoblotting. Tandem Electron Microscopy. Nanoparticle Tracking Analysis.	CD63 and HSP70 increased following exercise, immediately after exercise and 4 hours later. miRNA content was testing using RT-PCR.

				RT-PCR	
LOVETT *ET AL*., 2018	PPP	5-minute warm up quadricep resistance followed by 10 sets of 10 plyometric jumps at 90% of their maximum achievable jump height.	Size Exclusion Chromatography.	Tandem Electron Microscopy. Nanoparticle Tracking Analysis. qPCR to determine the expression of some pre-selected miRNA cargo.	No difference in EV size and number both pre-exercise plasma and plasma taken 2 hours post exercise, using NTA. TEM was used to visualise sEVs. miRNA content was testing using RT-PCR.
WHITHAM *ET AL*., 2018	PFP	Cycling bout: Starting at 50W and increasing power by 50 W every 3 minutes until exhaustion.	Differential centrifugation (2 x 1h at 20,000g).	NTA Cryo-EM Nano-ultra-high-performance liquid chromatography tandem mass spectrometry (UHPLC-MS/MS).	Significant difference of >300 proteins in sEV lysates between pre-exercise and immediately post exercise. There was no significance between pre-exercise and 4 hours post recovery.
BRAHMER *ET AL*., 2019	PFP	Cycling bout: Starting at 40W and increasing power by 40 W every 3 minutes until exhaustion.	Size Exclusion Chromatography.	Nanoparticle Tracking Analysis. Tandem Electron Microscopy.	There was no statistically significant increase in overall EV count between pre and post exercise conditions using NTA. An increase was noted in CD9, CD63 and CD81

				Flow Cytometry based immune-bead isolation.	positive EVs when using flow cytometry. There was a significant increase in several other potential EV markers: CD41, CD42, CD62P, CD4, CD8, CD14 and MHC-II.
RIGAMONTI *ET AL*., 2020	PPP	A moderate constant workload, corresponding to 60% of VO_2 max for 30 minutes or until voluntary exhaustion.	Samples were centrifuged at 1200 x g for 15 minutes before being run through a 0.10µm filter, followed by ultracentrifugation at 110,000 x g for 75 minutes.	Nanoparticle Tracking Analysis. Flow cytometry with CD14, CD61, CD62E, CD105, SCGA and FABP labelled.	Post-exercise vesicles were significantly decreased in both healthy and obese participants. The release was significantly reduced in those who were obese.
JUST *ET AL.*, 2020	PPP	Five sets of knee extensions to volitional failure.	Size Exclusion Chromatography.	Nanoparticle Tracking Analysis. Tandem Electron Microscopy. Western blot.	Significant increase in sEV seen 5 minutes after exercise. Neither concentration nor size distribution of isolated circulating EVs change one hour after exercise. miRNA content altered.
KOBAYASHI *ET AL*., 2021	Serum	Cycling bout: 8 exercise bouts comprising 20 S at	Size Exclusion Chromatography.	Flow cytometry.	Changes in protein cargo occur between pre-HIIT, T0

		140% of VO_2 max and rest for 10 S.		Nano liquid chromatography tandem mass spectrometry. Western blots.	and T30, with 20 protein levels being significantly difference between the three time periods.
VANDERBOOM *ET AL*., 2021	PPP	Cycling bout: 5 bouts of 4 minutes at > 90% of VO2 max with 3 min pedalling at no load between bouts.	Platelet poor plasma was collected and isolated using common isolation methods: Differential Ultracentrifugation Polymer-based precipitation (ExoQuick) Membrane affinity (ExoEasy)	High resolution liquid-chromatography mass spectrometry.	Size Exclusion Chromatography identified more proteins with a higher precision than alternate methods of EV isolation.
	PPP		SEC. Size Exclusion Chromatography		321 sEV-associated proteins significantly increased post exercise.

1.7.3. sEVs and Ageing

Ageing, which is defined as the progressive impairment of the physiological functions of cells, tissues, and organs, is the leading cause of disease and death in developed countries (Schaum et al., 2020). The causes of ageing are interconnected and extremely complex, but the primary hallmarks are telomere erosion, defective proteostasis, genomic instability, epigenetic alteration, and chronic, low-grade inflammation (Manni et al., 2023). sEVs have been associated with all of the hallmarks of ageing (Mas-Bargues and Alique, 2023) as well as ageing-associated diseases Bodart-Santos et al., 2023) and senescence (Muñoz-Espín et al., 2013). Therefore, it can be hypothesised that sEVs may be implicated in the ageing process.

Eitan (et al., 2017) studied plasma from 74 participants (young aged 30-35 years old; middle aged 40-55 years old; elderly aged 55-64 years old) over a 4–6-year period. They showed not only that sEVs fell with age, but that elderly sEVs were more readily taken up by B cells and monocytes, suggesting phenotypical changes in sEVs. These findings have been recapitulated several times since (Rani et al., 2017, Zhang et al., 2017, Alibhai et al., 2020, Zhang and Jin, 2020). Further data has shown no change in sEV counts between adults aged 21 to 92 (Alberro et al., 2016), whereas other studies have shown a significant increase in sEVs in those who are aged 75 – 83, compared to those aged 20 – 28 years old (Alique et al., 2017). One suggestion is that this decreased concentration of sEVs may be due in part to increased internalisation (Eitan et al., 2017). As we delve further into discussing the quantification of sEVs, it will become apparent that factors such as different isolation methods and different means of

quantification, discussed earlier, can have a significant impact of recorded results, which may explain these conflicting findings.

Zhang *(*et al., 2023) injected aged mice with both young blood and a control. These mice injected with young blood had an increased lifespan, and a drastic reduction in epigenetic factors associated with ageing in the liver and blood. Interestingly, the rejuvenation effect persisted 2 months beyond the initial treatment (Zhang et al., 2023) . It is unclear what drives this effect, but as sEVs are part of the circulatory system, it stands to reason that they may be at least partially responsible. This further supports previous findings, which showed that sEVs derived from adipose-derived stem cells improved multiple age associated parameters such as motor coordination, fatigue resistance, fur regeneration, renal function and grip strength when injected into old mice (Sanz-Ros et al., 2022). There was also a significant decrease in frailty. Predicted epigenetic age was lower in the tissue of the treated mice, with a reduction in oxidative stress, cell senescence markers and inflammation in kidney and muscle tissue. These effects were also found in sEVs isolated from young mouse plasma (Prattichizzo et al., 2021). Taken together, these findings may suggest that sEVs are at least in part responsible for ageing, be this pathologically or so-called healthy ageing. The conflicting evidence concerning whether sEVs increase, decrease, or do not change in ageing is also cause for further investigation, as these differences may be due to chosen isolation or research method.

1.7.4. sEVs and Senescence

A contributor to ageing and age-related disease is senescence. Cellular senescence is a state in which cells lose their ability to divide, leading to irreversible growth arrest. Although cellular senescence occurs naturally throughout the lifespan as a protective mechanism to prevent the proliferation of damaged or harmful cells, including during embryogenesis (Muñoz-Espín et al., 2013), senescence cells accumulate during the ageing process (van Deursen, 2014). It is well established that cells undergoing senescence release more sEVs through the activation of the ceramide pathway, or the p53 pathway (Mato-Basalo et al., 2022). sEVs form part of the senescence-associated secretory phenotype (SASP), in which senescent cells secrete increased levels of growth factors, proteases, immune modulators and inflammatory cytokines (Coppé et al., 2010). This makes sEV cargo particularly interesting as potential biomarkers of senescence, as they may reflect senescent burden. They are also relatively easily accessible via routine blood sampling.

1.8. Specific Thesis Objectives

As summarised, sEVs appear to carry a lot of information that might inform key biological processes in the context of exercise, health, and the ageing process. However, interpreting previous findings is challenging due to the aforementioned lack of consistency in analytical approach.

In light of this, the aims of each chapter of this thesis are as follows:

- Determine whether there were a significant difference in circulating sEV number after a bout of high intensity cardio-based exercise (**Chapter 2**); and
- to further investigate the proteome of sEVs released found within sEVs released during senescence, and whether any of these could have been candidate biomarkers (**Chapter 3**); and
- identify whether there were any significant quantitative or proteomic differences in circulating sEVs in response to ageing or chronic exercise (**Chapter 4**).

The overarching aim of this thesis is to investigate the impact that exercise (both acute and chronic), ageing and senescence have on the sEV count and protoeme, with an aim to determine the utility of studying sEVs in these wider contexts.

Chapter 2 -

Single vesicle analysis of circulating sEVs in response to high intensity intermittent exercise

Data presented in this chapter have been published in the following journal article:

McIlvenna, L.C.*, **Parker, H-J**.*, Seabright, A.P., Sale, B., Anghileri, G., Weaver, S.R.C., Lucas, S.J.E. and Whitham, M. (2023), Single vesicle analysis reveals the release of tetraspanin positive extracellular vesicles into circulation with high intensity intermittent exercise. The Journal of Physiology, 601:5093-5106.

2.1. Abstract

Purpose

Small extracellular vesicles (sEVs) are nano-sized particles containing proteins, metabolites, lipids, and RNA that can be transferred between cells. Previous research using methodologies such as nanoparticle tracking analysis, flow cytometry and mass spectrometry have suggested that there is a significant increase in the release of sEVs into circulation during an acute bout of aerobic exercise. Despite this, there is no gold standard for the isolation of sEVs from complex biofluids like plasma, raising the question of whether these results are due to bias introduced during different isolation approaches. It is also unclear to what extent the presence of platelets introduces bias into these data.

Method

Single EV particle analysis can be used without an isolation step, by immobilizing tetraspanin positive extracellular vesicles (CD9, CD63, CD81 and CD41a) onto a chip directly from plasma using the EV-TERA-P kit. EDTA-treated blood was collected from 7 participants, both pre and post a bout of high intensity interval training (HIIE) (4 x 30 s cycling at a work-rate corresponding to 200% of individual maximal power (watts), interspersed by 4.5 min of active recovery). Platelet poor and platelet free plasma samples were derived from 1 or 2 centrifugal spins at 2500 x g.

Results

A lower number of platelets were identified in the platelet free plasma than the platelet poor plasma, which was associated with lower numbers of CD9, CD63 and CD41a positive sEVs. HIIE induced an increase in fluorescence counts in CD9, CD63 and CD81 positive sEVs in both platelet poor plasma and platelet free plasma.

Conclusion

These data support previous research suggesting sEVs are released into circulation with exercise, despite any bias that may have been introduced with any additional isolation steps. Furthermore, platelet-free plasma is preferable in the study of phenotype during exercise, but if the effect is significant enough will be visible in platelet poor plasma. These data support the use of single EV particle analysis for wider analysis in this thesis.

2.2.2. Introduction

Small extracellular vesicles (sEVs) are cell-derived lipid membrane particles, which are capable of carrying molecules such as protein between cells. It is not currently known whether long term exercise and ageing alter circulating sEVs. There are several suggestions that sEVs may change during ageing, as discussed in **chapter 1**, but there is little research into whether long term exercise has an impact on this. This is a challenge that is also encumbered by the more straightforward question of whether acute exercise changes circulating sEVs. This is partially due to a lack of gold standard isolation methods for the study of sEVs.

Exercise is known to have a significant physiological effect on the body, with a plethora of molecular mechanisms all working concurrently throughout the body (Tung et al., 2019). One such example may be the release of sEVs into circulation. Several studies have shown that sEVs are released during acute exercise (Fruhbeis et al., 2015, Helmig et al., 2015, Brahmer et al., 2019). Further research shows significant changes to both the miRNA cargo of sEVs (Guescini et al., 2015, D'Souza et al., 2018, Lovett et al., 2018, Just et al., 2020, Rigamonti et al., 2020) and the protein cargo (Whitham et al., 2018, Kobayashi et al., 2021, Vanderboom et al., 2021). Of the proteins that were shown to increase, there were a large variety of biological processes that were implicated including adhesion molecules, lipid rafts and signalling molecules (Whitham et al., 2018). This indicates that exercise derived sEVs are associated with tissue crosstalk. Further studies into the timing of this release show that circulating sEV counts return to basal levels within 2 hours of exercise cessation (Lovett et al., 2018). It is likely

these sEVs localise to the liver (Whitham et al*.,* 2018), This indicates derived sEVs may be associated with tissue crosstalk.

Other research in rodents has shown no change to circulating sEVs post-exercise (Watanabe et al., 2022) or a reduction in sEV release in circulation in humans (Rigamonti et al*.,* 2019). These differences in results may be due to the choice of method by which sEVs are isolated from plasma, or the choice of quantification method. Due to these discrepancies, the exact impact of acute exercise of sEVs is unclear.

2.2.2. The problem with isolation methods

Another key factor which impacts the study of EVs is platelet contamination. To prevent the impact platelets may have on collected plasma, the ISEV guidelines (Théry et al., 2018) now suggest that samples are double spun. Thrombin-activated platelets trigger the release of further EVs (Spakova et al., 2021), which highlights the importance of correct plasma handling. It is also preferable to keep blood at room temperature prior to centrifugation, as platelet-derived EVs impacted by temperature change have different cargo in comparison to non-platelet-derived EVs. Of note, platelet-derived EVs are shown to release 1β57, HMGB1 and C-reactive protein, which are all key markers of inflammation (Miles and Calder, 2021). Furthermore, platelet-derived EVs support factor XII-dependent thrombin, which triggers the release of more platelets (Tripisciano et al., 2017). Platelet-derived EVs specifically exhibit higher thrombogenicity than EVs from unstimulated monocytic THP-1 cells (Tripisciano et al., 2017). Additionally, it has been reported that collected blood should be processed rapidly and only inverted as much as

is required to properly mix the relevant anticoagulant (Dhondt et al., 2023), due to movement of samples activating platelets, leading to their EV release (Puhm et al., 2020). Berckmans (et al., 2019) repeated a study of theirs from 2001 focusing on the function of EVs in blood from health adults, using more up to date plasma preparation methods. They initially suggested that EVs lead to low grade thrombin generation, but with newer plasma preparation methods, this does not appear to be the case (Berckmans et al., 2019). This suggests that research conducting using platelet poor plasma must be considered with care. In light of differences in plasma handling, sEV isolation and analytical approach in the published literature, these factors combined lead to uncertainty over whether circulating sEVs do truly change during acute exercise, or whether these results are simply the result of biased research data, or platelet contamination.

2.2.3. Single EV Particle Analysis

In recent years, single EV particle analysis array technology has emerged. Samples are characterised for tetraspanin antibodies which are found on the surface of sEVs, as well as the size and yield. For the human tetraspanin plasma kit (EV-TERA-P), CD9, CD63, CD81, CD41a and Mouse IgG (control) are measured. Vesicles which are positive for these will bind to antibody spot chips and with the aid of fluorescent conjugated antibodies to the same tetraspanin proteins, fluorescence intensity equates directly to sEV concentration. Colocalisation between the fluorescent antibodies and the size of sEVs above 50nm are also measured.

The key benefit of the single EV particle analysis technology is that no pre-purification of the vesicles is required, which constitutes an advantage over every other method to study extracellular vesicles.

2.2.4. Aims

- Determine whether there is a significant difference in sEV number between platelet free plasma and platelet poor plasma; and
- identify whether there is a significant difference in circulating sEV number after a bout of high intensity cardio-based exercise.

2.2.5. Hypothesis

- It is hypothesized that there will be a significant decrease in sEVs between single spun (platelet poor plasma) and double spun (platelet free plasma). Additionally, it is hypothesized that there will be a significant increase in sEVs during high intensity cardio-based exercise in platelet free plasma.

2.3. Methods

2.3.1. Ethical approval

Prior to the commencement of this study, ethical approval was obtained from the University of Birmingham Human Research Ethics Committee (Reference: ERN 17-1570), and all participants provided written informed consent prior to participation in accordance with the *Declaration of Helsinki*.

2.3.2. Participants and experimental procedures

Recruited via local advertisement, participants (aged 18-31) were requested to not consume food prior to the experiment (large meal < 4 hours, a light snack < 2 hours and from consuming caffeine < 6 hours) and to drink at least 0.5 litre of water within 4 hours and 0.25 litres of water within 15 minutes of the testing beginning, to prevent dehydration. Prior to commencement, all participants were determined to be healthy with no history of respiratory, cerebrovascular or cardiovascular disease and participants were required to not be taking any medication (with the exception of oral contraception in female participants).

2.3.3. Exercise Testing

An initial exercise testing session was conducted prior to the main testing, to determine the participant's power output, heart rate (Vyaire Medical, Basingstoke, United Kingdom), VO_2 max and $Watt_{max}$. Additionally, oxygen consumption was measured using a mask attached to a Vyntus Metabolic Cart (Vyaire Medical, Basingstoke, United Kingdom). These details were used to determine the subsequent exercise session intensities. An incremental aerobic cycling protocol was used (Lode ergometer, Groningen, Netherlands), which consisted of a warmup conducted at 50W for 5 minutes. This was followed by an increase protocol by loaded resistance, with resistance added every 3 minutes until exhaustion was reached. A 2-minute cool down period followed. Between 2 and 14 days after this session, a high intensity interval exercise (HIIE) set was conducted. This began with a general warm up period, followed by 4 x 30 seconds of cycling at 200% W_{max} with 4 minutes and 30 seconds of active

recovery at 50W between these sets. This was followed by a 5-minute cool down session.

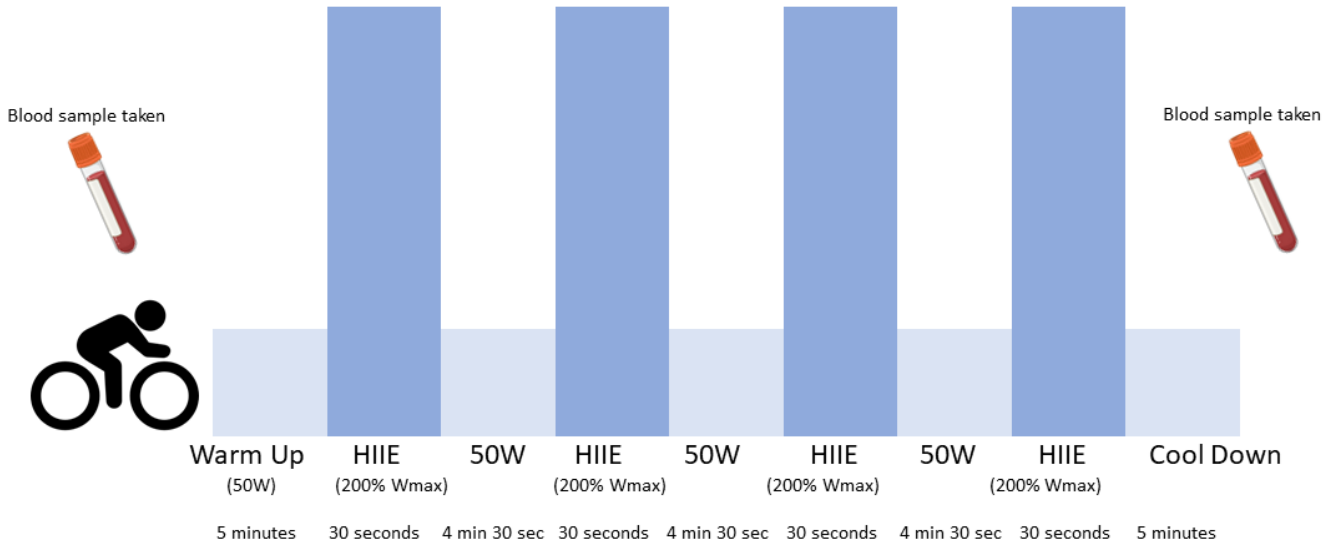

Figure 2.1. *The high intensity interval exercise protocol untaken by participants, cycling at 50W during the rest interval and 200% of their Wattmax during the exercise interval.*

Table 2.1 | *Participant anthropometric characteristics*

	N = 9
Age (years)	21 ± 2.93
Height (m)	1.70 ± 0.11
Weight (kg)	67.19 ± 10.31
BMI ($kg.m^{-2}$)	23.09 ± 1.70
VO2 Peak (ml·kg-1 ·min-1)	45.03 ± 4.41

Data presented as mean ± SD. Include both male participants (N=5) and female participants (N=4).

2.3.4. Blood Collection and plasma separation

A cannula was inserted into a vein within the cubital fossa prior to the exercise bout. This cannula was infused with saline and allowed to adjust for ~2 minutes. 2ml of venous blood was collected and disposed, to clear any cannulation contamination.

EDTA lined tubes were used. Pre-exercise, 5 x 10ml blood samples were collected after 10 minutes supine resting. Post-exercise, 5 x 10ml blood samples were collected within 30 seconds of cessation.

2.3.5. Platelet Poor Plasma and Platelet Free Plasma

Blood samples were spun within 2 minutes of sampling. Samples were centrifuged at 2500 x g for 15 minutes at room temperature. Plasma was collected using clean pastettes and placed into 15ml falcon tubes, leaving ~50mm to avoid the buffy coat. 2ml of this plasma was aliquoted separately as platelet poor plasma. The falcon tubes were then spun again at 2500 x g for 15 minutes at room temperature. This produces platelet free plasma. Both platelet poor plasma and platelet free plasma samples were stored at – 80°C for further use, with aliquots saved for ExoView to prevent any freeze-thaw cycles.

2.3.6. Platelet Count

20µl of plasma was placed into the aspiration chamber. This was then collected by the Horiba Medical Yumizen H500 (HORIBA, Northampton, United Kingdom) and delivered to the dilution chamber, where ABX Diluent was added to a final dilution of 1/201 (plasma: ABX Diluent). The platelet count was run in triplicate, with the mean value of these counts presented.

2.3.7. Single EV particle analysis

Plasma samples were analysed using the ExoView human tetraspanin plasma Kits (EV-TERA-P) in accordance with the manufacturer's instructions (Unchained Laboratories, Pleasanton, CA, USA) as described in detail in **Chapter 6: General Methods**. 10µl of

diluted plasma was applied to each chip containing antibody capture spots for CD9, CD63, CD81 and CD41a, as well as mouse IgG to act as a negative control. Bacurski (et al. 2019) showed that fluorescence intensity and fluorescent count results were similar to other methods of studying EVs, but that the label free SP-IRIS technology, which does not use fluorescent antibodies, that is additionally available on ExoView is inaccurate. When conducting concentration-based tests, using label-free SP-IRIS and fluorescent counts, Khan et al., (2021) showed that the label free IM (interferometric imaging) data did not increase in line with the increased sample concentration, whilst fluorescent counts did as would be expected. Due to this, the decision was made to focus on mean fluorescence intensity, which reflects total protein expression, and the fluorescent count data, which reflects quantitative counts of individual sEVs, using IM only for CD41a positive sEVs as there is no fluorescent marker. Further details about this analysis can be found in **Chapter 6: General Methods.**

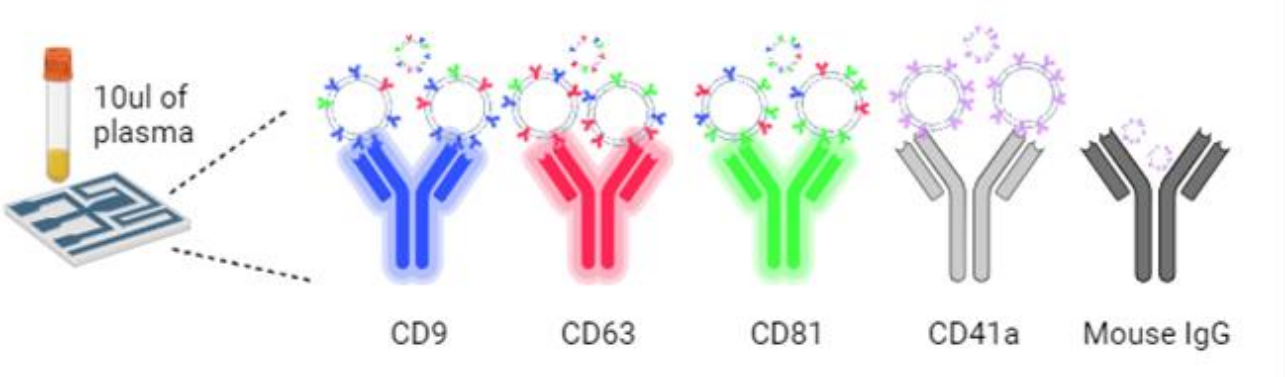

Figure 2.2 *The single particle immunofluorescence array works by reading the fluorescence emitted by binding specific tetraspanins on the surface of sEVs to those on a microfluidic chip.*

2.3.8. Follow-up assessment

In an additional follow up study to assess whether the effect on HIIE on sEV release prevails in platelet poor plasma, the same exercise protocol was used. Five participants completed the protocol (3 females, 2 males, age 21 ± 3 years, 41.0 ± 4.4 ml/kg/min). Platelet poor plasma, pre and post exercise plasma samples were analysed for tetraspanin positive sEVs as detailed above.

2.3.9. Statistical Analysis

When analysing fluorescent counts and mean fluorescent intensity, t-tests were used to denote statistical significance. Data are presented in figures as fold change. Colocalisation data is unchanged. All single particle statistical analysis was conducted using GraphPad Prism version 9.4.1. Statistical significance of pre and post exercise EV markers, platelet poor plasma and platelet free plasma EV markers and platelet counts were analysed using a paired two-tailed t-test. All data has been plotted with individual data points, with the mean +/- SD. Differences were considered statistically significant at $P< 0.05$ *.

2.4. Results

2.4.1. A significant difference in tetraspanin-positive sEVs is observed between platelet poor plasma and platelet free plasma.

As discussed previously, platelets are a known source of sEVs, meaning that any biological sample data may be impacted by platelet release. A significant decrease (*P = 0.0029* **) in platelets was observed between plasma which was centrifugated once (Platelet Poor Plasma) and plasma which was centrifugated twice (Platelet Free

Plasma) [Figure 2.3]. Platelet free plasma fluorescent counts, representing particle (sEV) number, fell in CD9 and CD63 (*P=0.0254 *; 0.0190 * respectively)* but did not fall in CD81 (*P = 0.222*) [Figure 2.3]. Additionally, interferometric counts taken from the CD41a binding spots significantly decreased once platelets are cleared from plasma (*P = 0.0027* **). Clearing of platelets was associated with a significant decrease in the size of CD9 (*P = 0.0125* *) and CD41a (*P = 0.0118* *) positive sEVs, but the magnitude of the change, in light of the size range of sEVs (20 – 300nm) is unlikely to be biologically meaningful.

CD63 (*P = 0.0430* *) and CD81 (*P = 0.0137* *) mean fluorescence intensity, representing total protein expression, irrespective of particle count, significantly decreased once plasma is spun for a second time. These data, along with the visual representation of fluorescence from the antibody spots [Figure 2.3] indicate that there are significantly more sEVs in platelet poor plasma than in platelet free plasma. These data suggest that a higher platelet count correlates with higher sEV count and that sEVs are released from remnant platelets ex vivo.

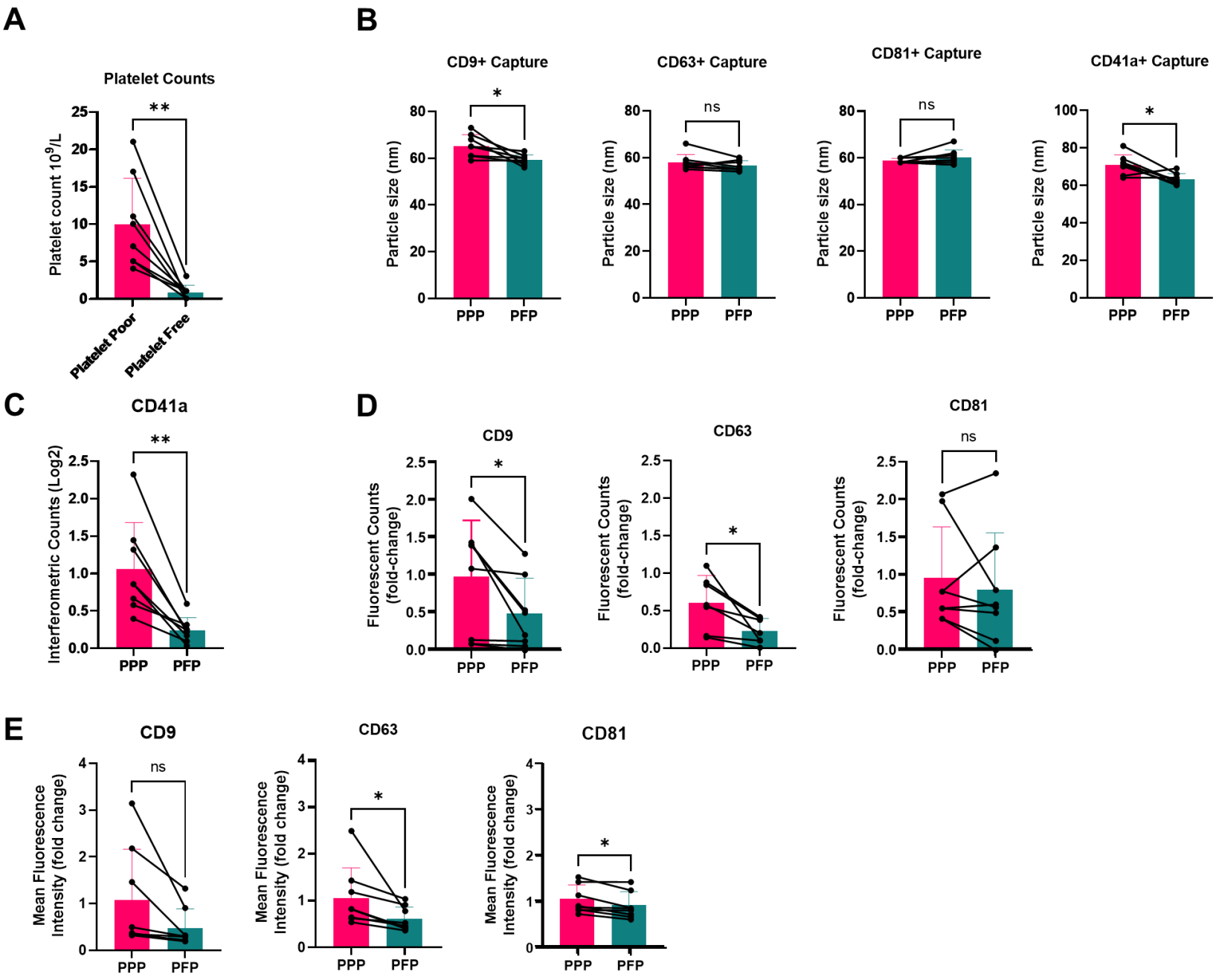
A
Platelet Counts
Platelet count 10^9/L
**
Platelet Poor
Platelet Free
B
CD9+ Capture
CD63+ Capture
CD81+ Capture
CD41a+ Capture
Particle size (nm)
*
ns
ns
*
PPP
PFP
C
CD41a
Interferometric Counts (Log2)
**
PPP
PFP
D
CD9
CD63
CD81
Fluorescent Counts (fold-change)
*
*
ns
PPP
PFP
E
CD9
CD63
CD81
Mean Fluorescence Intensity (fold change)
ns
*
*
PPP
PFP

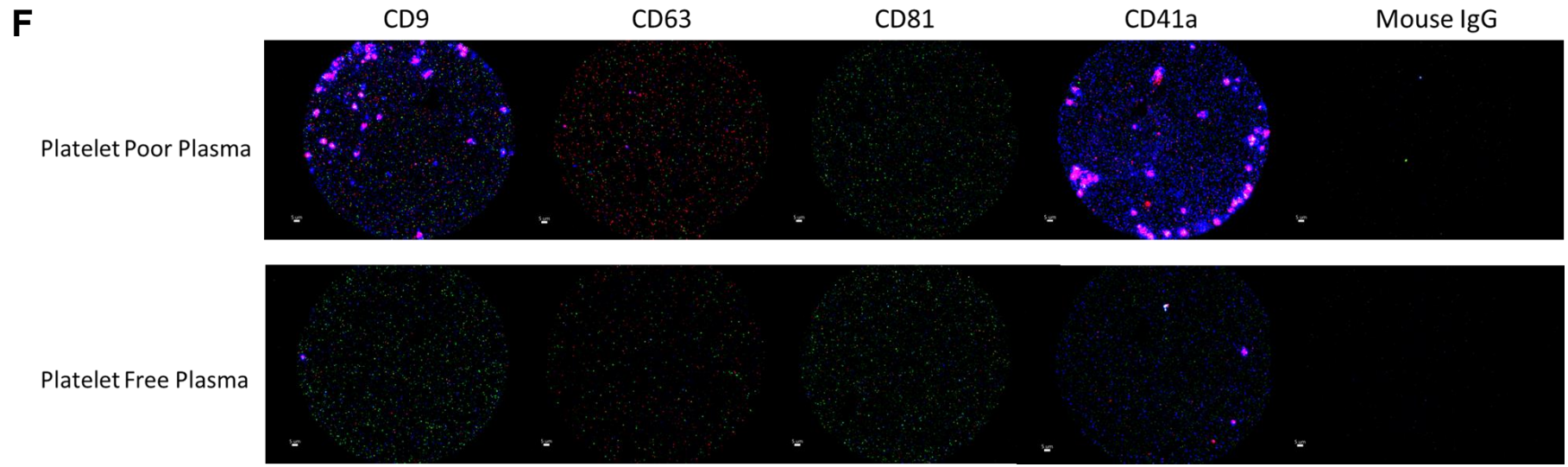

Figure 2.3. *A). A comparison of platelet count (10^9/L) for platelet poor and platelet free data (N = 8). B). Particle sizes for spot specific bound particles for platelet poor plasma and platelet free plasma, measured by SP-IRIS (N = 8) C). Fold change of interferometric counts of all particles bound on CD41a for platelet poor plasma and platelet free plasma (N = 8). D). Colour specific fluorescent counts, measured by using immunofluorescent imaging and analysed as fold-change between platelet poor plasma and platelet free plasma (N = 8). E). Mean fluorescence intensity of fold-change difference between platelet poor plasma and platelet free plasma measured by the intensity of the colour-specific antibody on each spot (N = 8). F). Representative spot images of platelet poor plasma and platelet free plasma taken using immunofluorescent imaging. All data previously referenced is collected from spots such as these. A representative mark denoting 5 µm is present on each image. For the ExoView figures, statistical analysis was conducted using paired t-tests using GraphPad Prism. $p<0.05$ indicated by *, $p<0.01$ indicated by **.*

2.4.2 High Intensity Interval Exercise leads to an increase in the number of circulating tetraspanin positive small extracellular vesicles.

A bout of high intensity interval exercise (HIIE) was validated using heart rate data [Figure 2.4], with mean HR showing large increases following each effort, indicating that the exercise protocol was maximal. A significant increase [Figure 2.4] was noted between all sEV counts. Fluorescent counts were significantly increased in all three measured tetraspanins (CD9 *P = 0.0180 * d=0.863*; CD63 *P = 0.0323 * d=1.229*; CD81 *P = 0.0412 * d=0.289*). Similarly, interferometric counts showed a significant increase in CD41a (*P = 0.0128 * d=0.466*). Mean fluorescence intensity was significantly increased in CD9 (*P = 0.0081 ** d=2.106*) and CD63 (*P = 0.0034 ** d=1.225*), further suggesting the release of sEVs during HIIE. This can be seen visually across representative capture spots, showing the present fluorophores (*CD9: Blue, CF488; CD63: Red, CF647; CD81: Green, CF555*) for both pre-exercise and post-exercise sEV images [Figure 2.4]. CD41a positive sEVs are shown to significantly increase in size post-exercise (*P = 0.013 **), but as previously discussed this is unlikely to be biologically relevant.

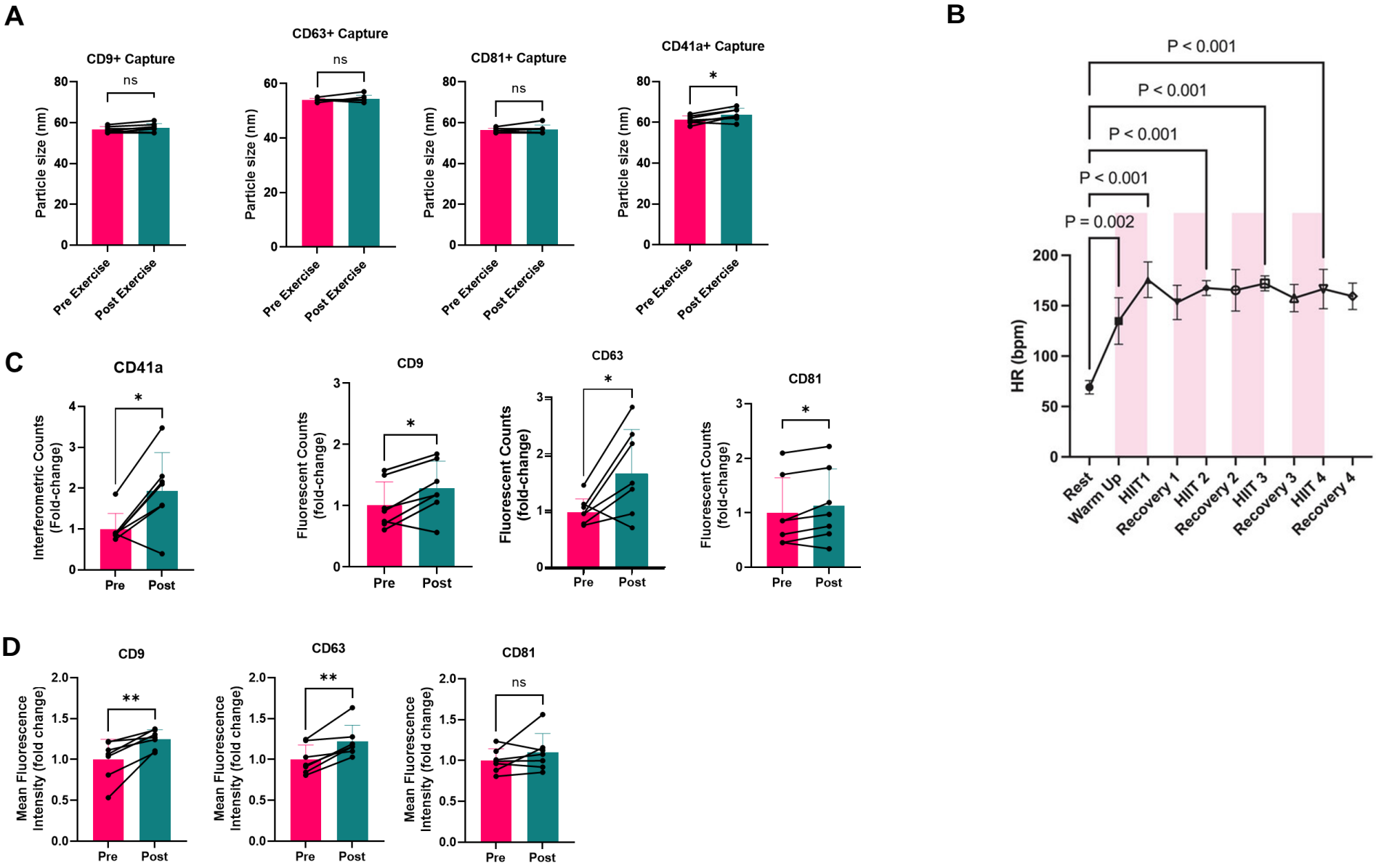
A
CD9+ Capture
CD63+ Capture
CD81+ Capture
CD41a+ Capture
Particle size (nm)
ns
*
Pre Exercise
Post Exercise
B
P < 0.001
P < 0.001
P < 0.001
P < 0.001
P = 0.002
HR (bpm)
Rest
Warm Up
HIIT1
Recovery 1
HIIT 2
Recovery 2
HIIT 3
Recovery 3
HIIT 4
Recovery 4
C
CD41a
CD9
CD63
CD81
Interferometric Counts (Fold-change)
Fluorescent Counts (fold-change)
Pre
Post
D
CD9
CD63
CD81
Mean Fluorescence Intensity (fold change)
**
ns

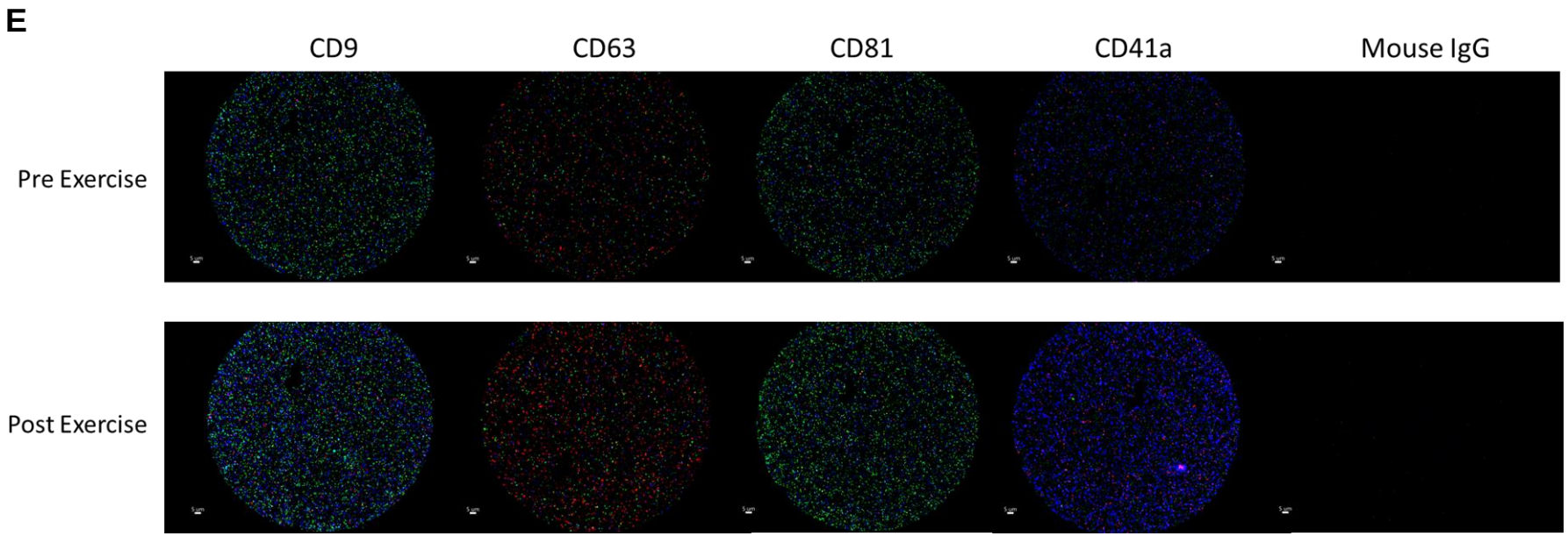

Figure 2.4. *A). Particle sizes for spot specific bound particles for pre and post exercise plasma, measured by SP-IRIS. (N = 7, paired t-test). B). Heart rate was significantly elevated by each exercise effort (one-way ANOVA and Dunnett's multiple comparison test). C). Fold change of interferometric counts of all particles bound on CD41a for pre and post high intensity interval exercise (N = 7). D). Colour specific fluorescent counts, measured by using immunofluorescent imaging and analysed as fold-change between pre and post high intensity internal exercise. (N = 7). E). Mean fluorescence intensity of fold-change difference between pre and post high intensity interval exercise measured by the intensity of the colour-specific antibody on each spot. (N = 7) F). Representative spot images of the CD9, CD63, CD81, CD41a and Mouse IgG control spots for pre and post high intensity interval exercise plasma taken using immunofluorescence imaging. All data previously referenced is collected from spots such as these. For the ExoView figures, statistical analysis was conducted using paired t-tests using GraphPad Prism. p<0.05 indicated by *, p<0.01 indicated by **. Cohen d effect size is denoted by d= .*

.

2.4.3 CD9 positive sEVs colocalise with other tetraspanin positive sEVs during exercise

Colocalisation data shows whether vesicles which have one tetraspanin on their membrane also show another tetraspanin [Figure 2.5]. This provides further characterisation of the vesicles and provides an insight into potential different subpopulations of sEVs. Blue fluorescence on another bound spot shows CD9 is present, red fluorescence on another bound spot shows CD63 is present and green fluorescence on another spot shows CD63 is present. For the CD63 spots and CD81 spots, no significant change in colocalisation between pre and host HIIE was identified (**CD63 Spot**: Blue, *P = 0.4520*; Red, *P = 0.0701*; Green, *P = 0.1489*. **CD81 Spot**: Blue, *P = 0.8509*; Red, *P = 0.2032*; Green, *P = 0.2368*). The CD9 spot showed significance against all three identified tetraspanins (***CD9 Spot**:* Blue*, P = 0.0050 **;* Red*, P = 0.0390 *;* Green*, P= 0.0362 **). The CD41a spot showed a significant increase in colocalisation of CD41a and CD9 positive vesicles (*P = 0.0472*) but does not show significance between CD41a and CD63 (*P = 0.0936 **), nor CD41a and CD81 (*P = 0.2275*) [Figure 2.5]. While colocalisation data may be difficult to interpret in the context of the research question, the prevalence of a significant effect of exercise in CD9 positive sEVs might implicate CD9 as a significant driver of the sEV exercise response.

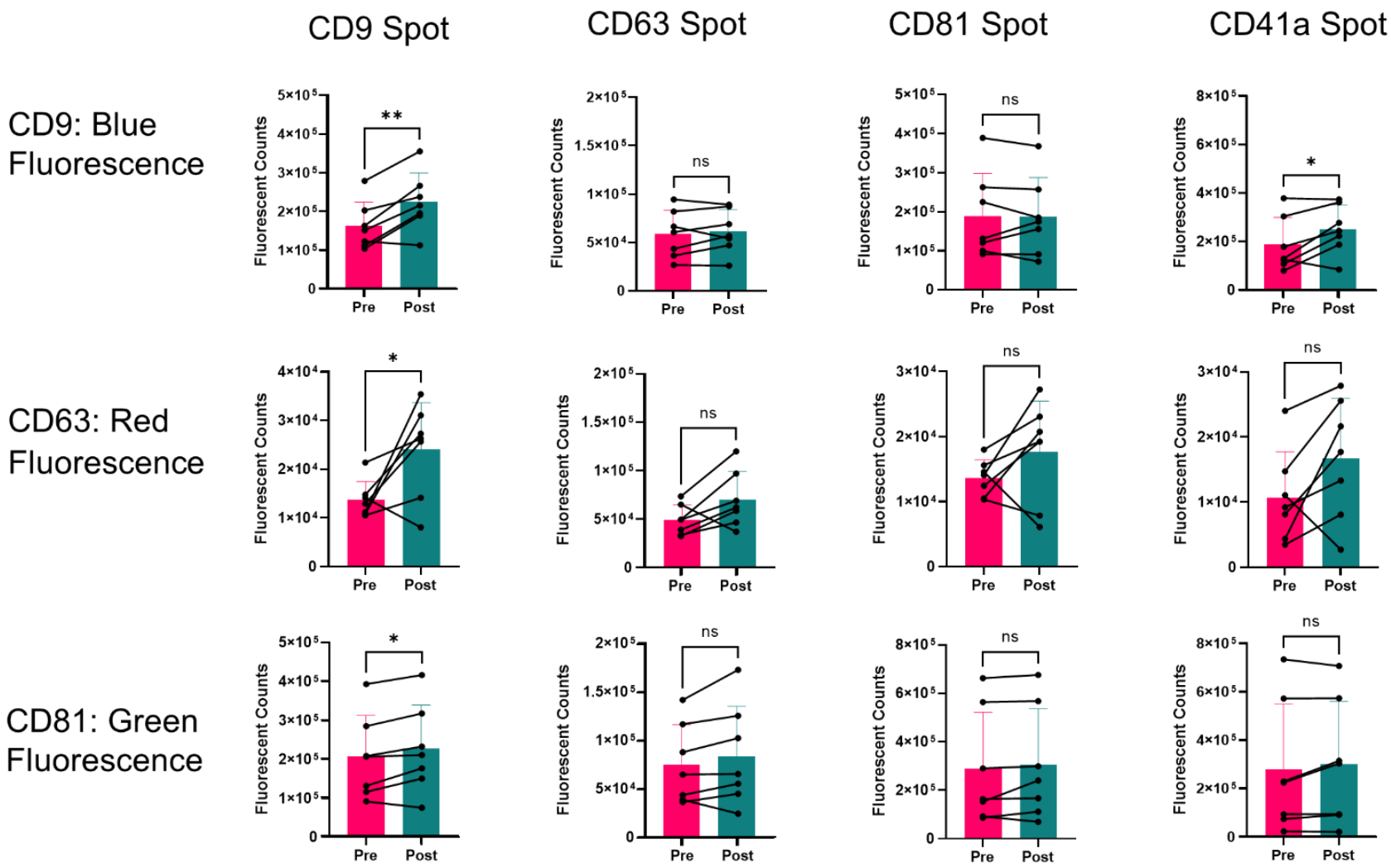

Figure 2.5. *Colocalisation of each colour (CD9: Blue; CD63: Red; CD81; Green) on each specific antibody binding spot both pre and post exercise. N = 7. Statistical analysis conducted using paired t-tests using GraphPad.* p<0.05 indicated by *, p<0.01 indicated by **.

2.4.4. The effect of HIIE on sEV count prevails in single spun plasma

The same manner as the platelet free plasma study [Figure 2.3], a bout of high intensity interval exercise (HIIE) was conducted. A significant increase [Figure 2.6] was noted between all sEV counts. Fluorescent counts were significant increased in all three measured tetraspanins (CD9 *P = 0.0230 *;* CD63 *P = 0.0028 *;* CD81 *P = 0.048 **). Interferometric counts similarly showed a significant increase in CD41a (*P = 0.023 **). Mean fluorescence intensity was significantly increased in CD9 (*P = 0.029 **), but not in CD63 nor CD81 positive sEVs. This recapitulates findings that sEVs are released during HIIE, an effect which can be seen despite the presence of remnant platelets in each sample, potentially increasing sEV count ex vivo.

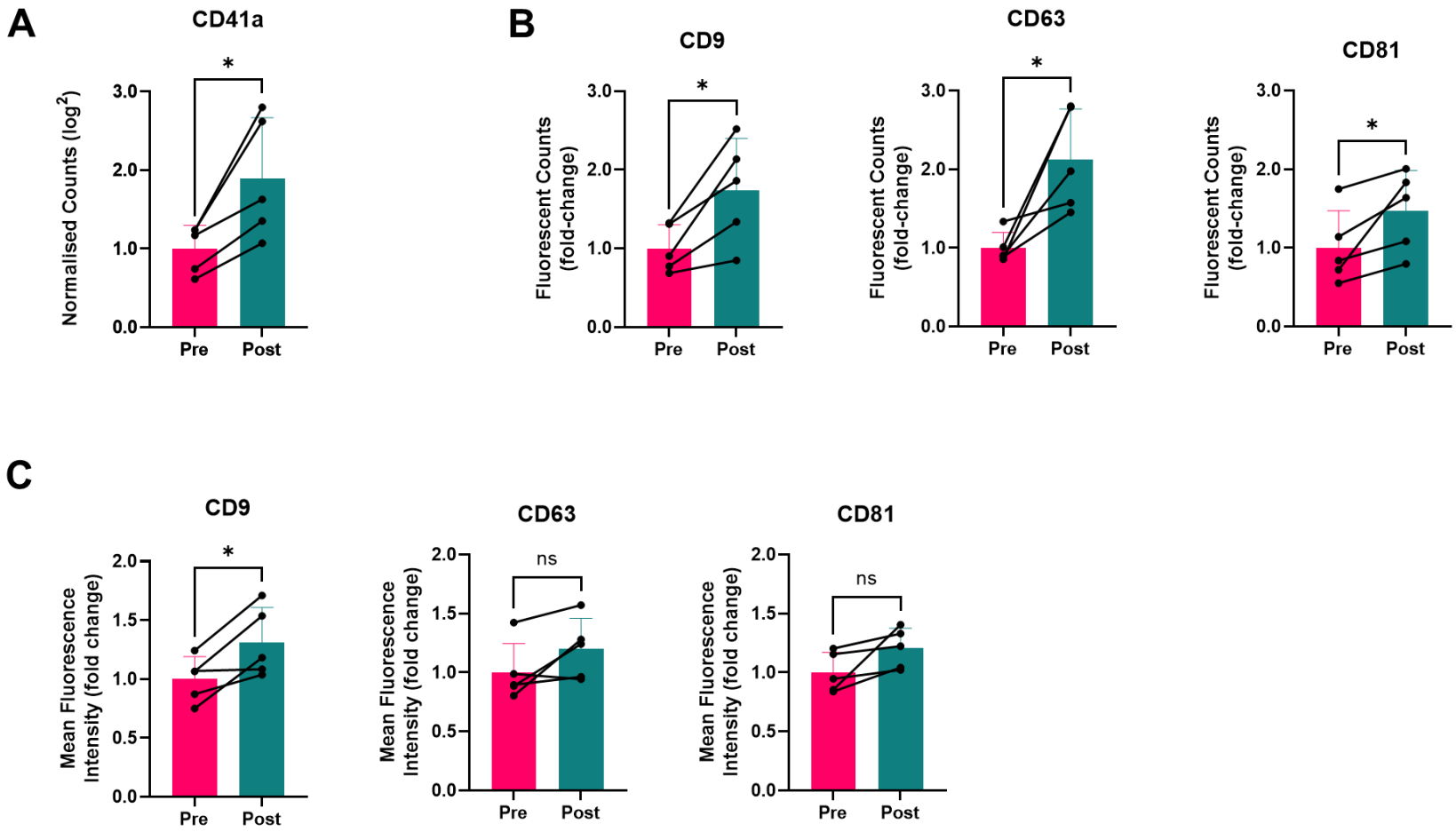

Figure 2.6. *A). Fold change of interferometric counts of all particles bound on CD41a for platelet poor pre and post exercise plasma (N = 5). B). Particle sizes for spot specific bound particles for platelet poor pre and post exercise plasma, measured by SP-IRIS. (N = 5, paired t-test). C) . Mean fluorescence intensity of fold-change difference between platelet poor pre and post high intensity interval exercise measured by the intensity of the colour-specific antibody on each spot. (N = 5)*

2.5. Discussion

As previously introduced, since 2015 (Fruhbeis et al.,) there has been increasing data suggesting that sEVs are released during a single bout of acute exercise. This is both applicable to individual counts of sEVs (Fruhbeis et al., 2015; Helmig et al., 2015; Just et al., 2020) and with regards to increased release of specific protein cargo during exercise (Whitham et al., 2018; Kobayashi et al., 2021; Vanderboom et al., 2021). Despite these findings, there are concerns that these results may be heavily influenced by the researcher's chosen method of sEV isolation and analytical approach, leading to the introduction of potential bias. For example, it is thought that the failure to adequately remove platelets from plasma might introduce sEVs into the plasma sample ex vivo. Using a single particle immunofluorescence analysis array, we show a significant difference in tetraspanin positive sEVs in platelet free plasma versus platelet poor plasma, suggesting that the former is a more representative analyte when assessing sEV number. Using the same array, it was also shown that sEVs increase with high intensity interval training, both using PPP and PFP. This reinforces the concept of sEV release during acute exercise and demonstrates that single particle immunofluorescence array is an important tool in the assessment of sEV number and phenotype.

As sEVs increase during exercise and have previously been shown to contain cargo related to a variety of biological processes (Whitham *et al*., 2018; Kobayashi *et al*., 2021; Vanderboom *et al*., 2021), the sEVs response to exercise may be biologically relevant.

CD9, in particular, is shown to be heavily impacted in all aspects of this study. CD9 significantly decreases in platelet depleted plasma. CD9 is also significantly increased in both platelet free and platelet poor plasma, in terms of both mean fluorescence intensity, which reflects total protein expression, and the fluorescent count data, which reflects quantitative counts of individual sEVs. CD9 positive sEVs have been implicated with the uptake of sEVs in in vitro studies (Nigri et al., 2022). This, combined with the increase of colocalised CD9 post exercise, feeds speculation that perhaps CD9 may be involved in both biogenesis and the uptake of sEVs.

A limitation of the single EV particle analysis array is that it assumes that CD9, CD63, CD81 and CD41a are the most appropriate markers to count sEVs. Kugeratski et al., (2021) conducted an in-depth analysis of EVs to identify representative protein markers. This was achieved by using super-SILAC, combined with high-resolution mass spectrometry, quantifying 1212 proteins from sEVs derived from 14 different cell lines. They showed that many sEV markers are not ubiquitous across all cell types, including CD9, CD63 and CD81. Despite this, the Kugeratski data focuses primarily on in vitro cell lines, meaning the data may not be applicable for more complex biological fluid samples, such plasma. Furthermore, the manner of combining all tetraspanins as a sum used here is likely to immobilise all sEVs across all capture spots.

Another point to note is that although platelet poor plasma and platelet free plasma show an increase in sEV counts during HIIE, and thus suggesting that PPP may be suitable to study sEV counts, this may not be the case when studying changes to sEV

cargo. As Vanderboom (*et al.,* 2021) previously showed, the proteome of sEVs from platelet poor and platelet free plasma is comprehensively different, likely due to the presence of remnant platelets. This would mean that any sEV cargo identified in platelet poor plasma may not accurately reflect the plasma proteome, due to the influence of remnant platelet-derived sEVs. Other potential confounders that can impact sEV count and cargo include postprandial status (Rome and Tacconi, 2024), donor age (Eitan et al., 2017), pregnancy (Nakahara et al., 2020), biological sex and menopause (Hooten et al., 2022). To mitigate these, none of the participants were or had previously been pregnant, nor had entered menopause. Participants were also required to fast prior to the experiment. The presence of lipoproteins from the diet will impact EV biogenesis, EV lipid composition and sEV cargo (Rome and Tacconi, 2024). sEV counts were taken using freshly collected plasma to prevent any impact from storage (Thery et al., 2018).

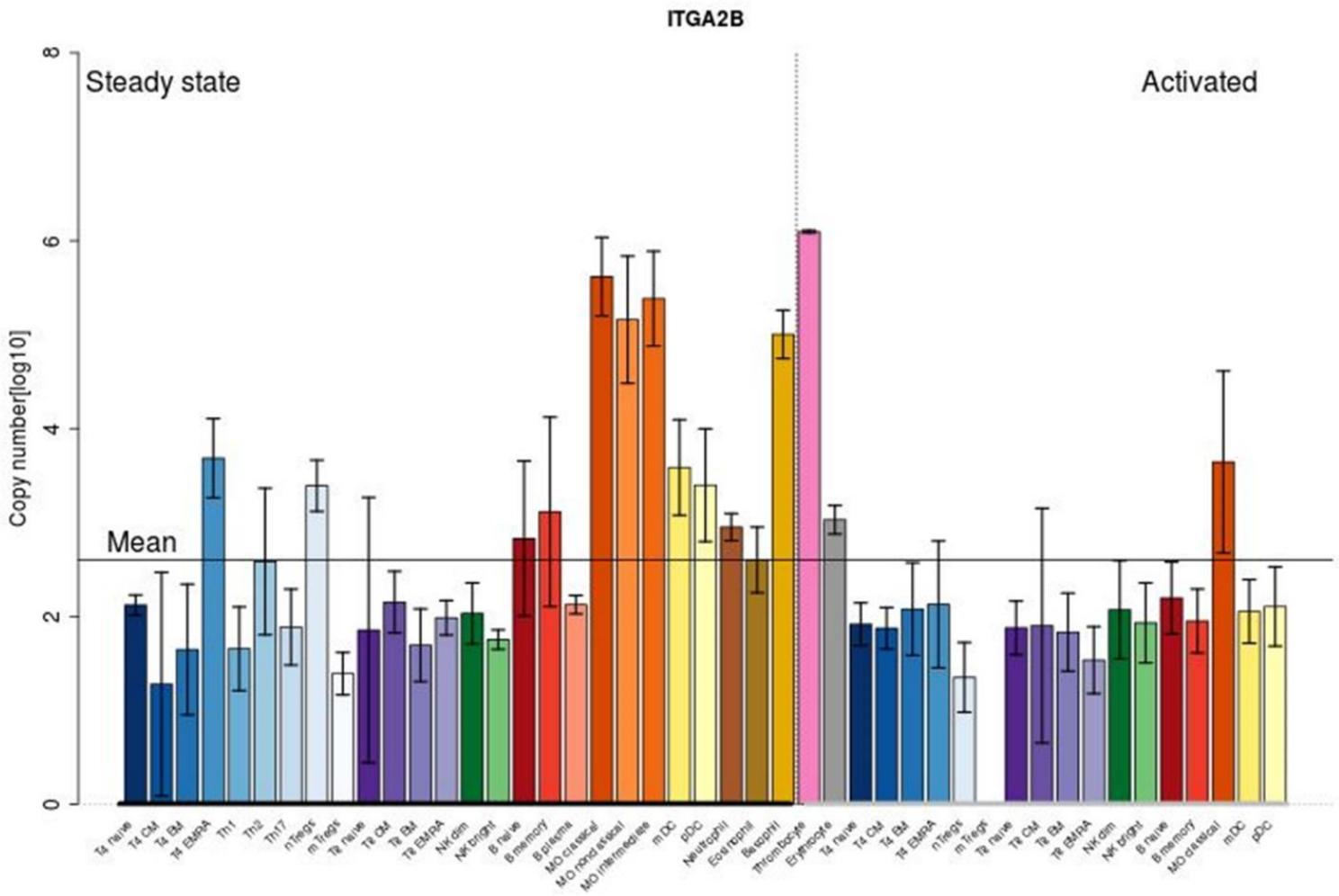

Figure 2.7. *An image collected as part of the Immprot study (Rieckmann et al., 2017) which characterised 28 primary human hematopoietic cell populations in both steady state and activated steps using high-resolution mass-spectrometry-based proteomics. This image features cells which feature CD41a in their proteome.*

Additionally, CD41a is used as part of the EV-TERA-P kit as a platelet marker, as it is frequently regarded as such (Mutreja *et al*., 2017). However, it is becoming more apparently that CD41 is not a unique to platelets. The Immprot database (Rieckmann et al., *2017)* features shared data of more than 300 studies, focusing on biomarkers identified on different types of cells. The Immprot database comprises single analysis of sorted cells by quantitative proteomics. Although thrombocytes have the highest concentration of CD41 [Figure 2.7], high levels of CD41 were identified on several types of monocytes. This indicates that although our research shows a significant difference in the presence of CD41a positive vesicles between platelet poor plasma and platelet free plasma, it does not necessarily mean the source of these is platelets.

2.6. Conclusion

Based on the findings in this study, it can be proposed that there is a significant release of sEVs during high intensity interval exercise. There is a significant increase in tetraspanin-positive sEVs post-exercise in both platelet poor and platelet free plasma. This recapitulates previous findings that showed an increase in sEVs post exercising using platelet poor plasma. These findings also confirm the single particle immunofluorescence array is a useful tool to calculate sEV numbers in the wider context of chronic exercise and ageing.

Chapter 3 -

Quantitative proteomics of the sEV proteome in the context of cellular senescence

3.1. Abstract

Purpose

Small extracellular vesicles have been previously shown to be released as part of the senescence-associated secretory phenotype, and may modulate senescent burden, A universal biomarker for senescence would be extremely beneficial as it could allow for quantification of biological ageing. This could aid in early detection and prevention of ageing related diseases.

Methods

Three models of senescence were induced in BJ-5ta cells: mitochondrial dysfunction associated senescence using antimycin A, oxidative stress induced senescence using hydrogen peroxide and oncogene induced senescence using inducible RAS which is activated by 4OHT. sEVs were isolated from conditioned media via ultracentrifugation (110,000 x g for 2 hours at 4°C x2). Samples were then analysed via nano ultra-high performance liquid chromatography-tandem mass spectrometry (nano UHPLC-MS/MS) and processed using MaxQuant. This was followed by a T-test with an S_0 of 0.1 and permutation-based FDR correction $P<0.05$.

Results

Senescence was confirmed in each model with a significant increase in phospho-histone h2aX and p16-INK4A. Senescence induced a pronounced increase in the abundance of proteins in sEVs with 991, 409, and 49 proteins increasing in response to mitochondrial dysfunction associated senescence, oxidative stress induced senescence and oncogene induced senescence respectively. Gene ontology enrichment also showed an increase in enrichment of genes associated with senescence.

Union of these significantly affected proteins identified seven potential biomarkers of senescence.

Conclusion

Senescence induced large changes in the sEV proteome. NIT2, CARS, EEF1A2, GSTO1, PGAM 1, PGAM 2 and NAMPT were identified as candidate universal markers of senescence.

3.2.1. Introduction

First proposed in 1961 (Hayflick and Moorhead), senescence was identified to trigger cells to enter and remain in the arrest phase of the cell-cycle. Cellular senescence is a biological process which plays a physiological role within embryonic morphogenesis and tissue homeostasis, making it imperative for normal development. Although senescence is important biologically, especially in early life and in tumour suppression, it is also associated with poor health outcomes (Seitz-Holland et al., 2023). Senescent cells begin to accumulate, mainly within renewable tissues and within tissues which have experienced inflammation for a prolonged time during the ageing process (Dimri et al., 1995).

Senescence is triggered by a multitude of factors such as cytoplasmic chromatin fragments, DNA damage, mitochondrial dysfunction, telomere shortening, Reactive Oxygen Species (ROS) and Senescence-associated β Galactosidase Activity. These are all processes which occur naturally during biological ageing (Mylonas and O'Loghlen, 2022). Although there are many molecular mechanisms which have an impact on biological ageing, senescence plays a significant role (Di Micco et al., 2021). Of note, the senescence phenotype has been shown to play a role within a variety of ageing-related diseases such as osteoarthritis, atherosclerosis, and Alzheimer's disease (McHugh and Gil, 2018). Senescence is heavily associated with increased frailty, showing that senescent burden is associated with biological ageing, not just the development of ageing related diseases and disorders (Boccardi and Mecocci, 2020). Frailty is a clinical syndrome, typically observed in older adults. Characteristics include weight loss, exhaustion, slowness, low physical activity, and weakness (Xue, 2011).

Frailty is heavily associated with systemic inflammation, a key trigger of cellular senescence. Senescent cells release inflammatory factors such as TNF-alpha and IL-6, leading to a long-term chronic state of inflammation which is a precursor to frailty (Sathyan et al., 2020). This senescence leads to further inflammation, and the eventual deterioration of mental and motor function, further increasing the frailty of the patient (Marcozzi et al., 2023).

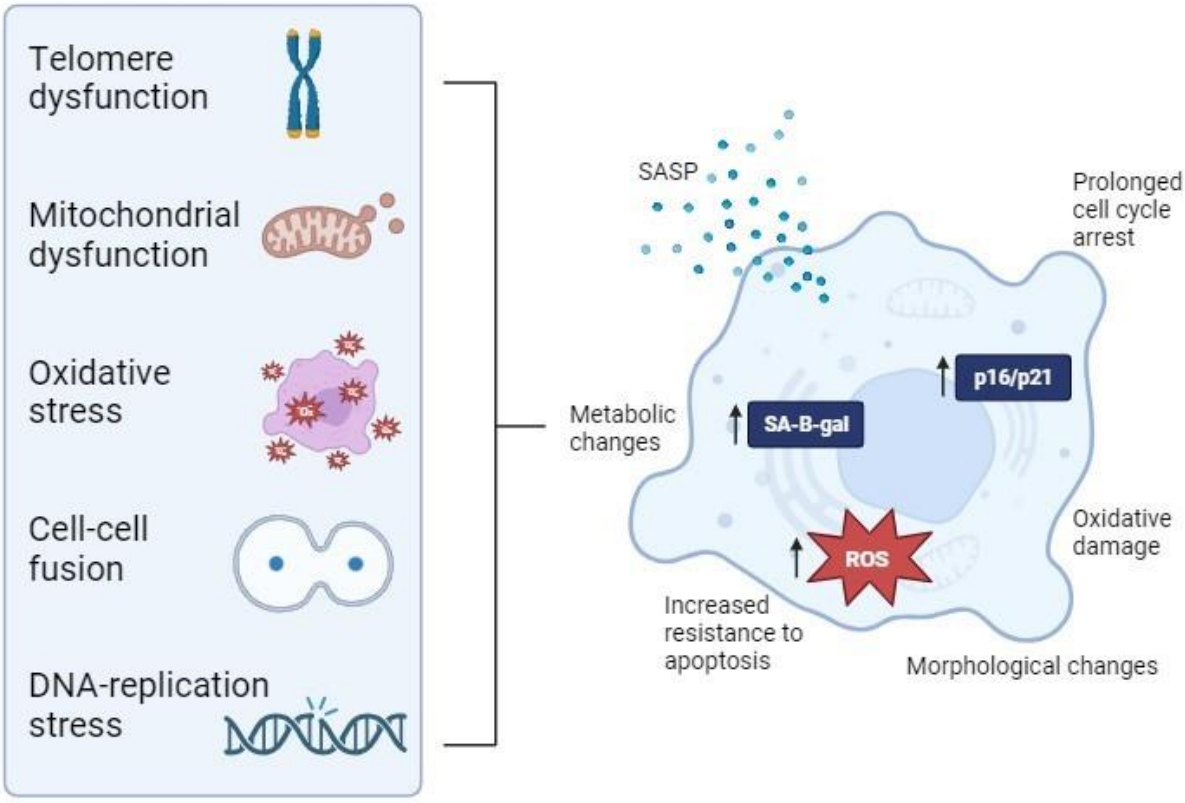

Figure 3.1. *An overview of senescence induces and the changes in cell physiology they trigger when accumulated.*

3.2.2. Senescence-associated secretory phenotype

Senescence leads to changes to the cellular microenvironment such as changes in gene expression (Kumari and Jat, 2021). These changes eventually lead to the senescence-associated secretory phenotype (SASP) (Wallis et al., 2020). The SASP is

characterised by the release of soluble signalling factors, secreted proteases, and insoluble proteins/extracellular matrix components (Coppé et al., 2010). A key reason for the interest in senescence with relation to sEVs is that senescent cells release sEVs which are capable of inducing senescence in nearby cells, termed paracrine senescence (Lehmann et al., 2008, Kavanagh et al., 2017, Takasugi et al., 2022). This suggests that sEVs can modulate senescent burden, making it worthwhile to study them for markers of senescence. It is well established that senescent cells release more sEVs, with these senescent sEVs triggering senescence in neighbouring cells (Marcozzi et al., 2023). These so called senescent sEVs have repetedly been shown to different phenotypically to their non-senescent counterparts (Buratta et al., 2017, Jeon et al., 2019, Alibhai et al., 2020, Fafián-Labora and O'Loghlen, 2021), but the biological purpose and specific composition changes are not fully understood. Although research is increasing to identify potential biomarkers for senescent burden (Buratta et al., 2017, Jeon et al., 2019, Alibhai et al., 2020, Fafián-Labora and O'Loghlen, 2021), no specific indicator of senescent burden which can be identified as part of a liquid biopsy has yet been confirmed. A liquid biopsy in this context refers to the detection of potential senescent biomarkers using patient blood or urine samples (Domen et al., 2022).

3.2.3. Biomarkers of Senescence

There have been several attempts to identify biomarkers of senescence, but these are not perfect. The most commonly used is Senescence-Associated B-Galactosidase (SA-β-gal), a hydrolase enzyme that is often cited as being found only in senescent cells. The marker is detectable in most types of senescent cell, and is infrequently found in immortal, transformed, quiescent or pre-senescent cells. SA-β-gal is however found in

overconfluent cells within tissue culture and cells which have been serum-starved. Additionally, they have also been shown to be found within some macrophages and in some post-mitotic cells (de Mera-Rodríguez et al., 2021), meaning it may not be specific markers of senescence.

Another well regarded marker of senescence is $p16^{ink4a}$. P16 is a kinase inhibitor that is found within the p53 tumour suppressor pathway. It is found to accumulate in senescent cells. In particular, p16 is used as a senescent marker in senescent tissues and cultured cells. However, p16 is not expressed ubiquitously, meaning it may not be suitable as a general senescent marker (Safwan-Zaiter et al., 2022). P16 is also found to be highly expression in some tumour cell lines, meaning it may register these cells as senescence incorrectly. Phosphorylated H2A histone family member X (γ-H2AX) is another commonly used marker of senescence. Histone γ-H2AX is associated with telomere shortening and double-stranded DNA breaks. The concern with using γ-H2AX as a biomarker of senescence is that it may not be specific to senescence. For example, telomere dysfunction may be reversible, and thus may not reflect senescence (Epel, 2012). Additionally, γ-H2AX is associated with ionizing radiation, meaning it may not be an appropriate marker when a radiation model is used (Redon et al., 2009). Additionally, these markers of senescence are useful for analysis of senescent cells, usually via lysates (Bernadotte et al., 2016, Safwan-Zaiter et al., 2022). Having a soluble biomarker, or one enclosed within an sEV would be more practical in a clinical setting as they could be used for liquid biopsies.

The identification of a biomarker for senescent burden would be extremely beneficial for many reasons. It would allow for the early detection and prevention of ageing related conditions, allow for the prediction of healthspan and longevity, and the quantification of biological ageing.

The identification of universal senescence biomarkers is dampened by the fact these markers may differ by the initial trigger of senescence. It is for this reason that we choose to use multiple methods of inducing senescence for this study.

3.2.4. Proteomics to identify a biomarker of senescence.

Proteomic techniques are used to create high-resolution, large mass-spectrometric data sets and can be used with several different labelling techniques, including label-free quantification (Tyanova et al., 2016). The key benefit of quantitative proteomics is that is facilities a hypothesis free, unbiased appreciation of the array of proteins contained in sEVs. This accelerates discovery in comparison to hypothesis driven approaches which require pre-selected proteins to be targeted.

The benefits in quantitative proteomics are strengthened by programmes such as Perseus which allow us to meet several bioinformatic needs: Exploratory analysis and normalisation, data integration, statistical analysis, visualisation, and any other specialised tools. Perseus is particularly useful for its ability to provide statistical analysis within the software, allowing for the comparison of proteins between conditions. Different sets of data can also be overlaid on top of each other, allowing for identification of proteins which correlate between different samples or different

conditions. A great advantage of this data-driven approach is that data can be shared and made available on public repositories such as PRIDE (Perez-Riverol et al., 2021).

3.2.3. Aims

- To induce senescence in BJ-5ta fibroblasts via mitochondrial dysfunction, oxidative stress and via the activation of the Ras oncogene; and
- to further investigate the proteome of sEVs released from said senescent models as part of the senescence-associated secretory phenotype (SASP) using mass spectrometry; and
- identify candidate markers of senescence.

3.3. Methods

3.3.1. Cell Culture Protocols

For this study, it was decided that fibroblasts would be the most appropriate cell type for this study. Fibroblasts are common models of senescence as they show morphological and phenotypic changes in response to senescence, meaning it is possible to clearly identify that senescence has been induced (Chen, Li and Tollesbol, 2013.. Additionally, fibroblasts release large amounts of vesicles in response to senescence, providing the required protein levels (Zou et al., 2022). For this reason, BJ-5ta fibroblasts were used in accordance with a well-established protocol to induce senescence in vitro (Neri et al., 2021). The selected methods of inducing senescence were:

- Mitochondrial Dysfunction-Associated Senescence (MiDaS) via Antimycin A
- Oxidative Stress-Induced Senescence (OSIS) via Hydrogen peroxide

- Oncogene-induced senescence (OIS) via 4-hydroxytamoxifen (4OHT) activation of the Ras pathway

Cells were seeded and cultured in DMEM containing 10% FCS, 1% Glutamine supplement and Penicillin-Streptomycin. Any deviations for inducing senescence are noted in **Table 3.1.**

30 separate T175 flasks with a total cell count of 2 x 10^6 fibroblasts were seeded:

- 5 for antimycin-A condition and 5 for the corresponding DMEM media control
- 5 for hydrogen peroxide condition and 5 for the corresponding carrier control (DMSO)
- 5 for 4-OHT condition and 5 for the corresponding carrier control (ethanol)

The protocol for this can be found in figure 3.2.

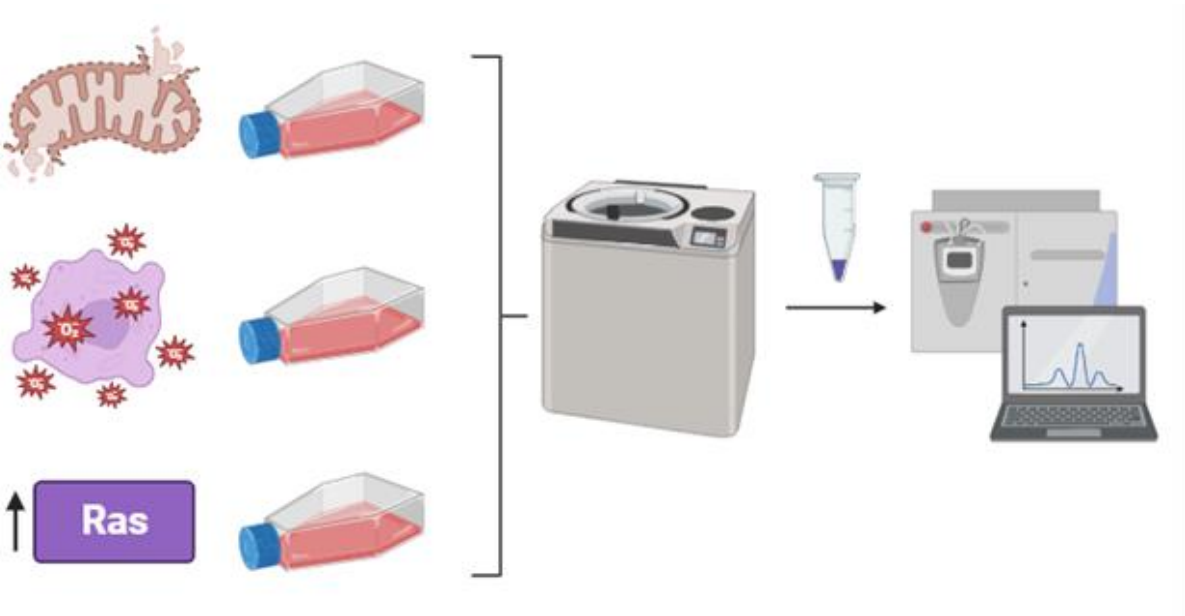

Figure 3.2. *Senescence is induced within the cells via mitochondrial dysfunction, oxidative stress, and oncogene. sEVs were then isolated from conditioned media using UC and analysed using nano UHPLC-MS/MS.*

Table 3.1 **|** *The protocol for each method of inducing senescence in BJ-5ta cells and the corresponding control.*

	INITIAL CONDITION	TREATMENT	SPLIT	MEDIA COLLECTION
MITOCHONDRIAL DYSFUNCTION-ASSOCIATED SENESCENCE	BJ-5ta fibroblasts were seeded in 5 separate T175 flasks at a density of 2 x 10^6 fibroblasts.	Antimycin A at a concentration of 250nm was added to the media on days 2,4,6 and 8.		Media was changed to serum free on day 9. Media is collected and frozen at -20°C on day 11.
OXIDATIVE STRESS-INDUCED SENESCENCE	BJ-5ta fibroblasts were seeded in 5 separate T175 flasks at a density of 2 x 10^6 fibroblasts.	Days 2 and 7, cells are treated with a hydrogen peroxide solution with a final concentration of 300nm, diluted in DMSO, for 2 hours. They are then washed with a pre-prepared media.	On day 6, cells were split at a density of 2 x 10^6	Media was changed to serum free on day 9. Media was collected and frozen at -20°C on day 11.
ONCOGENE INDUCED SENESCENCE	BJ-5ta fibroblasts were seeded in 5 separate T175 flasks at a density of 2 x 10^6 fibroblasts. 4-OHT was dissolved in ethanol, and added to DMEM Complete Media, to a final concentration of 333nM.	Every second day, the culture media was replenished with fresh DMEM Complete Media containing 4-OHT, for a total of 17 days		Media was changed to serum free on day 17. Media is collected and frozen at -20°C on day 19.
DMEM COMPLETE MEDIA (CONTROL)	BJ-5ta fibroblasts were seeded in 5 separate T175 flasks at a density of 2 x 10^6 fibroblasts.	Media was changed on days 2, 6 and 8.	On day 7, cells were split at a density of 2 x 10^6	Media was changed to serum free on day 9. Media was collected and frozen at -20°C on day 11.

DMSO MEDIA (CONTROL)	BJ-5ta fibroblasts were seeded in 5 separate T175 flasks at a density of 2 x 10^6 fibroblasts.	Media was changed on days 2, 6 and 8.	On day 7, cells were split at a density of 2 x 10^6	Media was changed to serum free on day 9. Media was collected and frozen at -20°C on day 11.
ETHANOL TREATED MEDIA (CONTROL)	BJ-5ta fibroblasts were seeded in 5 separate T175 flasks at a density of 2 x 10^6 fibroblasts.	Every second day, the culture media was replenished with fresh DMEM Complete Media containing ethanol, for a total of 17 days	On day 15, cells were split at a density of 2 x 10^6	Media was changed to serum free on day 17. Media is collected and frozen at -20°C on day 19.

3.3.2. Lysates

Cell lysates were collected on the final day of each experiment to validate senescence. Flasks were placed on ice, and cells were washed with ice-cold PBS. 2ml of Ice-cold lysis buffer (25 mM Tris-HCl, pH 7.6, 150 mM NaCl, 1% NP-40,1% sodium deoxycholate, 0.1% SDS) was added to flasks. Flasks were then incubated for 20 minutes on ice, and cells scraped from the surface. Resulting lysate was then added to microfuge tubes and centrifuged for 10 minutes at 12,000 x g at 4°C. The supernatant was retained and frozen at -80°C.

3.3.3. Western Blotting

3.3.3.1. Protein Assay and sample preparation

The Protein Assay was completed in accordance with the provided instruction manual (https://www.bio-rad.com/webroot/web/pdf/lsr/literature/LIT448.pdf). Absorbances were read at 750nm using the FLUOstar OMEGA microplate reader.

3.3.3.2. Gel Electrophoresis

To run the sodium dodecyl sulphate-polyacrylamide gel electrophoresis (SDS-PAGE), 10µg of isolated sEV protein was prepared in x1 Laemmli buffer (ThermoFisher Scientific, Leicestershire, UK), and loaded into 4% - 12% Bis/Tris precast gels (Bio-Rad Laboratories, Watford, UK). Gels were ran using a PowerPac HC High-Current Power Supply (Bio-Rad Laboratories, Watford, UK) in 1x MOPS buffer (ThermoFisher Scientific, Leicestershire, UK) for approximately 90 minutes at 130V.

3.3.3.3. Transfer and Blocking

Using the wet transfer method, proteins were transferred onto Immobilon-P PVDF membranes (Merck-Millipore, Hertfordshire, UK) for 1 hour at 100V. The PVDF membrane was blocked in 3% Bovine Serum Albumin (BSA) in TBS-T (20mM Tris-

base 7.5, 137mM sodium chloride, 0.1% (v/v) Tween-20) for an hour whilst rocking.

3.3.3.4. Primary Antibody

Primary antibodies were diluted in TBST with 3% Bovine Serum Albumin. The membranes were then rocked overnight at 4°C in the relevant primary antibody.

3.3.3.5. Secondary Antibody

The primary antibody is removed and retained. Membranes were washed in TBST, and then incubated with their relevant secondary antibodies whilst rocking at room temperature for one hour. Membranes were then washed in TBST.

The following primary and secondary antibodies were used for analysis.

Table 3.2 | Antibody details

Antibody	Dilution	Source	Manufacturer	Catalogue no.
Histone H2A X (S139)	1:1000	Rabbit	Cell Signalling	#9719
p16 INK4A (D7C1M)	1:1000	Rabbit	Cell Signalling	#80772
Anti-Rabbit IgG	1:1000	Goat	CST	#7074

3.3.3.6. Imaging

Membranes were imaged using a G: BOX Chemi XT4 imager, using GeneSys capture software (Syngene, Cambridge, UK). Manual band quantifications were performed, and corrections were completed to remove the effects of background signal using Fiji/ImageJ (National Institutes of Health, USA).

3.3.4. Quantitative proteomic sample prep

sEVs were isolated with two centrifugal spins of 110,000 x g for 2 hours at 4°C. 5µg of sample were added to a LoBind tube (Eppendorf, Hamburg, Germany). Lysis buffer (0.1M HEPES ph 8.0, 6M UREA, 2M Thiourea) was added to reach a reagent

total of 10µl.This was followed by reduction with DTT (Fisherscientific, A39255) and alkylation with iodoacetamide (Thermofisher, A39271). Samples were then digested with LysC and underwent acidification with 1% TFA. The samples were then loaded into equilibrated SDB-RPS tips (Rappsilber et al., 2007) and peptides eluted in three different fractions. Samples were then dried on a SpeedVac (Eppendorf, Hamburg, Germany) for ~40 minutes at 45°C. Further details can be found in **Chapter 6: General Methods**

3.3.5. Mass Spectrometry

Samples were analysed by nano ultra-high performance liquid chromatography-tandem mass spectrometry (nano UHPLC-MS/MS) using the Q Exactive HF-X Hybrid Quadrupole-Orbitrap system (ThermoFisher Scientific, Brisbane, Australia). Resuspended samples were run in DDA mode, selecting the top 20 most intense peptide ions, using a 120min linear gradient at a flow rate of 200nl/min. MS spectra were acquired at a resolution of 70,000, m/z scan range between 300 to 1650, and a target value of $3e^6$ ions. Raw files were searched against the human UniProt database using MaxQuant (Cox and Mann, 2008) at an FDR of 0.01 with variable (Oxidation (M), Acetyl (Protein N Term) and fixed (carbamidomethyl (C)) modifications. Protein quantification was performed using the label free algorithm and match between runs enabled to maximise proteomic coverage (Cox et al., 2014).

3.3.6. Bioinformatics analysis

Proteomic samples were analysed using Perseus v1.6.15.0 (Tyanova et al., 2016). Data was filtered to remove proteins identified only by modification site, probable contaminants and protein sequences which matched artificially generated decoy

sequences. Each row representing a protein were then filtered based on valid values, requiring 2 positive values (40%) for each protein in each group (per model). Data were normalised to the median of the control condition in each model. Following log^2 transformation and visual check for normal distribution [Figure 3.4], data were analysed via Two sample T tests with an S_0 of 0.1 and permutation-based FDR correction P<0.05. Gene ontology enrichment was also completed on the proteins which were shown to be significantly increased in the senescent markers. This was done by comparing which proteins were significantly enriched in the senescence models against the proteins within the relevant control.

Significantly increased proteins from each model were then overlaid against each other to identify which proteins were significantly increased in all three senescence models. Datasets were uploaded to the same matrices in Perseus, before employing the 'matching row by gene name' function. UniProt Gene identifiers were matched across each dataset, and a final dataset was presented which showed proteins that were significantly increased across all three datasets. The datasets were uploaded to https://bioinformatics.psb.ugent.be/webtools/Venn/ to provide a visual representation of the union between models.

3.4. Results

3.4.1 Validation of senescence

Phospho Histone-H2AX was significantly increased in each treatment when matched to the relevant control: Oncogene-induced senescence (OIS) via 4-hydroxytamoxifen (4OHT) activation of the Ras pathway (*P = 0.0044* **), Mitochondrial Dysfunction-Associated Senescence (MiDaS) via Antimycin A treatment (*P = 0.0077* ***) and Oxidative Stress-Induced Senescence (OSIS) via hyodrogen peroxide (*P = 0.0066*

**). p16-INK4A was also significantly increased in the senescent models of OIS and MiDaS (*P = 0.0456* *, *P = 0.0138* * respectively), whilst OSIS was not (*P = 0.1720*). Due to the presence of at least one senescent marker in each sample, it can be shown that the cell model succesfully reproduced senescence.

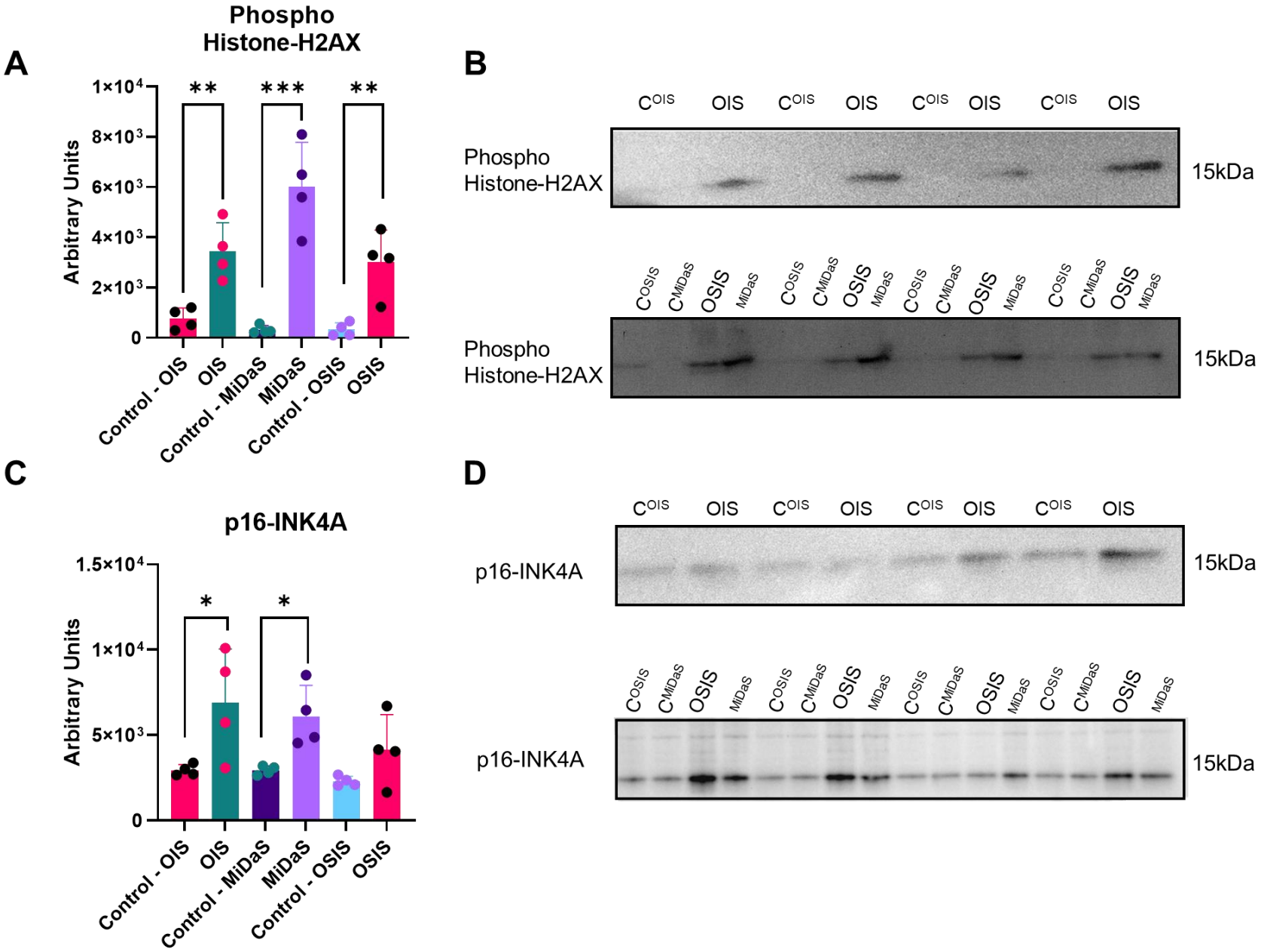
A
Phospho
Histone-H2AX
Arbitrary Units
1×10⁴
8×10³
6×10³
4×10³
2×10³
0
**
***
**
Control - OIS
OIS
Control - MiDaS
MiDaS
Control - OSIS
OSIS
B
C^OIS
OIS
Phospho
Histone-H2AX
15kDa
C^OSIS
C^MiDaS
OSIS
MiDaS
C
p16-INK4A
Arbitrary Units
1.5×10⁴
1×10⁴
5×10³
0
*
*
D
p16-INK4A
15kDa

Figure 3.3. *A). Signalling of phospho-histone h2aX to identify whether the senescent cell model successfully induced senescence. B). Western blots of phospho-histone h2ax in conditioned media from each sample of the senescent cell model. C). Signalling of p16-INK4A to identify whether the senescent cell model successful induced senescence. D). Western blots of p16-INK4A in lysates from each sample of the senescent cell model. Values are presented as individual data points and means +/- SEM. Statistical analysis was conducted using paired t-tests using GraphPad Prism. N = 4. p<0.05 indicated by *, p<0.01 indicated by **, p<0.001 indicated by ***. Key: C^{OIS} = Control for OIS, C^{MiDaS} = Control for MiDaS, C^{OSIS} = Control for OSIS.*

3.4.2. Proteomic analysis of sEVs derived from the SASP

Data was normalised to the median of the control condition of its relevant model, and this was confirmed visually via histogram [Figure 3.4]. Principle component analysis was also completed to identify whether there was clustering of senescent data. This allowed us to identify whether there were likely to be variances within the data in the form of clusters [Figure 3.4]. The oncogene-induced senescence (OIS) model (4OHT) had 3037 total identified proteins within sEVs, the mitochondrial dysfunction-associated senescence (MiDaS) model (Antimycin-A) had 3424 total identified proteins within sEVs, and the oxidative stress-induced senescence (OSIS) model (H_2O_2) had 4086 total identified proteins within sEVs. 991 proteins significantly increased in the OIS model, 409 proteins significantly increased in the MiDaS model, and 49 proteins significantly increased in the OSIS model of senescence [Figure 3.4]. These significantly increased proteins reflect the effect that senescence has on the sEV proteome.

To further understand the significantly increase proteins, the enriched proteins in each senescent model were analysed via gene ontology enrichment against the proteins within the relevant control. All three senescence models showed an increase in senescence-associated pathways such as cellular translation, cell projection assembly and organonitrogen compound biosynthetic processes (OIS), cellular organisation, nucleation and polymerisation (MiDaS) and cellular detoficiation and responses to toxic substances (OSIS).

A.

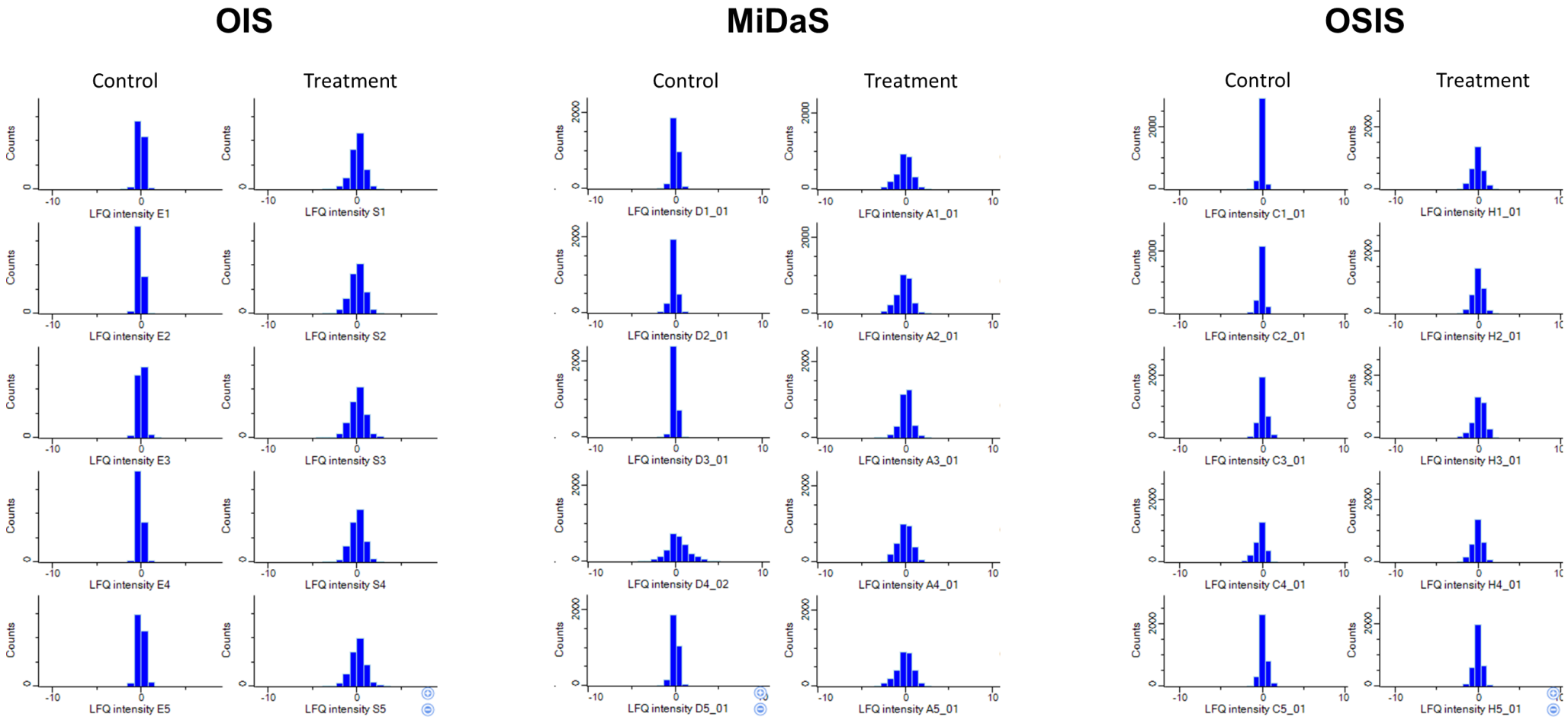
OIS
MiDaS
OSIS
Control
Treatment
Counts
LFQ intensity E1
LFQ intensity S1
LFQ intensity E2
LFQ intensity S2
LFQ intensity E3
LFQ intensity S3
LFQ intensity E4
LFQ intensity S4
LFQ intensity E5
LFQ intensity S5
LFQ intensity D1_01
LFQ intensity A1_01
LFQ intensity D2_01
LFQ intensity A2_01
LFQ intensity D3_01
LFQ intensity A3_01
LFQ intensity D4_02
LFQ intensity A4_01
LFQ intensity D5_01
LFQ intensity A5_01
LFQ intensity C1_01
LFQ intensity H1_01
LFQ intensity C2_01
LFQ intensity H2_01
LFQ intensity C3_01
LFQ intensity H3_01
LFQ intensity C4_01
LFQ intensity H4_01
LFQ intensity C5_01
LFQ intensity H5_01

B.

OIS

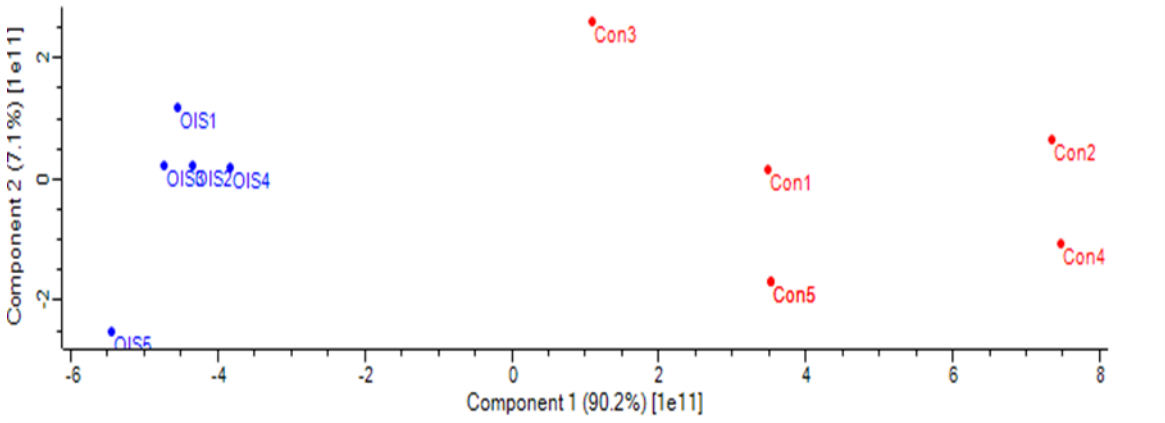

MiDaS

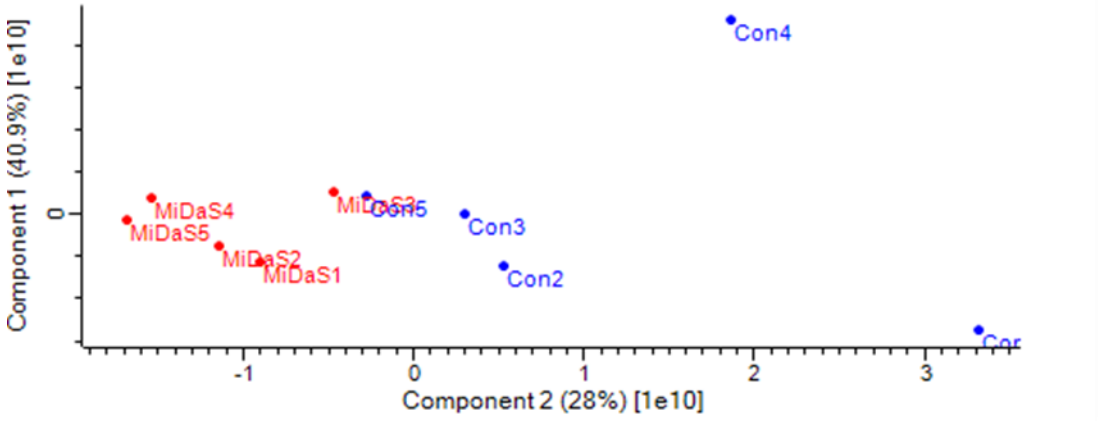

OSIS

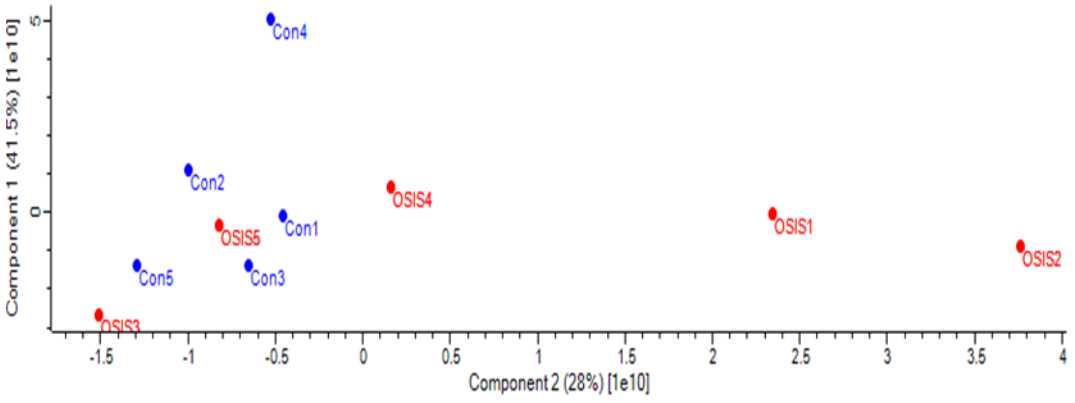

C.

OIS

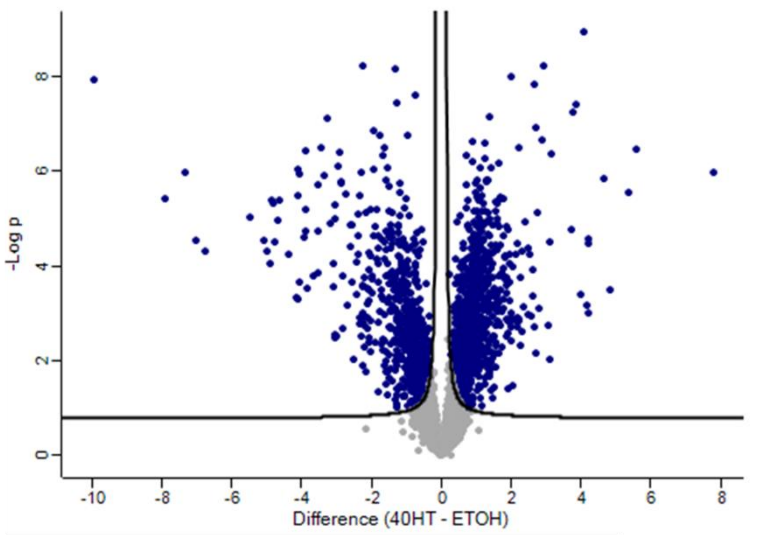

MiDaS

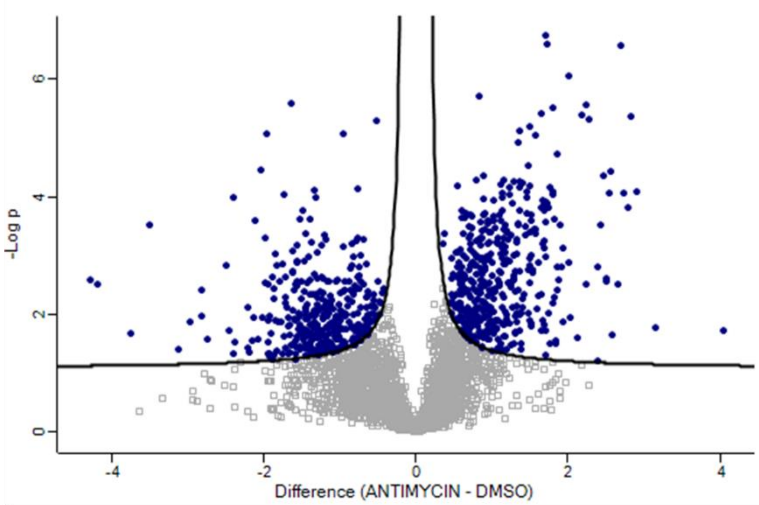

OSIS

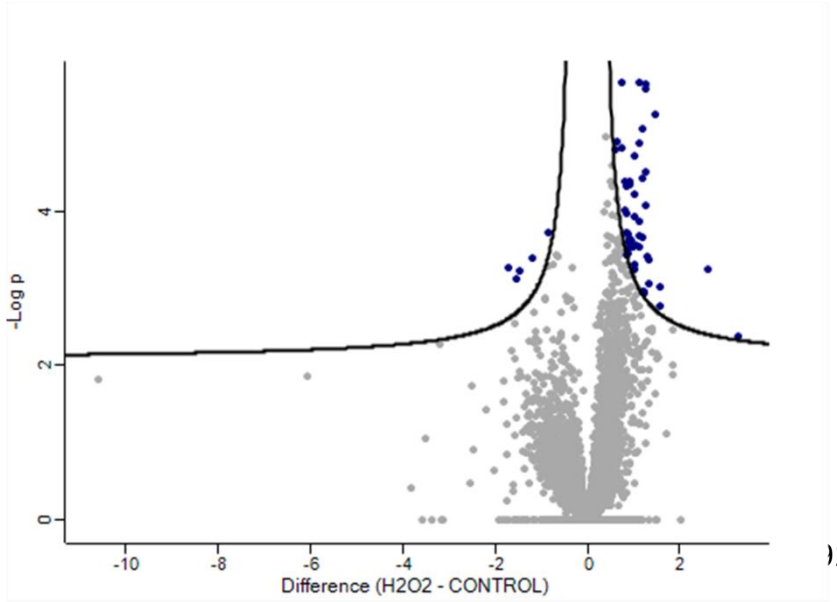

D.

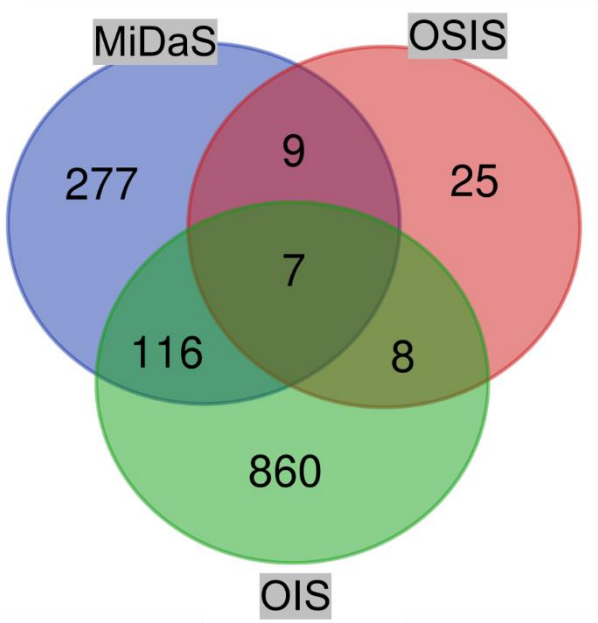

E.

OIS

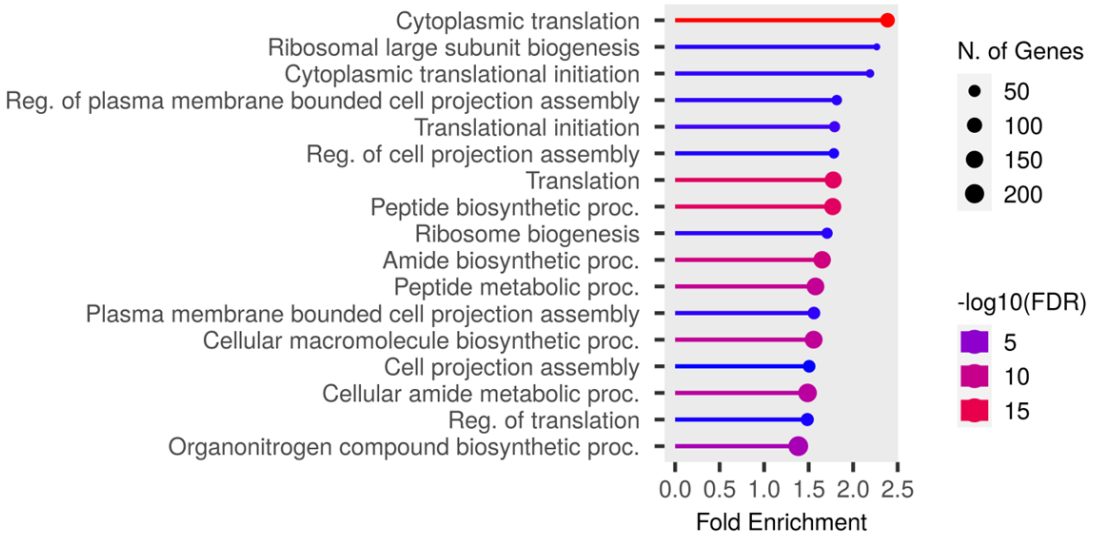

MiDaS

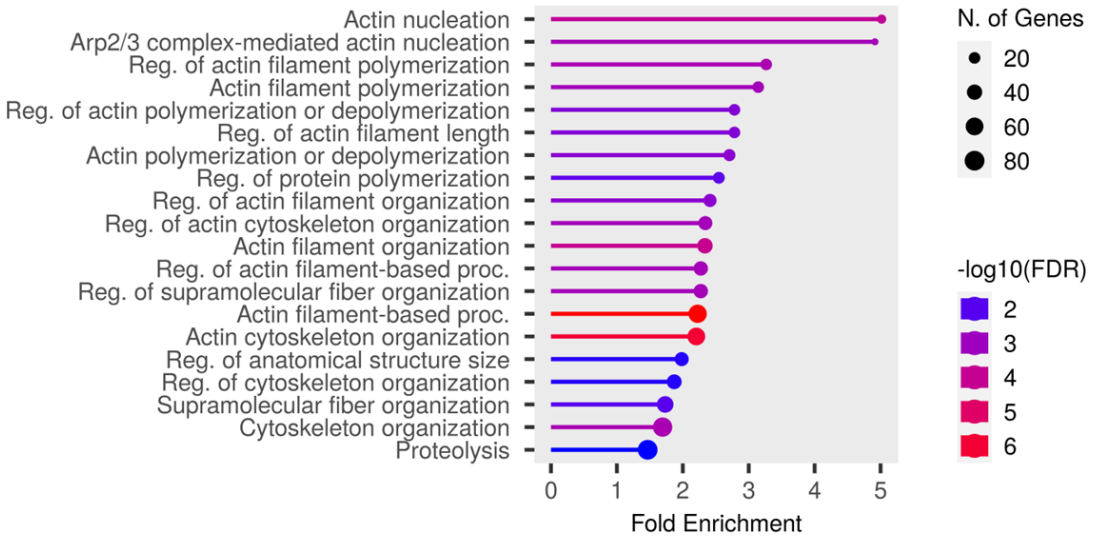

OSIS

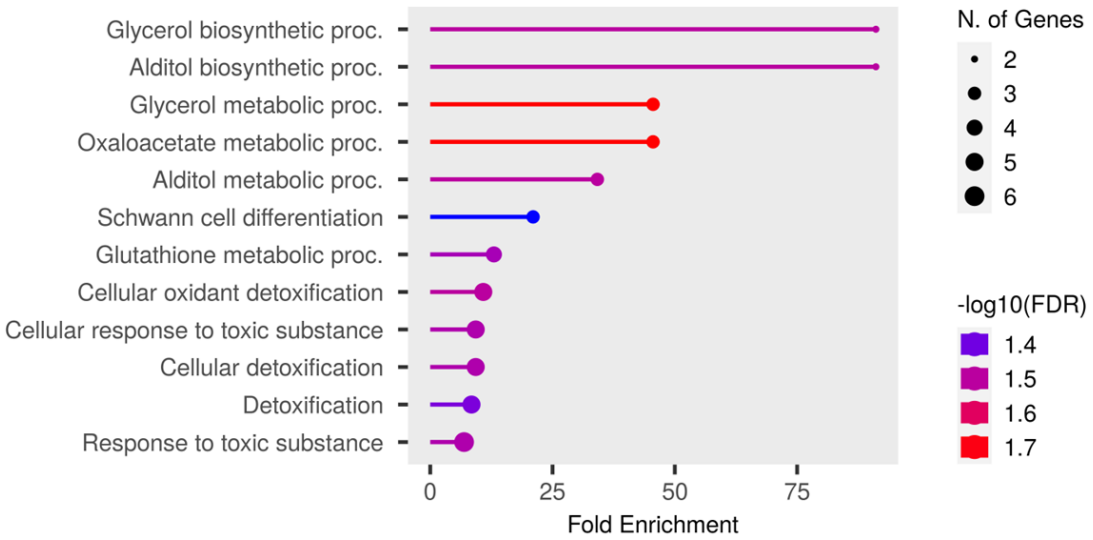

Figure 3.4. *A). Validation that the protein numbers were normalised correctly. B). Principal component analysis of the proteome of sEVs measured in the senescent model and their relevant control. C). Volcano plots showing proteins which statistically decrease, and increase based on comparing an oncogene-induced senescence (OIS) model to a control, a mitochondrial dysfunction-associated senescence (MiDaS) model to a control, and an oxidative stress-induced senescence (OSIS)model to a control. Statistically increased proteins are displayed in blue. Statistical analysis was completed using the Perseus v1. 5. 5. 2. D). An overlay of the significantly increased proteins for each of the three senescence models. E). Gene Oncology enrichment of biological processes associated with the genes which were significantly increased in senescence treated cell models (Ge et al., 2019).*

Table 3.3 **|** *Potential biomarkers identified using an in-house cellular model of senescence and proteomic analysis.*

Gene Symbol	Protein Name
NIT2	Nitrilase Family Member 2
CARS	Cysteinyl-TRNA Synthetase 1
EEF1A2	Eukaryotic Translation Elongation Factor 1 Alpha 2
GSTO1	Glutathione S-Transferase Omega 1
PGAM1	Phosphoglycerate mutase 1
PGAM2	Phosphoglycerate mutase 2
NAMPT	Nicotinamide Phosphoribosyltransferase

Based on the union of these three models of senescence, 7 proteins were positively associated with senescence. It is possible these may serve as potential circulating biomarkers for senescence.

3.5.1 Discussion

sEVs from senescent cells have been shown to induce senescence, but the responsible proteins are unclear. A benefit of this analysis is the potential to propose candidate biomarkers for senescence which could be used in liquid biopsies. These would allow for early detection and prevention of ageing related conditions, allow for the prediction of healthspan and longevity and allow quantification of biological ageing. Therefore, we carried out unbiased assessment of proteins released in sEVs using three senescent models: mitochondrial dysfunction associated senescence (MiDaS), oxidative stress induced senescence (OSIS), and oncogene induced senescence (OIS).

sEVs from these models were isolated using ultracentrifugation and then analysed using nano ultra-high performance liquid chromatography-tandem mass spectrometry

(nano UHPLC-MS/MS). Lysates from these cellular models were probed for p16-INK4A and phospho-histone h2aX to identify whether the models were indeed senescent. These markers were selected due to their standing as well-established markers of cellular senescence as they can be found within senescent lysates (Rayess et al., 2012, Merighi et al., 2021). Once the senescence models were overlaid onto one another using their UniProt ID, seven potential biomarkers for senescence were identified: NIT2, CARS, EEF1A2, GSTO1, PGAM 1, PGAM 2 and NAMPT.

In our study, there were large increases in sEV derived proteins in each senescent model: 991 proteins significantly increased in the OIS model, 409 proteins significantly increased in the MiDaS model, and 49 proteins significantly increased in the OSIS model of senescence. This is much wider coverage than other studies focusing on sEVs as mediators of senescence were able to achieve (Borghesan et al., 2019, Basisty et al., 2020). Borghesan identified an increase in 310 proteins in response to DNA damage associated senescence, and an increase in 343 proteins in response to ionizing radiation associated senescence. Basisty induced senescence via two models: iRAS and iRR models of senescence, which had 42 significantly increased proteins and 520 significantly increased proteins respectively. These studies proposed interferon-induced transmembrane protein 3 (Borghesan et al., 2019), growth/differentiation factor 15 (GDF15), stanniocalcin 1 (STC1) and serine protease inhibitors (SERPINs) (Basisty et al., 2020). None of these potential markers were identified as potential candidates within our own models. Borghesan (et al., 2019) isolated sEVs using a combination of SEC and UC, Batisty et al., 2020 used UC. As with any isolation method, there may in

consistencies or damage caused to the vesicles. This may have an impact of any results. Additionally, these models may not have been as senescent as our own model. Each of these models of senescence were validated using SA-β-gal staining (Borghesan *et al.,* 2019; Basisty *et al.,* 2020).

Interestingly, of the 7 proteins we associated with senescence, 4 of them were significantly increased in plasma samples taken from a large cohort of participants taken across the lifespan (Lehallier et al., 2019): CARS, NAMPT, PGAM, GSTO1.

CARS (Cysteinyl-tRNA synthetase 1) is an enzyme that is essential for protein synthesis (Kamtekar et al., 2003). Although no specific mechanism for the impact CARS has on senescence has been identified, it is well known that there is disruption to protein synthesis during the ageing process (Anisimova et al., 2018). CARS is also associated with several types of senescence related cancers (Sung et al., 2022) and is known to be able to induce cell death (Zhang et al., 2022). NAMPT (Nicotinamide Phosphoribosyltransferase) is a metabolic enzyme which is an endogenous mediator of inflammation. NAMPT is a modulator of inflammation, which is released to induce NAD biosynthesis and reduced further inflammation (Audrito et al., 2020). This response has been linked to senescent related diseases such as obesity, diabetes, and cancer. NAMPT has previously been found to be increased both within senescence cells and in sEVs released as part of the SASP (Kuehnemann et al., 2022). GSTO1 is the first of the omega class glutathione transferases, which are within the cytosolic glutathione transferase superfamily. Despite being in the GST family, GSTOs have distinctive biological attributes compared to the rest of the family (Board and Menon, 2016).

GSTO1 is linked to inflammation and is critical in the TLR4-like pro inflammatory response (Menon et al., 2017) which is heavily associated with the SASP (Hari et al., 2019). An example of this link to inflammation in a senescence related disorder is that GSTO1 is shown to be increased not only during active Alzheimer's (Allen et al., 2012), but also prior to the onset of symptoms (Umlauf et al., 2016). GSTO1 has also been shown to increase with age in mice. Interestingly, GSTO1 begins to reduce again once the mice are approaching being elderly, but this reduction is still an increase on GSTO1 within young mice (Xu et al., 2018). Phosphoglycerate mutase (PGAM) have two subunits: PGAM 1 and PGAM 2. It is the catalyst used in the glycolytic pathway (3-PGA to 2-PGA). When PGAM was increased in a cellular model, the capacity of respiration by isolated mitochondria was decreased, and the generation of reactive oxygen species were significantly increase (Okuda et al., 2013). Another interesting role of PGAM is its role within the Warburg effect (Mikawa et al., 2020). The Warburg effect is the manner in which cancer cells can increase their rate of glucose uptake and utilise lactate production in the presence of oxygen (Liberti and Locasale, 2016). The Warburg effect has been shown to occur in ageing non-cancerous cells (Morris et al., 2020), making PGAM interesting from a biological ageing perspective. As a key benefit of the use of this style of proteomics is the public availability of published datasets, it is planned that the data from these models were created will be published on the PRIDE Archive (PRoteomics IDEntifications Database) (Perez-Riverol et al., 2021) once published.

3.5.2. Limitations

When compared to both the MiDaS and the OIS models, the OSIS model has both lower overall protein counts, and significantly increased proteins found within the sEVs. When considering this and the western blot quantification of senescence, it is apparent that there may have been less senescence in this model than the other two models. This may be a limitation as proteins which may have been released from a more senescent model may be missed. However, this could also be considered a benefit as it will provide a marker for general senescence, rather than an overwhelming senescent burden.

Although there are significant benefits to the use of cell models, such as the ability to harvest large amounts of vesicles and the ability to control for different types of senescence, there are cons to the use of cellular models. In addition to the aforementioned isolation and purification challenges, there is also the lack of in vivo complexity to consider. Vesicle behaviour may differ in vivo than they would within a complex biological system like would appear within a human (Yáñez-Mó et al., 2015). This could mean that key molecular interactions may not be accounted for. Additionally, cellular models limit representation of heterogeneity within sEVs (Altschuler and Wu, 2010). Cellular models also provide a statistic environment, which would not be representative of what occurs within humans. It could also be of interest to attempt to replicate this study using muscle-derived cells, either in the form of C2C12 myotubes or Primary Human Skeletal Muscle Cells. This could provide data concerning how senescence could impact muscle-derived sEV release.

As with any work which requires sEV isolation, the decision had to be made as to which isolation method was suitable. Ultracentrifugation was selected. UC may not isolate pure sEVs, but all of our candidate biomarkers appear on the Vesiclepedia database (Pathan et al., 2019), showing that they are present in sEVs. Also, as the sEVs are isolated from conditioned media, they are less likely to contain contaminants than biofluids such as plasma would.

There is also a need to validate these proposed markers of senescence. This would be achieved by completing targetted analysis on a very large patient population to determine whether the markers are present in circulating sEVs dependent on age.

3.6. Conclusion

Three models of inducing senescence were used to create a high coverage proteomic resource of sEV changes in the context of senescence. In all three models of senescence, proteomic changes between the control and the senescent model noted were large. NIT2, CARS, EEF1A2, GSTO1, PGAM 1, PGAM 2 and NAMPT are all candidates for universal markers of senescence, with CARS, GSTO1, NAMPT and PGAM positively associated with ageing. These require further validation as universal markers of senescence.

Chapter 4 -

Single vesicle and proteomic analysis of circulating sEVs in relation to ageing and chronic exercise

4.1 Abstract

Purpose

There is mixed evidence concerning both the quantitative changes of circulating sEVs associated with ageing and the corresponding sEV proteome due to the lack of gold standard for isolation of sEVs. Determining whether ageing and a history of chronic exercise is responsible for changes to the numbers of, and the proteomic cargo of circulating sEVs will be a useful step in uncovering the molecular mechanisms of these processes.

Methods

Single EV particle analysis was used to determine counts of tetraspanin-positive extracellular vesicles. EDTA-treated blood was collected from young participants (20.0 ± 2.8), older participants (69.8 ± 4.1) and Masters athletes (67.1 ± 6.4) (N=12). Plasma was isolated for single EV particle analysis (3000 x g for 10 minutes at 4°C) and sEVs were isolated for proteomic analysis via ultracentrifugation (110,000 x g for 2 hours at 4°C x2). Samples were then analysed via nano ultra-high performance liquid chromatography-tandem mass spectrometry (nano UHPLC-MS/MS), followed by an ANOVA with an S_0 of 0.1 and permutation-based FDR correction $P<0.05$.

Results

There was a significant difference in CD9 positive fluorescent counts in older adults compared to the young cohort, and a significant decrease in the CD9 positive mean fluorescence intensity in Masters athletes compared to the young cohort. Otherwise, there were no overarching difference in tetraspanin positive sEV counts between

cohorts. There was not an identifiable large change to the sEV proteomes of these three cohorts, as only four proteins were shown to significantly increase in the older cohort compared to the young: BANF1, ATP1A1, CCT8 and BSG. None of the potential biomarkers of senescence identified in **Chapter 3** were different between groups.

Discussion

Single EV particle array suggests that there is no significant difference between sEV numbers between young, older adults and Masters athletes. Quantitative mass spectrometry-based proteomics also showed a limited effect of age and chronic exercise on the sEV proteome.

4.2.1. Introduction

It is long established that exercise is beneficial to the ageing process, with journal articles from the late 1960s reporting health benefits to those who are elderly and complete regular exercise (Shock, 1967, Lester et al., 1968). Over half a century later, we have a deeper understanding of the large number of molecular pathways involved with both exercise and ageing, with exercise having a positive benefit on areas such as sarcopenia (Lu et al., 2021), cardiovascular health (Chen et al., 2022) and osteoporosis (Watson et al., 2018). As discussed previously, exercise [**Chapter 2]** and senescence [**Chapter 3**] have a large effect on sEV release, suggesting sEVs might inform a combination of these biological processes in participants in a chronic way. There is also evidence that regular cardiovascular exercise is able to reduce senescent burden in CD8+ T cell populations (Donovan et al., 2021, Englund et al., 2021) and in the colon mucosa of older adults (Demaria et al., 2023).

Research quantifying sEVs and how they change with age is currently up for debate due to large variations in the data that have been published. Several groups have reported a decrease in the quantity of circulating sEVs that corresponds with an increased age (Eitan et al., 2017, Rani et al., 2017, Zhang et al., 2017, Alibhai et al., 2020, Zhang et al., 2020)

In contrast, sEVs isolated from human serum from 21 to 92 years olds were found to have no significant change in quantity (Alberro et al., 2016). Another found sEVs increased in elderly participants in comparison to younger participants (Aliquet et al., 2017). Each of these studies used NTA to quantify sEV counts. As discussed previously in **Chapter 1**, NTA is biased by lipoprotein contamination, as they are counted

alongside sEVs due to their size. Brownian methods have been employed within NTA in an attempt to reduce this bias in comparison to methods such as flow cyometry (van der Pol et al., 2014), but NTA is still liable to count lipoproteins within samples, and to produce different data dependent on the user. This difference can be up to 25% between samples (Vestad et al., 2017), which may be a large enough difference to significantly influence results. NTA also requires isolation prior to its use. Although each of these studies used NTA to provide quantitative counts for EVs, they used a variety of isolation methods including ultracentrifugation (Yu et al., 2006; Alberro et al., 2016; Zhang et al., 2017), differential centrifugation (Lehmann et al., 2008); and immunoaffinity methods (Eitan et al., 2017; Rani et al., 2017; Alibhai et al., 2020; Zhang et al., 2020). None of these immunoaffinity methods used single particle EV analysis, instead using fluorescence-activate cell sorting (FACS), which is liable to bias induced by the gating strategy set by the user (Cossarizza et al., 2021).

It remains unclear whether these differences in results occur due to biological differences due to these inconsistencies that arise from NTA, whether it is due to isolation method or whether it is due to differences within the participant populations. In particular, isolation and analysis methods need to be considered as circulating lipoprotein counts are impacted by age (Upmeier et al., 2011, Johnson and Stolzing, 2019), which may impact these reported results.

Studies focusing on the differences in sEV cargo are generally focused on identifying specific markers, rather than a comprehensive proteomic analysis of circulating sEVs.

Eitan (et al., 2017) found MUCIN16 and CD151 within sEVs increased with age. Other significant differences in cargo include a significant decrease in active mitochondria respiration associated cargo with age (Zhang and Jin, 2020) and a reduction in proteins associated with pluripotent stem cell differentiation (Enjeti et al., 2017). There is a clear lack of quality proteomic data focusing on sEVs in circulation in the context of ageing. There is also a lack of data concerning whether the impact of sEV release during acute exercise has an impact on chronic exercise and health ageing. Due to the combination of these aforementioned studies associated sEVs with ageing (Alberro et al., 2016, Alique et al., 2017, Eitan et al., 2017, Rani et al., 2017, Zhang et al., 2017, Alibhai et al., 2020, Zhang and Jin, 2020), as well as previous research indicating that senescence (Coppé et al., 2010, Mato-Basalo et al., 2022) and exercise (Frühbeis et al., 2015, Guescini et al., 2015, Whitham et al., 2018, Brahmer et al., 2019) alter sEVs, it stands to reason that sEVs may be implicated in any physiological adaptations which occur in the ageing and senescent process due to exercise.

To counter these aforementioned concerns previous data, single EV particle analysis is a useful tool to analyse sEV count within these cohorts (McIlvenna, Parker *et al.,* 2023) without the bias that occurs due to pre-isolation method. Nano ultra-high performance liquid chromatography-tandem mass spectrometry (nano UHPLC-MS/S) is also a useful unbiased tool for understanding any differences in the protein cargo of sEVs that might be brought about by the ageing process or the attenuation of this via regular exercise.

4.2.2. Aims

- To identify whether there are any significant quantitative differences in the number of circulating sEVs in young versus old, and in those who have completed lifelong exercise; and
- to determine whether there are any changes in the proteome of circulating sEVs in response to age and chronic exercise.

4.3. Methods

4.3.1. Ethical approval

Prior to the commencement of this study, ethical approval was obtained from the West Midlands/Solihull Research Ethics Committee (16/WM/0167), and all participants provided written informed consent prior to participation in accordance with the *Declaration of Helsinki*.

4.3.2. Participant recruitment

Participants were recruited using a combination of local advertisements, the League of Veteran Racing Cyclists, and the British Masters Athletics Federation. To be eligible for study participation, young participants (aged 18 – 35) and elder untrained participants (aged 60 – 80) must have maintained habitual activity and not previously completed any non-recreational structured exercise training. Masters athletes (aged 60 – 80) were required to have maintained continuous endurance training, at least twice per week for no less than 20 years. Additionally, participants could not regularly use analgesic or anti-inflammatory drugs.

Table 4.1| Participant anthropometric characteristics (*McKendry, 2019).*

	Young (N=12)	Elder (N=12)	Masters Athlete (N=12)
Age (years)	20.0 ± 2.8	69.8 ± 4.1	67.1 ± 6.4
Height (m)	1.80 ± 0.04	1.80 ± 0.07	1.7 ± 0.06
Weight (kg)	78.9 ± 13.3	77.5 ± 14.2	68.7 ± 6.6
BMI ($kg.m^{-2}$)	24.6 ± 3.6	24.5 ± 3.8	23.0 ± 2.0
VO2 Peak (ml·kg-1 ·min-1)	53.2 ± 7.3	36.7 ± 6.5	49.3 ± 3.6

Data presented as mean ± SD. All male participants.

On the day of the study, young participants, elder untrained participants, and elder Masters athletes were required to fast overnight prior to their laboratory session. $V0_2$ max was calculated for each participant using the Ekblom-Bak test (Bjorkman *et al*., 2016) performed on an exercise bike (Lode Ergometer, Groningen, Netherlands) using a Vyntus Metabolic Cart (Vyaire Medical, Basingstoke, United Kingdom). Blood samples were taken.

4.3.3. Blood Collection and plasma separation

A cannula was inserted into a vein within the cubital fossa prior to the exercise bout. This cannula was infused with saline and allowed to adjust for ~2 minutes. 2ml of venous blood was collected and disposed, to clear any cannulation contamination. EDTA lined tubes were used. 5 x 10ml blood samples were collected after 10 minutes supine resting. These samples were then centrifuged at 3000 x g for 10 minutes at 4°C. Plasma was then stored at -80°C.

4.3.4. Single EV particle analysis

Plasma samples were analysed using the ExoView human tetraspanin plasma Kits (EV-TERA-P) in accordance with the manufacturer's instructions (Unchained Laboratories, Pleasanton, CA, USA). Fluorescent counts indicate the number of tetraspanin positive sEVs bound to the antibody spot, as determined by interferometric counts. Mean fluorescence intensity is the intensity of fluorescence emitted from tetraspanin positive sEVs bound to the antibody spot. Non-fluorescent interferometric counts reflect the presence fluorescent particles bound to the CD41a positive spot. Further details about this analysis can be found in **Chapter 6: General Methods.**

4.3.5. Statistical Analysis on single EV particle analysis array

For analysis of fluorescent counts, mean fluorescence intensity and IM data were normalised to the mean of the young control group. Colocalisation data was unchanged. All single EV particle analysis statistical analysis was conducted using GraphPad Prism version 9.4.1. Statistical significance between any counts and fluorescent intensity were analysed using ordinary one-way ANOVA, with Tukey's multiple comparisons test to identify significance between groups. All data has been plotted with individual data points, with the mean +/- SD. Differences were considered statistically significant at $P < 0.05$ *.

4.3.6. Quantitative proteomic sample prep

sEVs were isolated with two centrifugal spins of 110,000 x g for 2 hours at 4°C. Further details can be found in **Chapter 6: General Methods**. Protein was precipitated from

sEV lysates via ice cold acetone and overnight incubation -20°C. Protein was pelleted at 5000 x g for 10 minutes and resuspended in 20µl of fresh urea lysis buffer (0.1M HEPES ph 8.0, 6M UREA, 2M Thiourea), before sonicating the sample. Qubit was then conducted to quantify protein. 5µg of sample were added to a LoBind tube (Eppendorf, Hamburg, Germany). Lysis buffer (0.1M HEPES ph 8.0, 6M UREA, 2M Thiourea) was added to reach a reagent total of 10µl. This was followed by reduction with DTT (Fisherscientific, A39255) and alkylation with iodoacetamide (Thermofisher, A39271). Samples were then digested with LysC and underwent acidification with 1% TFA. The samples were then loaded into equilibrated SDB-RPS tips (Rappsilber et al., 2007) and peptides eluted in three different fractions. Samples were then dried on a SpeedVac (Eppendorf, Hamburg, Germany) for ~40 minutes at 45°C. Further details can be found in **Chapter 6: General Methods**

4.3.7. Mass Spectrometry

Normalised samples (5 µg) were analysed by nano ultra-high performance liquid chromatography-tandem mass spectrometry (nano UHPLC-MS/S) using the Q Exactive HF-X Hybrid Quadrupole-Orbitrap system (ThermoFisher Scientific, Brisbane, Australia). Samples were run in DDA mode, selecting the top 20 most intense peptide ions, using a 120min linear gradient at a flow rate of 200nl/min. (Rappsilber et al., 2007) . MS spectra were acquired at a resolution of 70,000, m/z scan range between 300 to 1650, and a target value of $3e^6$ ions. The mass spectral data was then run through MaxQuant v2.4.2.0 against the human UniProt database (Cox and Mann, 2008) for label free quantitation, match-between-runs and statistical analysis.

4.3.8. Bioinformatics analysis

Proteomic samples were analysed using Perseus v1.6.15.0 (Tyanova et al., 2016). Data were filtered to remove proteins identified only by modification site, probable contaminants and protein sequences which matched artificially generated decoy sequences. Each row representing a protein were then filtered based on valid values, requiring 2 positive values (40%) for each protein in each group (per model). Data were normalised to the median of the young plasma condition against each aged condition. Following $\log^2$ transformation and visual check for normal distribution, data were analysed via ANOVA with an S_0 of 0.1 and permutation-based FDR correction $P<0.05$.

4.4. Results

4.4.1. Despite a difference in CD9 positive sEVs, there was no overall difference in tetraspanin positive sEVs associated with age nor a history of chronic exercise

When comparing sEV sizes for young participants (Y), older participants (O) and Masters athletes (MA), there were no significant differences in the sizes of tetraspanin positive sEVs [Figure 4.1]. There were no between group differences in the number of CD63 and CD81 positive sEVs. There was a significant group difference in CD9 positive fluorescence counts (*F = 3.488, P = 0.0423 **) and CD9 positive mean fluorescence intensity (*F = 4.736, P = 0.0156 **). CD9 positive fluorescent counts significantly lower in older adults compared to young participants (*P = 0.0372 **). Masters athletes had a lower CD9 positive mean fluorescence intensity than the young cohort (*P = 0.0206 **) according to Tukey's post-hoc comparison. This is not the case for CD9 mean fluorescence intensity between any other participant group, or within different tetraspanins. These data, along with the visual representation of fluorescence from the

single EV particle array spots [Figure 4.1] indicates that although there is a significant differences in CD9 positive sEVs this does not indicate an overarching change in sEV counts. This is because one would expect that if there was a clear effect of age or chronic exercise of sEVs, it would be visible in all CD9, CD63 and CD81 immobilised sEVs. Due to these differences in CD9 positive sEVs, it may be that there are subpopulations of CD9 positive sEVs that differ dependent on age. Colocalisation data will allow us to identify which tetraspanins jointly appear on the same vesicle, providing further information about these potential subpopulations.

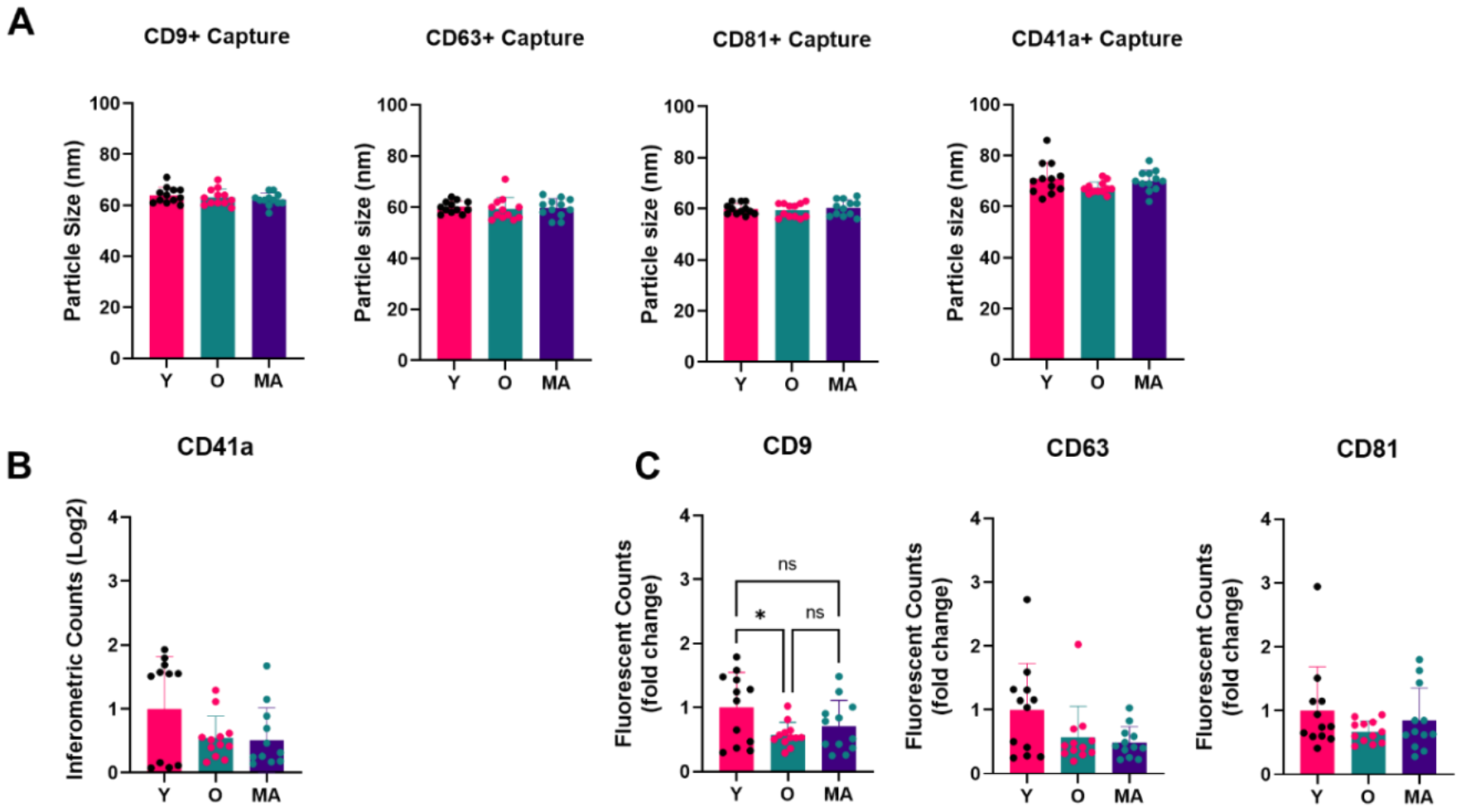
A
CD9+ Capture
CD63+ Capture
CD81+ Capture
CD41a+ Capture
Particle Size (nm)
Particle size (nm)
Y
O
MA
B
CD41a
Inferometric Counts (Log2)
C
CD9
CD63
CD81
Fluorescent Counts (fold change)
ns
*

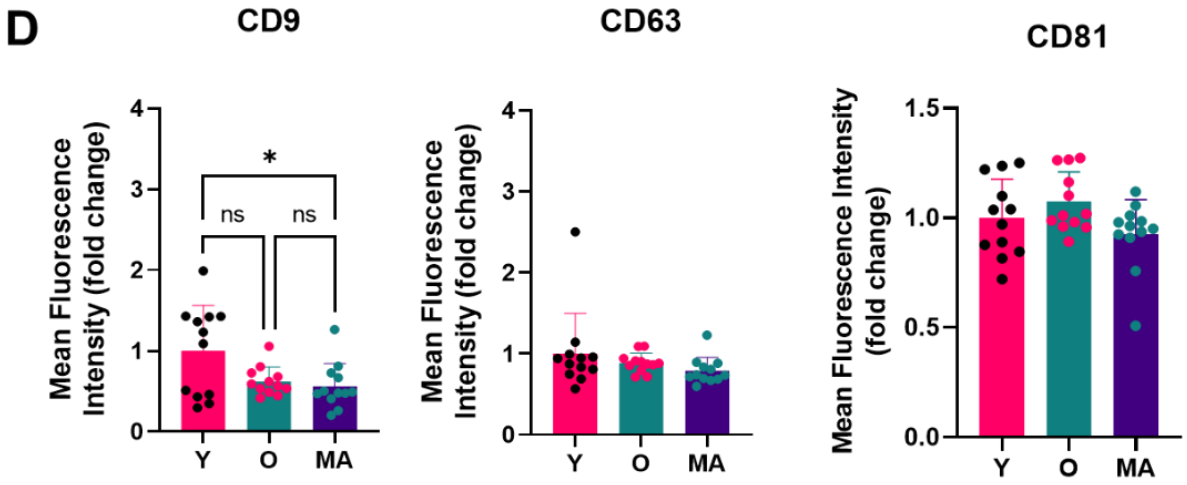
D
CD9
CD63
CD81
Mean Fluorescence Intensity (fold change)
Mean Fluorescence Intensity (fold change)
Mean Fluorescence Intensity (fold change)
*
ns
ns
0
1
2
3
4
0.0
0.5
1.0
1.5
Y
O
MA

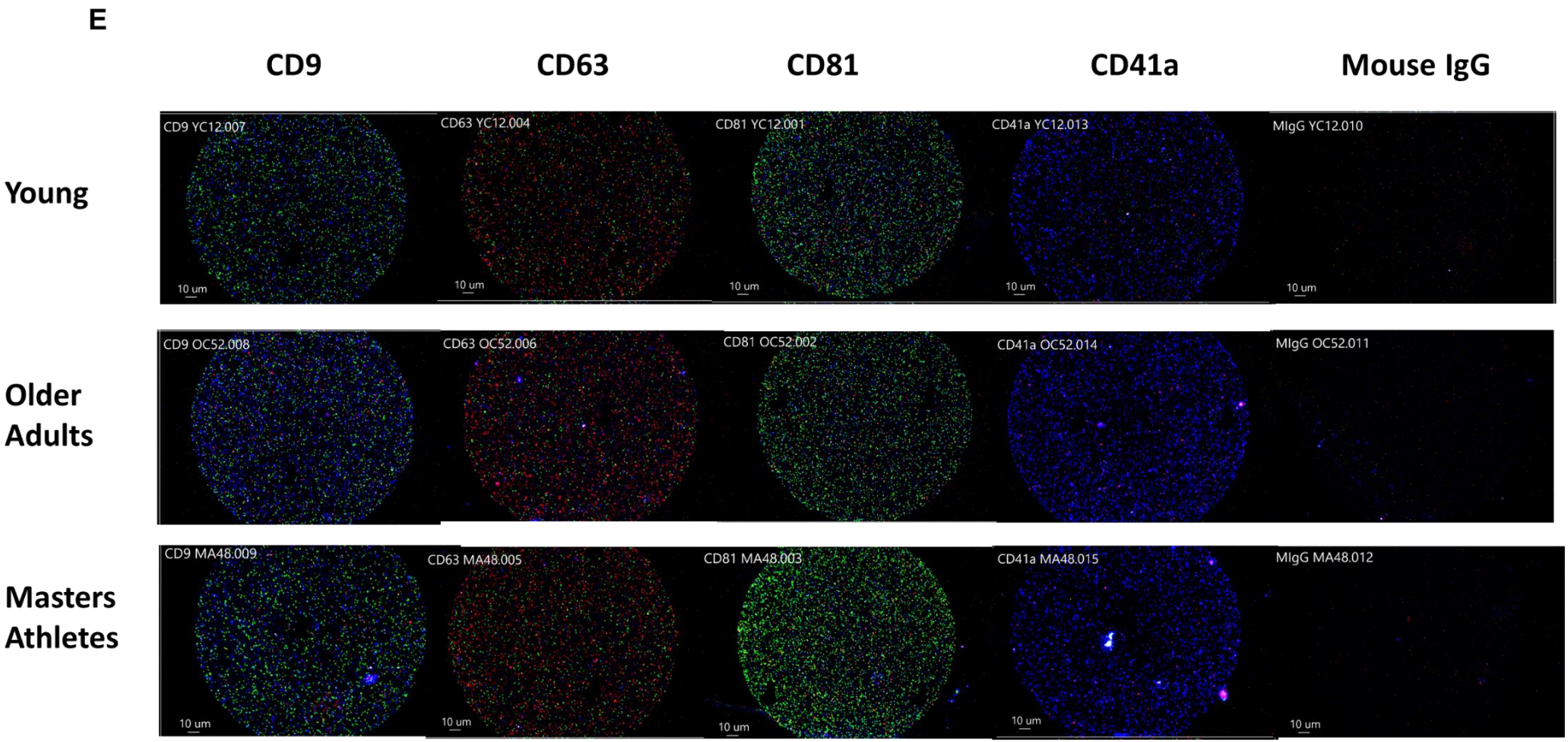

Figure 4.1. *A). Particle sizes for spot specific bound particles measured by Single EV Particle Array. B). Fold change of interferometric counts of all particles in plasma bound on CD41a. C). Colour specific fluorescent counts, measured by interferometric microscope and analysed as fold-change. D). Mean fluorescence intensity of fold-change difference E). Representative spot images taken using interferometric imaging. All data previously referenced is collected from spots such as these. A representative mark denoting 5um is present on each image. Graph key: young participants (Y), older participants (O) and Masters athletes (MA). N = 12. All analysis conducted on plasma. For the ExoView figures, statistical*

*analysis was conducted using Ordinary one-way ANOVA, followed by Tukey's test using GraphPad Prism. p<0.01 indicated by *, p<0.01 indicated by **. F = F-Distribution*

.

4.2. Colocalisation data shows little difference between sEV counts associated with age or a history of chronic exercise.

Colocalisation data shows whether there are subpopulations of SEVs responding to ageing and chronic exercise [Figure 2.2]. There were no between group differences in the colocalisation of sEVs immobilised on the CD81 positive spot. There were also no between group differences in CD9 positive immobilised sEVs colocalised with CD9 or CD81; no between group differences in CD63 positive immobilised sEVs with CD63 or CD81; nor any between group differences in CD41a positive immobilised sEVs with CD9 or CD81. For the CD9 positive spot (*F = 7.218, P = 0.0025* **), there was a significant difference in CD63 positive vesicles between young sEVs and older sEVs (*P = 0.0354* *) and young sEVs and Masters sEVs (*P = 0.0163* *) according to Tukey's post-hoc comparison. For the CD63 spot *(F = 6.012, P = 0.0059* **), there was a significant decrease in CD9 positive vesicles between young sEVs and older sEVs (*P = 0.0042* **). For the CD41a spot (*F = 7.576, P = 0.0020* **),, there was a significant decrease in CD63 positive vesicles between young sEVs and older sEVs (*P = 0.0026* **) and young sEVs and Masters sEVs (*P = 0.0128* *), but not in other tetraspanin colocalisation combinations. This may suggest that vesicles which have either both CD63 and CD9 on their surface or have CD63 and CD41a on their surface decrease with age, and this is not dependent on chronic exercise. Of note, this was not seen when considering CD63 in isolation. If there was a genuine effect on the sEVs within these samples, it could be argued there would be a visible change in sEVs between participant groups irrespective of the tetraspanin target, as is seen in **Chapter 2**.

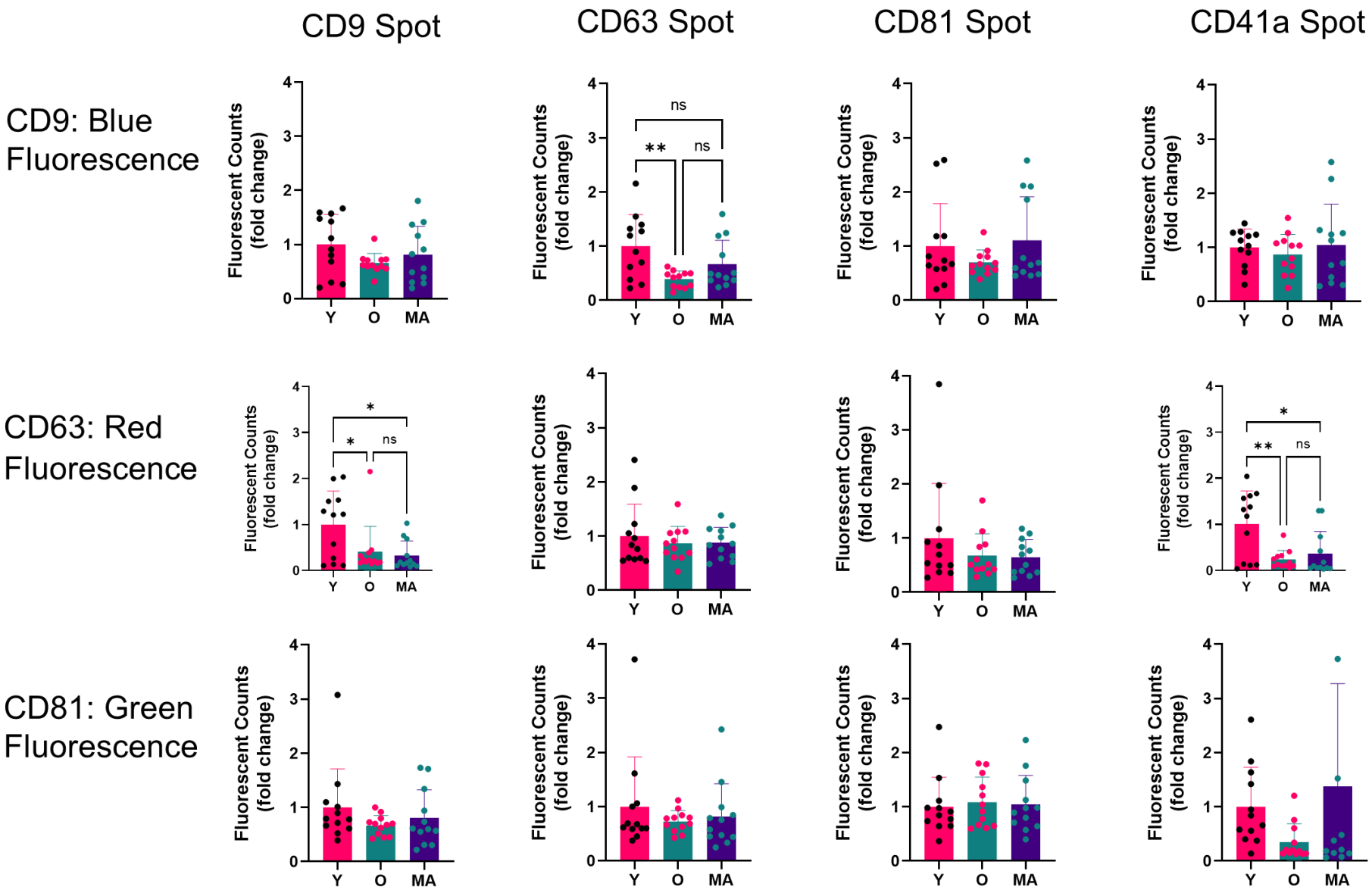
CD9 Spot
CD63 Spot
CD81 Spot
CD41a Spot
CD9: Blue Fluorescence
CD63: Red Fluorescence
CD81: Green Fluorescence
Fluorescent Counts (fold change)
Y
O
MA
ns
**
*

Figure 4.2 *Colocalisation of each colour (CD9: Blue; CD63: Red; CD81; Green) on each specific antibody binding spot for young (Y), older (O) and Masters athlete (MA) participants. N = 12. Statistical analysis was conducted using Ordinary one-way ANOVA, followed by Tukey's test using GraphPad Prism. p<0.01 indicated by *, p<0.01 indicated by **. F = F-Distribution*

4.4.3 Proteomic Analysis shows little difference in sEV cargo irrelevant of age or chronic exercise.

Data was normalised to the median of the control condition of its relevant model, and this was confirmed visually via histogram [Figure 4.3]. As sEVs can differ in their protein cargo independent of sEV number, proteomic analysis was completed of the sample groups. In total, 669 proteins were identified across all three conditions. An ANOVA was completed to determine whether there were any proteins which significantly changed between young, old and Masters athlete sEVs. There were no significant differences in proteins between young participants and Masters athletes, nor between older participants and Masters athletes. When comparing groups independently by T test with permutation-based P value correction, 4 proteins were significantly increased between young participants and old participants: BANF1, ATP1A1, CCT8 and BSG. The proteins IgH, Igg1 and Ig-like dom were significantly decreased in older participants compared to younger participants.

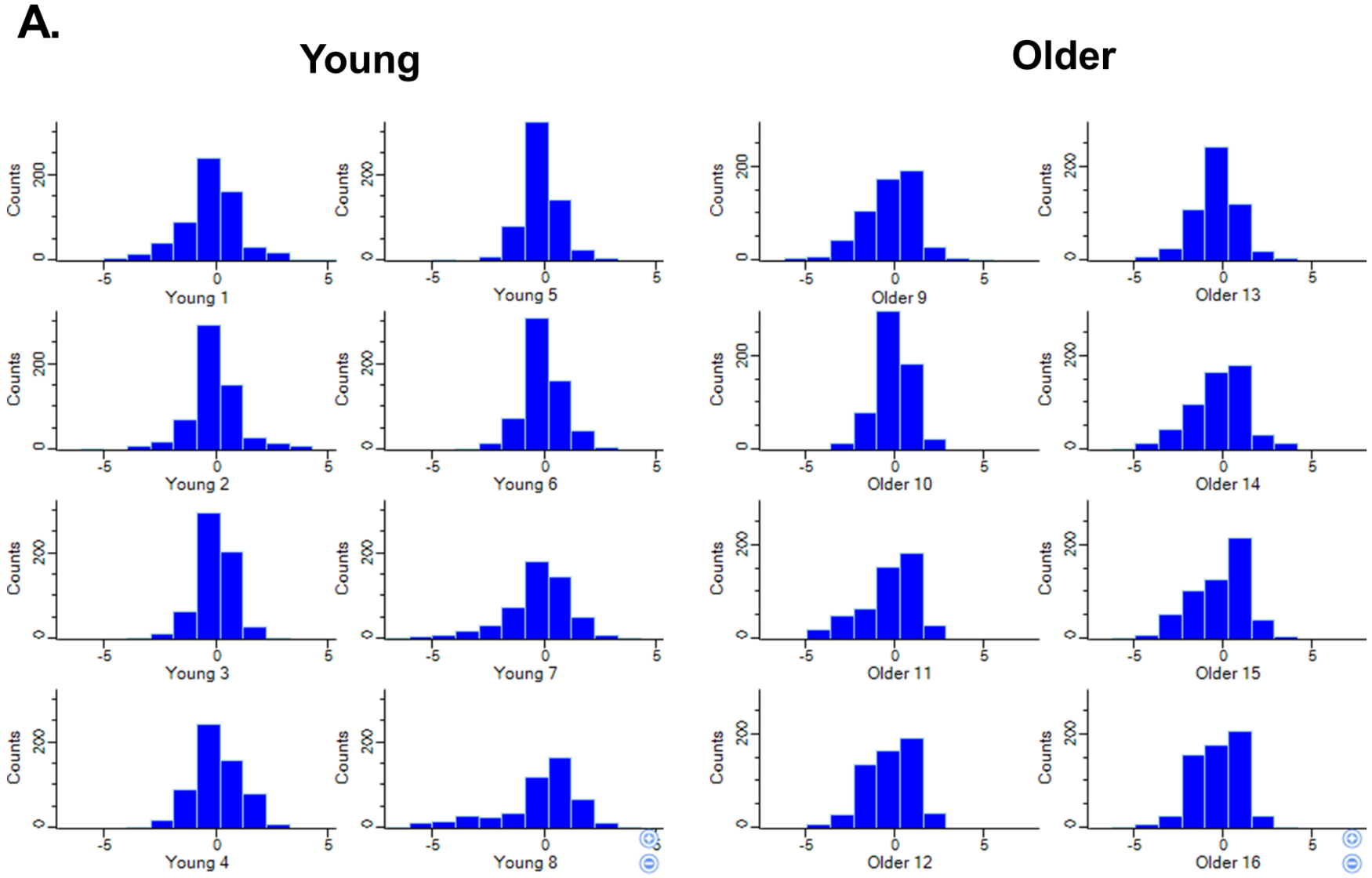
A.
Young
Older
Counts
Young 1
Young 2
Young 3
Young 4
Young 5
Young 6
Young 7
Young 8
Older 9
Older 10
Older 11
Older 12
Older 13
Older 14
Older 15
Older 16

Masters

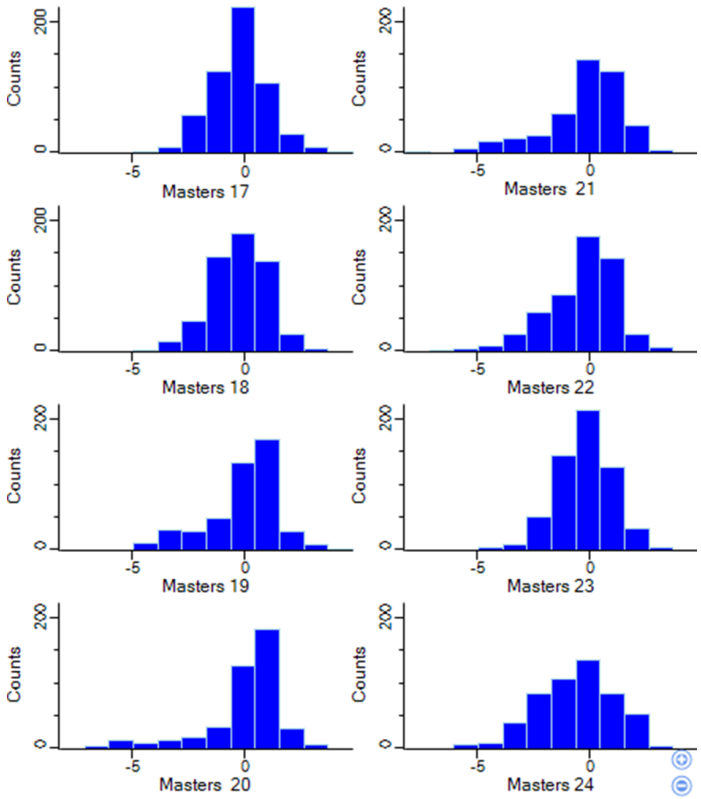

B

Young vs Older

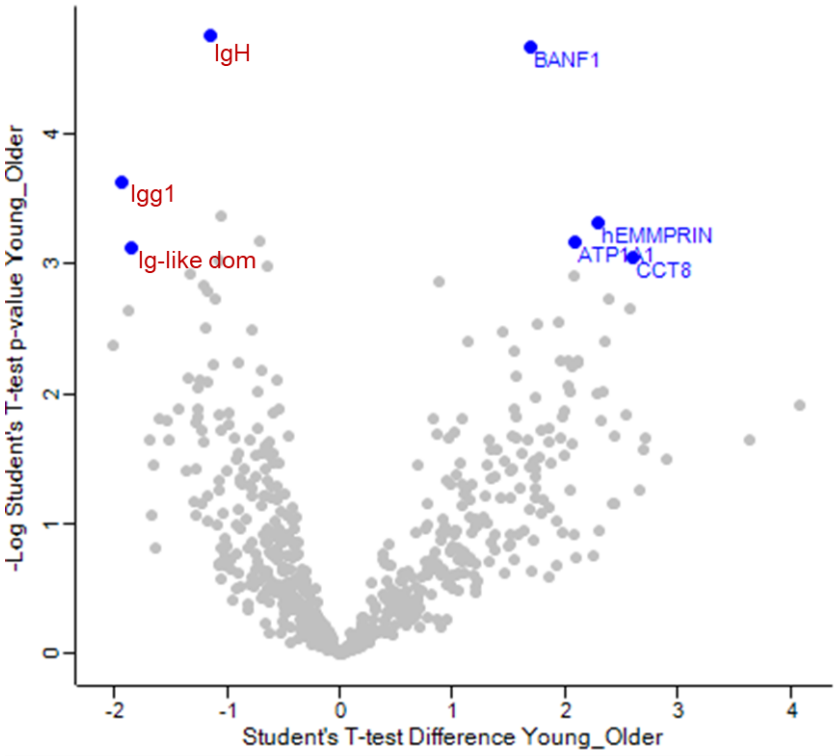

Young vs Masters Athletes

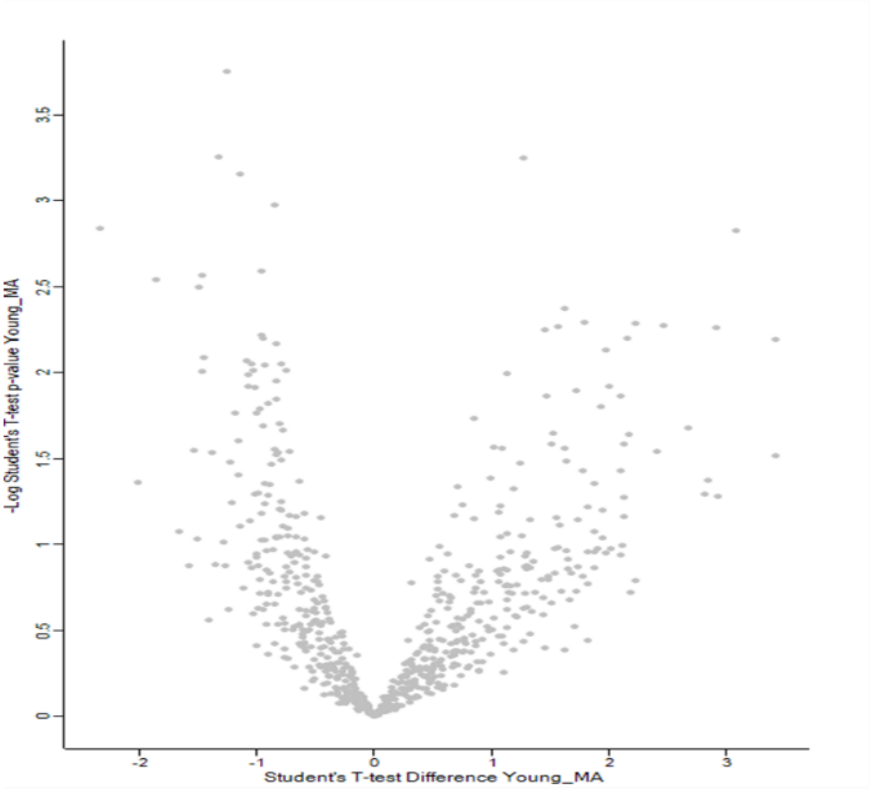

Older vs Masters Athletes

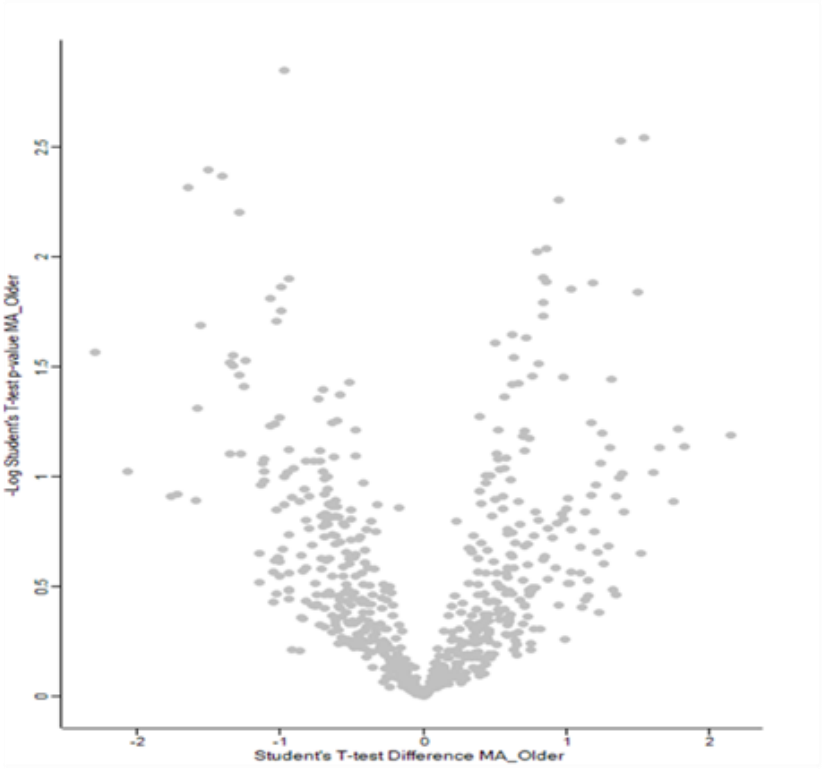

Figure 4.3. *A). Validation that the protein numbers were normalised correctly. B). Proteins which statistically change (left side of the graph) and increase (right side of the graph) based on comparing young participant plasma to older participant plasma, young participant plasma to Masters athlete participant plasma and older participant plasma to Masters athlete participant plasma. Statistically increased proteins are displayed in blue. Statistical analysis was completed using the Perseus v1. 5. 5. 2.*

The following proteins are changed in the older cohort in comparison to the young cohort.

Table 4.2 | *Proteins identified as significantly higher in older participants compared to younger participants.*

Gene Symbol	Protein Name
BANF1	BAF Nuclear Assembly Factor 1
ATP1A1	ATPase NA+/K+ Transporting Subunit Alpha
CCT8	T-Complex Protein 1 Subunit 8
BSG	Human Extracellular Matrix Metalloproteinase Inducer

4.5.1. Discussion

There could be great utility in understanding how sEV count and protein cargo change due to the ageing process, and whether chronic exercise has an impact on these. Not only do senescence and exercise have a large effect on the release of sEVs, but exercise has been shown to mediate the impact of senescent burden (Donovan et al., 2021, Englund et al., 2021, Demaria et al., 2023). The results showed there were no significant difference between the overarching sEV count of each cohort depending on age group nor chronic exercise.

Early studies suggested that sEVs increase during senescence (Yu et al., 2006, Lehmann et al., 2008) and these researchers extrapolated that this would also be the case in aged participants. There were several limitations to these studies. Both Yu (et al., 2006) and Lehmann (et al., 2008) conducted analysis to confirm the presence of sEVs using a combination of electron microscopy and western blots for the target Hsp90β and TSG101 respectively, neither of which provide counts for single EV

particles. Although identified within vesicles, Hsp90β has been shown to be enriched within sEVs from some types of senescence associated cancers (Ono et al., 2018), so the sEVs measured by Yu as part of a model of senescence may have been similarly enriched. Although initially thought of as a homogenous marker for sEVs, TSG101 has been proposed as a marker specifically for tetraspanin-enriched sEVs (Tucher et al., 2018). TSG101 is also found to be reduced in samples which have undergone ultracentrifugation in comparison methods which do not cause biological disruption e.g. SEC (Willms et al., 2018). Studies focusing on aged participants have shown mixed results, with some suggesting sEVs decrease (Eitan et al., 2017; Rani et al., 2017; Zhang et al., 2017; Alibhai et al.,2020; Zhang et al., 2020), some suggesting they increase (Aliquet et al., 2017) and another proposing they do not change (Alberro et al., 2016). Unlike these studies, where quantification occurred using NTA, our use of single EV particle analysis prevents the bias introduced by introducing an isolation method. Additionally, the use of three different tetraspanin markers, rather than measuring sEVs by size, means that potential contaminants such as lipoproteins do not contribute to potential counts.

In the analysis of sEVs derived from human plasma, there were 4 proteins which had not previously been identified in our analysis, but there were significant differences in older participants: BSG, ATP1A1, BANF1 and CCT8.

hEMMPRIN (Human Extracellular matrix metalloproteinase inducer), is also known as basigin (BSG). BSG is a transmembrane glycoprotein which sits within the immunoglobulin superfamily, and has roles in cell proliferation, tumour cell migration,

differentiation, apoptosis, differentiation and inflammation (Kim et al., 2021). BSG7 is heavily correlated with several markers of inflammation, including c-reactive protein and neutrophil/lymphocyte ratio (Pennings et al., 2010). BSG also has strong associations with ageing, playing a key role in age-associated changes in myocardial age (Huet et al., 2015) and the severity of ischemic strokes and risk of secondary haemorrhage (Patrizz et al., 2020), all of which are associated with senescent burden. More recently, BSG has been linked with severity of SARS-CoV-2, in a platelet activation dependent manner (Maugeri et al., 2022; Ghasemzadeh et al., 2022). It is possible these links to inflammation are linked to platelet stimulation, as BSG is found on the surface of 20.45% of platelets (Pennings et al., 2010). As well as being found on platelets, BSG has been identified within extracellular vesicles using Vesiclepedia (Panthan et al., 2019).

CCT8 (Chaperonin containing TCP1 subunit 8) is involved in the transport and assembly of newly synthesised proteins, specifically through the cellular molecular chaperone complex (Liao et al., 2021). CCT8 is also heavily associated with proteostasis, with normal T cell biology being critically dependent on CCT8 (Oftedal et al., 2021). Overexpression of CCT8 leads to proteostasis decline, which is heavily associated with an increase in senescence (Sabath et al., 2020). The overexpression of CCT8 is both heavily associated with poor prognosis of several senescence related cancers such as lung cancer, endometrial cancer (Gong et al., 2023) and colorectal cancers (Liao et al., 2021). Conversely, the overexpression of CCT8 has also been associated with an increased lifespan, due to the increase of proteostasis (Noormohammadi et al., 2016), a decline of which is associated with ageing and

senescence (Sabath et al.,2020; Zhang et al., 2022). CCT8 has been identified within extracellular vesicles using Vesiclepedia (Panthan et al., 2019).

BANF1 (BAF Nuclear Assembly Factor 1) is a member of the barrier-to-autointegration factor family or proteins. It is a highly conserved DNA binding protein which is involved in mitosis, viral infection, gene regulation, DNA damage response, chromatin and mitosis (Jamin and Wiebe, 2016). One such DNA damage response is that BANF1 regulates poly [ADP-Ribose] polymerase 1 (PARP1) activity in response to oxidative DNA damage, which is associated with ageing and senescence (Bolderson et al., 2019). Interestingly, a mutation of BANF1 can trigger Nestor-Guillermo Progeria Syndrome (NGPS), which is also known as severe premature ageing syndrome, where children will experience ageing associated diseases such as lipoatrophy, osteolysis and osteoporosis (Paquet at al., 2014) due to premature senescence triggered by genome instability (Carrero et al., 2016). BANF1 has been identified within extracellular vesicles using Vesiclepedia (Panthan et al., 2019).

ATP1A1 (ATPase NA+/K+ Transporting Subunit Alpha 1) codes for the alpha subtype of the NKA protein. NKA is comprised of two such subunits, alpha and beta. The NKA protein is responsible for cell adhesion and motility. There is mixed research with regards to the alpha subunit itself, with some sources stating the alpha subunit decreases in older people (Mewes et al., 2017; Ding et al., 2018). Other sources link NKA a1 overexpression to several forms of senescence-associated cancers such as non-small cell lung cancer, and glioblastoma. Within these glioblastoma cells, NKA a1 was shown to have an antiproliferative and anti-migratory effect (de Silva et al., 2021). Due to these apparent contrasting results, it is clear further research into the impact

ATP1A1 has on senescence, if any, is needed. ATP1A1 has been identified within extracellular vesicles using Vesiclepedia (Panthan et al., 2019).

These proteins were not significantly different in the young participant cohort nor the Masters athlete cohort when compared against one another. This suggests that proteomics showed limited differences in protein cargo. Whilst sEVs appear to be different in in vitro models of senescence, there may be several reasons that is not the case within aged participants. It is important to note that BSG and ATP1A1 have both been proposed as sEV markers (Kugeratski et al., 2021).

One reason that there may be no significance between the three participant groups may be that there is not a large enough senescent burden to reflect a significant change in the proteome in these older individuals. The accumulation of senescent burden is associated with several diseases such as strokes (Torres-Querol et al., 2021), Alzheimer's disease (Liu et al., 2022), sarcopenia (He et al., 2021) and motor neuron disease (Trias et al., 2019). Participants within our study were required to be healthy and not have any major health concerns, it could be that we retrieved sEVs from the plasma of particularly healthy individuals who would not reflect this burden.

Another possibility could be that the sEVs analysed in **Chapter 3** may not accurately reflect senescent burden in vivo. The senescence models were induced using BJ-5ta fibroblasts, which may not be reflective of senescence within a healthy participant where

many molecular pathways are interacting. Additionally, the model may have been more senescent than would be viable within healthy participants.

4.5.2 Limitations

It is also key to note that perhaps the tetraspanins CD9, CD63, CD81 and CD41a are not the most relevant sEV targets to be considered in this analysis. Although these are widely regarded as classical markers, there are other markers such as EN01, GPI, YWHAB, CNTN1, CSF1R and HSPA5 which are similarly abundant in sEVs from all cell types (Garcia-Martin et al., 2022). It is also worth noting that different cell types are shown to produce varying proteomes with regards to their released sEVs (Garcia-Martin et al., 2022). The proteome between sEVs is not ubiquitous. Kugeratski (et al., 2021) showed that sEVs from different cell lines had different sEV markers. This is also applicable to cargo, as different cargo have been used to identify the potential biogenesis of sEVs (Burbidge et al., 2020).

Although the proteomic study did not show an increase in any of the previously identified potential senescence biomarkers, this does not automatically exclude them. Although there have been large improvements in mass spectrometry technology (Burnum-Johnson et al., 2022), there are still reasons that proteins may not be detected within samples. These include limits to the estimation of low abundance proteins (*Le et al., 2019*), inadequate identification of peptides (Mulvey et al., 2010) and the limitations in current mass spectrometry in only identifying a limited number of peptides, and thus only a small number of amino acids (Sinitcyn et al., 2023).

Another key thing to note is that the plasma samples used were platelet poor plasma (single spun). As discussed previously, it is preferable to use platelet free plasma (double spun), as residue platelets impact count and phenotype (McIlvenna, Parker *et al.,* 2023). As platelets are reduced in the elderly (Jones, 2016) and increased in those who exercise (Heber and Volf, 2015), it is difficult to identify whether these differences that could potentially occur are due to in vivo or ex vivo considerations. We cannot accurately determine whether the proteins identified within the proteomics comparing young, older and Masters athletes are indeed due to significant differences in these participation groups, rather than due to platelet count. This is especially pertinent as CD9 (Dale et al., 2009, Lazareth et al., 2019, Schotte et al., 2020) and CD63 (Israels and McMillan-Ward, 2005, Choudhury et al., 2007, Blair et al., 2018) have both been associated with activated platelets, indicating platelet count may be the reason for a reduction in CD9 the older participants.

Of the four proteins which were significantly different between participant groups, three of them were found within the proteome of platelets: BSG, ATP1A1 and CCT8 (Boyanova et al., 2012). This could suggest that any increase in these proteins may be linked to platelet presence. None of these proteins were shown to increase in any of our models of inducing senescence (**Chapter 3**), which would not have platelets in as they are from conditioned media. This highlights the limitation of liquid chromatography mass spectrometry, in that plasma is liable to containing contaminants due to the more complex biological interactions with occur ex vivo (Pietrowska et al., 2019). However, as platelets have been shown to have a significant effect on sEV counts (McIlvenna, Parker et al., 2023), it is likely that if platelets had impacted these results, it would be in

a more significant way. This contamination is further highlighted by the 3 proteins which were significantly lower in older participants. These would not be relevant as potential biomarkers for senescence as they are not present in sEVs (Pathan et al., 2019) so are likely to be contaminants.

4.6 Conclusion

Despite mixed evidence with some studies indicating an increase in sEV counts and some indicating a reduction, the single EV particle array suggests that there is no significant difference between sEV numbers between young, older adults and Masters athletes. Single EV particle analysis does not require an additional isolation step, so data should be less biased than samples which require isolation. Unbiased analysis of sEVs via quantitative mass spectrometry-based proteomics also showed limited effect of age and chronic exercise on the sEV proteome.

Chapter 5 -

General Discussion

5.1. Introduction

Small extracellular vesicles (sEVs) are nano-sized particles (40-150nm) comprising of lipid bilayers. Their purpose is to carry proteins, lipids, and miRNA between cells, aiding in cellular and organ crosstalk. sEVs have been implicated in many biological processes such as ageing (Alberro et al., 2016, Alique et al., 2017, Eitan et al., 2017, Rani et al., 2017, Zhang et al., 2017, Alibhai et al., 2020, Zhang and Jin, 2020), exercise (Frühbeis et al., 2015, Helmig et al., 2015, Guescini et al., 2015, Brahmer et al., 2019, Just et al., 2020, Whitham et al., 2018) and in senescence-associated diseases such as cardiovascular disease (Lu et al., 2018, Coly and Boulanger, 2022), Alzheimer's disease (Breijyeh and Karaman, 2020, Bodart-Santos et al., 2023), and cancer (Melo et al., 2015, Qiao et al., 2019, Balakrishnan et al., 2020). Some sEVs have been shown to be selectively released and taken up by cells, meaning they may provide great utility in increasing our understanding of the mechanisms behind exercise, ageing and senescence. By understanding when sEVs are released, and what cargo they carry during this release, we can understand what molecular processes are implicated in these molecular processes.

There have been attempts to identify candidate biomarkers of senescence and senescent burden within sEVs, but none have been successful as of yet. sEVs are notoriously difficult to study. They are difficult to isolate as their molecular surfaces have different markers dependent on the cell they were released from (Krylova and Feng, 2023). They are also difficult to isolate by size as they are often mistaken for lipoproteins (Brahmer et al., 2019). Although there are significant advancements in our

understanding of how sEVs play a role in senescence, ageing and exercise, there is a clear lack of understanding of the connection between these processes. Research into the release of sEVs during exercise is hampered by these concerns with isolation.

Therefore, this thesis had three main aims:

- Determine whether there were a significant difference in circulating sEV number after a bout of high intensity cardio-based exercise (**Chapter 2**); and
- to further investigate the proteome of sEVs released found within sEVs released during senescence, and whether any of these could have been candidate biomarkers (**Chapter 3**); and
- identify whether there were any significant quantitative or proteomic differences in circulating sEVs in response to ageing or chronic exercise (**Chapter 4**).

This discussion chapter will briefly summarise any key findings described in **Chapters 2**, **3** and **4** of this thesis. For the outline of **Chapter 2**, we will discuss the use of single EV particle analysis and whether there are any differences in circulating sEVs in response to level of platelet contamination and high intensity interval exercise. The outline of **Chapter 3** will consider the three senescence models we induced, and the proteomic analysis completed to further investigate the proteome of sEVs released during senescence. We will also discuss whether candidate biomarkers can be identified for general senescence. Finally, in **Chapter 4** we will discuss the impact that ageing and chronic exercise have on sEV counts and proteome within the circulation. This will be integrated with a discussion on the real-world implications of this research, followed by a discussion on experimental limitations and future directions.

5.2.1. Single vesicle analysis indicates an increase in circulating sEVs post high intensity intermittent exercise.

Although there are many sources indicating that sEVs are released as a result of an acute bout of high intensity intermittent exercise, some studies have shown that there is a decrease in sEVs during exercise or that there are no significant changes to the sEV count in circulation during exercise. This is due to the lack of gold standard for the isolation and study of sEVs. In addition, the vast majority of these studies used platelet poor plasma. In **Chapter 2**, using single EV particle analysis, a technique which does not require a pre- sEV isolation step, resting plasma samples were analysed. Plasma was centrifugated either once (platelet poor plasma) or twice (platelet free plasma). There was a significantly less sEVs in the platelet free plasma than in the plasma poor plasma [Figure 2.2]. implying that platelets have an impact on detected circulating sEVs. Following on from this, plasma samples taken pre and post exercise were quantified, to provide sEV counts and some detail about the presence of different tetraspanins on their surface. High intensity intermittent exercise triggered an increase in fluorescent sEV counts (CD9, CD61, CD81 and CD41a) and an increased mean fluorescence intensity (CD9, CD63) [Figure 2.3; Figure 2.6]. This suggests that there is indeed a significant increase in sEV release during HIIE, and this quantitative increase is seen even with the impact that platelet presence has on sEV profile.

5.2.2. Implications

These findings provide a highly sensitive evaluation of sEV dynamics during exercise through the analysis of individual EV particles. Due to this, we believe that the array will be a suitable complementary approach to understanding biological relevance of sEV

release into circulation with exercise. For example, by completing the use of the array with proteomic analysis to provide information on both counts and the proteome. As sEVs increase in circulation during HIIE, it is likely that sEVs contribute to molecular processes involved in exercise. Both sEVs and exercise have been linked to cellular signalling (Whitham et al., 2018), tissue repair and regeneration (Bussolati and Camussi, 2017; Kalluri et al., 2020), metabolic regulation (Kobayashi *et al.*, 2018), and adaptation to physiological stress (Khoury and Nagy, 2023). It stands to reason that sEVs may be responsible for these adaptations.

Furthermore, this information underscores the potential influence of platelet depletion on both the count and phenotype of sEVs. Despite this, the impact of exercise has such a large effect that the increase of sEVs was still apparently in platelet poor plasma. Due to this, we suggest that it is preferable to use platelet free plasma, but that if the effect being studied is large enough, platelet poor plasma is adequate

5.2.3. Limitations

One limitation to our study is in **Chapter 2,** where our N values are low. They are between 5 and 9 for the single EV particle analysis studies. To better understand the data here, post-hoc analysis was completed to determine the Cohen D effect size and statistical power. Cohen classified the effect size as small (d = 0.2), medium (d = 0.5), and large (d>0.8) (Sullivan and Feinn, 2012). Due to the majority of our data showing medium or large effect sizes, it is likely that our low N is sufficient.

A further limitation of this study is that it does not provide data about the source or destination of the released sEVs. As a further interest point of sEVs is that they may have a controlled release in response to stimuli such as acute exercise, knowing this information will provide a deeper understanding of their role within cellular and tissue crosstalk. As sEVs released from different cells have different signatures, single particle EV analysis could be used with different immunofluorescent markers. For example, CD86 and CD68 have been used as markers for sEVs released from macrophages (Wang et al., 2020). This would only be useful if there is already a clear understanding of which sEV markers are associated with a particular destination. An alternative could be to use DiR-labelling to detect the location of vesicles. DiR is a fluorescent cyanine dye, which can be used to create fluorecent images of labelled membranes, such as sEVs, to show presence within organs. DiR-labelling has been used previously to identify that sEVs localised to the liver after a bout of high intensity exercise (Whitham et al., 2018), and to track muscle cell derived sEVs in cell culture (Fulzele et al., 2019).

5.3.1. sEV LC-MS/MS analysis provides an insight into the proteome of senescence derived sEVs

sEVs derived from senescent cells are able to induce senescence in other cells. Due to this, there is utility in examining the cargo of these sEVs. Currently there are no identified biomarkers of senescence in sEVs. This is because many of the identified candidate biomarkers show differences dependent on the specific cell type that released the sEVs (Jurgielewicz et al., 2020). Additionally, different inducers of senescence show different biological markers (Garcia-Martin et al., 2022), further impacting current biomarkers of senescence. Identifying a biomarker which could be

used in liquid biopsies would be extremely beneficial in the early detection of senescent burden, allowing for the early identification of senescence-associated diseases. Initially, independent analyses of these data showed widespread changes in the sEV proteome in cellular models of senescence, but no clear universal markers were observable using nano ultra-high performance liquid chromatography-tandem mass spectrometry (nano UHPLC-MS/MS) analysis of sEVs isolated from three different senescent models:

- Mitochondrial dysfunction associated senescence (MiDaS)
- Oxidative stress induced senescence (OSIS)
- Oncogene induced senescence (OIS)

In general, we were able to identify much higher levels of significantly increased proteins in our models of senescence (991 for the oncogene stress, 409 for the mitochondrial dysfunction and 91 for the oxidative stress model) than in the aforementioned publicly available datasets. These proteins were overlaid on top of one another, matched by UniProt code, followed by comparison to the ageing dataset and the proteins found within sEVs database. This produced a list of 7 potential candidates as a biomarker of senescence: NIT2, CARS, EEF1A2, GSTO1, PGAM 1, PGAM 2 and NAMPT. Four those these had also been shown to significantly increase in association with ageing (Lehallier et al., 2019): CARS, GSTO1, NAMPT and PGAM.

5.3.2. Implications

If the seven proteins identified are indeed biomarkers of senescence, there could be many implications for advancing our understanding of ageing, improving disease diagnosis, and developing targeted therapeutic interventions for age-related conditions.

The most obvious implication of identifying a biomarker of senescence their use in early disease detection. By facilitating early detection of senescence associated diseases, there may be more timely intervention and an improvement in treatment outcomes. This is especially key for senescence-associated diseases where early intervention is able to increase outcome such as certain cancers (Crosby et al., 2022) and Alzheimer's disease (Rasmussen and Langerman, 2019). It may even be possible in the future to use such biomarkers as these to monitor ageing processes and susceptibility to senescence-associated conditions before the patient even has the disease. Additionally, with public health and ageing being one of the largest problems that our society faces (Mitchell and Walker, 2020), the identification of biomarkers of senescence would help to inform healthcare planning and disease prevention.

5.3.3. Limitations

A limitation that is impacted in **Chapter 3** is the vastness of the proteome, and the steps that go into researching it. 3037, 3424 and 4086 proteins were quantified from the OIS model, MiDaS model and OSIS model respectively after filtering methods were completed. Although there was an attempt to narrow these down through union of the three models using their UniProt IDs, this may still be too broad to identify specific markers.

Another issue is that using sEVs isolated from cell models do not accurately reflect senescence within their natural microcellular environment, meaning the data may not always be translational (Kapałczyńska et al., 2018). When collecting sEVs from the senescent models, the complexity of senescence and ageing within the human body

would be missed, as a multitude of molecular mechanisms and pathways interactions are not accurately represented.

5.4.1. Circulating sEVs do not illicit significant changes in their proteome dependent on age nor chronic exercise

Determining the link between ageing, a history of chronic exercise and the presence of sEVs in circulation will be extremely beneficial in providing knowledge about the underlying molecular mechanisms at play. If sEVs play an important role in all biological processes, and in particular senescence, it is conceivable that the process of ageing, which is also associated with senescent burden, is reflected within any released sEVs. Exercise has been shown to reduce senescent burden (Donovan et al., 2021, England et al., 2021, Demaria et al., 2023), so it stands to reason that any physiological benefit that occurs due to chronic exercise may be reflected within circulating sEVs. In **Chapter 4** we used the single EV particle analysis technology that was validated in **Chapter 2**. Resting plasma samples were tested from young participants, older participants, and Masters athletes. Although there were differences in CD9 positive sEVs associated with ageing and chronic exercise, these changes were not seen across all of the tetraspanin markers of sEVs. This implies that sEV count does not change depending on age or chronic exercise. To determine whether there were any proteomic differences in these proteins, the same samples were analysed using nano UHPLC-MS/MS. There were no large differences in the proteomes of these cohorts, as only four proteins were shown to significantly increase. These four proteins which were significantly higher in the older cohort than the young cohort: BANF1, ATP1A1, CCT8 and BSG. It is unclear however whether these proteins are indeed associated with the ageing process specifically as

they have been proposed as markers of sEVs (Kugeratski et al., 2021) and have been linked with platelets (Boyanova et al., 2012). **Chapter 2** supported that remnant platelets release sEVs, and as ageing reduces platelets, the use of platelet poor plasma may explain the lower CD9 protein markers seen in the older cohort compared to the young.

5.4.2. Implications

Chapter 4 showed no large differences between sEVs or their proteome in response to ageing nor chronic exercise. It was previously shown that sEVs containing proteins associated with glycolysis, membrane tracking and the cellular cytoskeleton (Whitham et al., 2018) are released after exhaustive exercise. Glycolysis is shown to increase in ageing cells (Murao et al., 2022), and the inhibition of glycolysis promotes healthy ageing and extends lifespan (Feng et al., 2016). Membrane tracking and the cellular cytoskeleton are both impacted within ageing, with calcium signalling have a direct association with mitochondrial damage that occurs during ageing (Schaum et al., 2020, Fox et al., 2021), and the cytoskeletal stability and function decline during the ageing process (Kim et al., 2022). Due to these factors, it could be implied that any significant difference in the proteome could be identified in response to a bout of high intensity interval exercise, where it would stand to reason that sEVs would be released. Additionally, as sEVs are involved in many biological processes, it may be that they are not specific enough to show clear differences within ageing.

5.4.3. Limitations

The analysis process for proteomics requires filtering proteins by arbitrary methods in an attempt to reduce this bias and remove potential contaminants. This filtering also

removes proteins which are not found in the majority of samples, meaning only proteins which are seen in abundance for the majority of sample groups are included. This could be at the detremient of proteins which could be relevant, as it is conceivable that senescence or ageing results in proteins being uniquely expressed within sEVs.

A key question that is worth considering throughout this thesis is whether there could even be a universal sEV-associated biomarker of senescence that could be used within liquid biopsies. Current techniques identifying senescence require the use of multiple markers to establish senescence (Rossi and Abdelmohsen, 2021). This is because senescence from different cells displays different molecular patterns. Senescent cells also trigger dysfunction within the tissue they interact with in different ways (Tripathi *et al.,* 2021). This may also have an impact on the validity of any potential biomarkers of senescence. It is unlikely that we would be able to identify any potential biomarkers with our cohort of 8 of each participant group. Using LC-MS/MS, at least 250 diseased and 250 controls are required to achieve 90% validation, which is required to be classed as clinically accurate (Skates et al., 2013).

Data could further be impacted by the blood handling that occurred for the samples used for this study. Due to the impact of the COVID-19 pandemic, samples were used which were not originally intended for sEV focused research. This means that considerations such as the use of platelet free plasma, plasma to be kept at room temperature, for care to be taken to prevent agitation and correct cannula flushing were not accounted for. These are all changes to methods which have been previously indicated to have an impact on sEV count and phenotype (Thery et al., 2018).

Additionally, as discussed in the limitations to this study, as we know exercise induces significant changes to the circulating sEV proteome, it could be that we would see the significant changes after a bout of high intensity exercise.

5.6. Future Research

Although none of our potential biomarkers from **chapter 3** were identified in the mass spectrometry data conducted in **chapter 4,** this could be due to the participant pool that were used. The older adult participants were required to be deemed healthy by completion of a general health questionnaire assessment. Such participants may not display a high level of senescence. Similar proteomic analysis should be completed across diseased cohorts who have a senescence-associated disease such as cancer, sarcopenia, or obesity. This testing should be done irrespective of what senescence-associated disease the participants have, to allow for the identification of a marker of senescence rather than marker for the specific disease.

To further our understanding in the impact that ageing and chronic exercise have on the proteome of sEVs, future research should consider conducting a high intensity interval training protocol. As discussed previously in the implications of **Chapter 4**, it may be the case that any significant differences of sEV cargo in the long term are only apparently as a response to cardio-based exercise.

5.7. Conclusions

Overall, this thesis contributes to our understanding in small extracellular vesicles in relation to exercise, ageing, and senescence. The findings of this thesis show that sEVs

are released during exercise, in a manner that is large enough to see within both platelet poor plasma and platelet free plasma. This is despite the fact that remnant platelets in plasma have a significant effect of sEV counts ex vivo. Furthermore, this thesis supported the concept that sEVs are implicated in cellular senescence and proposed sEV biomarker candidates of senescence. Finally, single EV analysis and quantitative proteomics showed there are limited differences in sEV count and protein cargo between young, old and Masters athletes. This implies that a broad look at sEVs does not inform the ageing process nor the impact of lifelong exercise.

Chapter 6 -

General Methods

6.1. Ultracentrifugation (UC)

Plasma was centrifuged for 10 minutes at 3000 x g at 4°C using a Sorvall Legend X1 centrifuge (ThermoFisher Scientific, Leicestershire, UK) **t**o remove any cellular debris. The supernatant was then placed into separate thick-walled tubes (ThermoFisher Scientific, Langenselbold, Germany) and spun at 110,000 x g for 2 hours at 4°C using the Sorvall MTX 50 Micro-ultracentrifuge (ThermoFisher Scientific, Langenselbold, Germany), to pellet sEVs. The pellet was then resuspended in PBS and spun at 110,000 x g for 2 hours at 4°C. The EV pellet was then lysed in 20µl of fresh urea lysis buffer (0.1M HEPES ph 8.0, 6M UREA, 2M Thiourea), sonicated using the Bioruptor Plus (Diagenode, Seraing, Belgium) for 4 rounds of 30 seconds, and protein quantified by Detergent Compatible assay (Bio-Rad Laboratories, Watford, UK). Samples were stored at – 80°C.

6.2.1. Single EV Particle Analysis

Single EV Particle Analysis was used in **Chapter 2** and **Chapter 4** of this thesis.

6.2.2. Assay Protocol

Samples were analysed using the ExoView® R100 (Unchained Labs, Pleasanton, CA, USA). Single EV particle analysis was completed in accordance with their provided protocol, with some slight variations (https://www.nanoviewbio.com/exoview-r100). One such deviation is that sEVs were not purified prior to incubation, due to the bias that isolation could introduce. Chips were pre-scanned using the ExoView® R100. Prior to incubation, the ExoView chips were stored at 4°C. They were removed ~20 minutes prior to use, to allow adjustment to room temperature. Individual chips were then placed

into wells of a 24 well plate, making sure that the antibody chip centre was facing upwards and that the chip was not touching the side of any of the wells. The tetraspanin kit contains antibody spots for anti-CD9, anti-CD63, anti-CD81, anti-CD41a, and Mouse IgG. A dilution of 1:100 was created (plasma: incubation solution), and 35ml of this solution was added onto each of the chips. The chips were covered and incubated at room temperature for 16 hours, making sure the chips were not disturbed at any point. The following morning, chips were washed in the provided wash solution, and shaken at 500rpm for 3 minutes on microplate shaker, a total of 4 times. Chips were then incubated within fluorescent marker infused blocking solution (CD9 Blue 1:500; CD63 Red 1:500; CD81 Green 1:500) on a 500-rpm plate shaker, covered at room temperature for an hour. Chips were then washed x3 in wash solution, before being transferred to a 10cm dish, containing purified water to rinse the chips. Rinsed chips were then dried on absorbent paper, and ran using the ExoView® R100, and analysed using ExoView Analyzer software version 3.1.4.

6.2.3. Analysis Protocol

The ExoView human tetraspanin plasma kits (EV-TETRA-P) were analysed in accordance with the provided protocol (https://www.nanoviewbio.com/exoview-r100) using the ExoView® R100 (Unchained Laboratories, Pleasanton, California, USA). When analysing the samples, the background cut offs were adjusted to account for any background fluorescence from non-sEV components of plasma. In accordance with company guidelines, these cut offs were set between 5-10%.

6.2.4. CD9, CD63 and CD81 Fluorescent Count and Mean Fluorescence Intensity Quantification

Fluorescence counts were determined by the total sum of all fluorescent counts per fluorophore across all capture spots (CD9: Blue, CF488; CD63: Red, CF647; CD81: Green, CF555) This is to say, blue fluorophores on each individual antibody spot denotes the presence of a CD9 positive vesicle. This was repeated with each tetraspanin and their respective antibody. The relevant recorded Mouse IgG background fluorescence was subtracted.

Mean fluorescence intensity is measured by summing the mean of the relevant fluorophore fluorescent intensity (CD9: Blue, CF488; CD63: Red, CF647; CD81: Green, CF555) across each of the bound antibody spots. For example, when calculating the mean fluorescence intensity of CD9, the mean fluorescence intensity of the blue fluorophore was calculated across all three CD9 spots, all three CD63 spots, all three CD81 spots and all three CD41a bound spots. These means were summed to provide the total mean fluorescence intensity. The relevant recorded Mouse IgG background fluorescence was subtracted.

6.2.5. CD41a Interferometric Counts

CD41a interferometric counts were calculated by the presence of fluorescent particles on the CD41a specific spots, using Single Particle Interferometric Reflectance Imaging Sensor (SP-IRIS). This is to say, the blue fluorophore counts, the red fluorophore counts, and the green fluorophore counts were summed. The relevant recorded Mouse IgG background fluorescence was subtracted.

The decision was made to focus on mean fluorescence intensity and the fluorescent count data, using IM only for CD41a positive sEVs as there is no fluorescent marker.

6.3.1. Proteomics

Proteomic analysis was used in **Chapter 3** and **Chapter 4** of this thesis.

6.3.2. Clean Up of Plasma Samples

For samples which are particularly impure, for example biological samples such as plasma, the samples required additional clean up steps prior to their digest. This was not completed on the sEVs collected from the cellular media. Lysis buffer was added to the EV lysate and then transferred to a fresh, chilled, LoBind tube (Eppendorf, Hamburg, Germany). Ice cold acetone was added at a 1:5 ratio (100µl of lysis: 500µl of acetone) and incubated at – 20°C overnight. The sample was then span at 5000 x g for 10 minutes, before the supernatant was aspirated and air dried. 20µl of lysis buffer was added, before sonicating the sample. Qubit was used to calculate protein count.

6.3.3. 5µg Digest

5µg of sample were added to a LoBind tube (Eppendorf, Hamburg, Germany). Lysis buffer was added to reach a reagent total of 10µl. Samples were reduced with DTT (Fisherscientific, A39255) to a final concentration of 10nM. Samples were then alkylated to a final concentration of 25mM iodoacetamide (Thermofisher, A39271). The same amount of DTT was added to lead to a final concentration of 20nM as part of a 5-minute quench reaction. The sample was then digested with LysC (Wako, 125-05061) (1:50) for 5 hours at room temperature, before CaCl was added, to lead to a final concentration of 1mM. The samples were then diluted in 5 volumes of 0.1M Hepes.

Trypsin was added at a 1:20 ratio, with CaCl added to a concentration of 1mM. These samples were then incubated overnight at 37°C. The following morning, samples were acidified to a final concentration of 1% TFA and span at 15,000 x g for 5 minutes at room temperature.

The samples were then loaded into equilibrated SDB-RPS tips (Rappsilber et al., 2007) and peptides eluted in three different fractions. Samples were then dried on a SpeedVac (Eppendorf, Hamburg, Germany) for ~40 minutes at 45°C.

6.3.4. Mass Spectrometry

Normalised samples (5µg) were analysed by nano ultra-high performance liquid chromatography-tandem mass spectrometry (nano UHPLC-MS/S) using the Q Exactive HF-X Hybrid Quadrupole-Orbitrap system (ThermoFisher Scientific, Brisbane, Australia). Single shot samples were run in DDA mode, selecting the top 20 most intense peptide ions, using a 120min linear gradient at a flow rate of 200nl/min. Prior to loading, samples were reduced in DTT, alkalised with IAA, and digested in LysC and Trypsin. Desalting and cleanup of the samples were completed via SDB-RPS stage tips (ThermoFisher Scientific, Brisbane, Australia). MS spectra were acquired at a resolution of 70,000, m/z scan range between 300 to 1650, and a target value of $3e^6$ ions. The mass spectral data was then run through MaxQuant v2.4.2.0 (Cox and Mann, 2008) for analysis.

6.3.5. MaxQuant

Normalised samples (5µg) were analysed by nano ultra-high performance liquid chromatography-tandem mass spectrometry (nano UHPLC-MS/S) using the Q Exactive HF-X Hybrid Quadrupole-Orbitrap system (ThermoFisher Scientific, Brisbane, Australia). Samples were run in DDA mode, selecting the top 20 most intense peptide ions, using a 120min linear gradient at a flow rate of 200nl/min. MS spectra were acquired at a resolution of 70,000, m/z scan range between 300 to 1650, and a target value of $3e^6$ ions. The mass spectral data was then run through MaxQuant v2.4.2.0 (Cox and Mann, 2008) for analysis searching against the Human UniProt database with label free quantitation and matched between runs algorithms enabled.

References

ALBERRO, A., SÁENZ-CUESTA, M., MUÑOZ-CULLA, M., MATEO-ABAD, M., GONZALEZ, E., CARRASCO-GARCIA, E., ARAÚZO-BRAVO, M. J., MATHEU, A., VERGARA, I. & OTAEGUI, D. 2016. Inflammaging and Frailty Status Do Not Result in an Increased Extracellular Vesicle Concentration in Circulation. *International Journal of Molecular Sciences,* 17.

ALIBHAI, F. J., LIM, F., YEGANEH, A., DISTEFANO, P. V., BINESH-MARVASTI, T., BELFIORE, A., WLODAREK, L., GUSTAFSON, D., MILLAR, S., LI, S. H., WEISEL, R. D., FISH, J. E. & LI, R. K. 2020. Cellular senescence contributes to age-dependent changes in circulating extracellular vesicle cargo and function. *Aging Cell,* 19**,** e13103.

ALIQUE, M., RUÍZ-TORRES, M. P., BODEGA, G., NOCI, M. V., TROYANO, N., BOHÓRQUEZ, L., LUNA, C., LUQUE, R., CARMONA, A., CARRACEDO, J. & RAMÍREZ, R. 2017. Microvesicles from the plasma of elderly subjects and from senescent endothelial cells promote vascular calcification. *Aging (Albany NY),* 9**,** 778-789.

ALLEN, M., ZOU, F., CHAI, H. S., YOUNKIN, C. S., MILES, R., NAIR, A. A., CROOK, J. E., PANKRATZ, V. S., CARRASQUILLO, M. M., ROWLEY, C. N., NGUYEN, T., MA, L., MALPHRUS, K. G., BISCEGLIO, G., ORTOLAZA, A. I., PALUSAK, R., MIDDHA, S., MAHARJAN, S., GEORGESCU, C., SCHULTZ, D., RAKHSHAN, F., KOLBERT, C. P., JEN, J., SANDO, S. B., AASLY, J. O., BARCIKOWSKA, M., UITTI, R. J., WSZOLEK, Z. K., ROSS, O. A., PETERSEN, R. C., GRAFF-RADFORD, N. R., DICKSON, D. W., YOUNKIN, S. G. & ERTEKIN-TANER, N. 2012. Glutathione S-transferase omega genes in Alzheimer and Parkinson disease risk, age-at-diagnosis and brain gene expression: an association study with mechanistic implications. *Molecular Neurodegeneration,* 7**,** 13.

ALTSCHULER, S. J. & WU, L. F. 2010. Cellular heterogeneity: do differences make a difference? *Cell,* 141**,** 559-63.

ANDREU, Z. & YÁÑEZ-MÓ, M. 2014. Tetraspanins in Extracellular Vesicle Formation and Function. *Frontiers in Immunology,* 5.

ANISIMOVA, A. S., ALEXANDROV, A. I., MAKAROVA, N. E., GLADYSHEV, V. N. & DMITRIEV, S. E. 2018. Protein synthesis and quality control in aging. *Aging (Albany NY),* 10**,** 4269-4288.

AUDRITO, V., MESSANA, V. G. & DEAGLIO, S. 2020. NAMPT and NAPRT: Two Metabolic Enzymes With Key Roles in Inflammation. *Frontiers in Oncology,* 10.

AUSTIN-SUTHANTHIRARAJ, P. P. & GRAVES, S. W. 2013. Fluidics. *Current Protocols in Cytometry,* 65**,** 1.2.1-1.2.14.

BABST, M., DAVIES, B. A. & KATZMANN, D. J. 2011. Regulation of Vps4 During MVB Sorting and Cytokinesis. *Traffic,* 12**,** 1298-1305.

BACHURSKI, D., SCHULDNER, M., NGUYEN, P. H., MALZ, A., REINERS, K. S., GRENZI, P. C., BABATZ, F., SCHAUSS, A. C., HANSEN, H. P., HALLEK, M. & POGGE VON STRANDMANN, E. 2019. Extracellular vesicle measurements with nanoparticle tracking analysis - An accuracy and repeatability comparison between NanoSight NS300 and ZetaView. *Journal of Extracellular Vesicles,* 8**,** 1596016.

BALAKRISHNAN, A., ROY, S., FLEMING, T., LEONG, H. S. & SCHUURMANS, C. 2020. The Emerging Role of Extracellular Vesicles in the Glioma Microenvironment: Biogenesis and Clinical Relevance. *Cancers (Basel),* 12.

BASISTY, N., KALE, A., JEON, O. H., KUEHNEMANN, C., PAYNE, T., RAO, C., HOLTZ, A., SHAH, S., SHARMA, V., FERRUCCI, L., CAMPISI, J. & SCHILLING, B. 2020. A proteomic atlas of senescence-associated secretomes for aging biomarker development. *PLOS Biology,* 18**,** e3000599.

BLAIR, T. A., MICHELSON, A. D. & FRELINGER, A. L. 2018. Mass Cytometry Reveals Distinct Platelet Subtypes in Healthy Subjects and Novel Alterations in Surface Glycoproteins in Glanzmann Thrombasthenia. *Scientific Reports,* 8**,** 10300.

BOARD, P. G. & MENON, D. 2016. Structure, function and disease relevance of Omega-class glutathione transferases. *Archives of Toxicology,* 90**,** 1049-67.

BODART-SANTOS, V., PINHEIRO, L. S., DA SILVA-JUNIOR, A. J., FROZA, R. L., AHRENS, R., GONÇALVES, R. A., ANDRADE, M. M., CHEN, Y., ALCANTARA, C. L., GRINBERG, L. T., LEITE, R. E. P., FERREIRA, S. T., FRASER, P. E. & DE FELICE, F. G. 2023. Alzheimer's disease brain-derived extracellular vesicles reveal altered synapse-related proteome and induce cognitive impairment in mice. *Alzheimers and Dementia,* 19**,** 5418-5436.

BOLDERSON, E., BURGESS, J. T., LI, J., GANDHI, N. S., BOUCHER, D., CROFT, L. V., BEARD, S., PLOWMAN, J. J., SURAWEERA, A., ADAMS, M. N., NAQI, A., ZHANG, S.-D., SINCLAIR, D. A., O'BYRNE, K. J. & RICHARD, D. J. 2019. Barrier-to-autointegration factor 1 (Banf1) regulates poly [ADP-ribose] polymerase 1 (PARP1) activity following oxidative DNA damage. Nature Communications, 10, 5501.

BORGHESAN, M., FAFIÁN-LABORA, J., ELEFTHERIADOU, O., CARPINTERO-FERNÁNDEZ, P., PAEZ-RIBES, M., VIZCAY-BARRENA, G., SWISA, A., KOLODKIN-GAL, D., XIMÉNEZ-EMBÚN, P., LOWE, R., MARTÍN-MARTÍN, B., PEINADO, H., MUÑOZ, J., FLECK, R. A., DOR, Y., BEN-PORATH, I., VOSSENKAMPER, A., MUÑOZ-ESPIN, D. & O'LOGHLEN, A. 2019. Small Extracellular Vesicles Are Key Regulators of Non-cell Autonomous Intercellular Communication in Senescence via the Interferon Protein IFITM3. *Cell Reports,* 27**,** 3956-3971.e6.

BOYANOVA, D., NILLA, S., BIRSCHMANN, I., DANDEKAR, T. & DITTRICH, M. 2012. PlateletWeb: a systems biologic analysis of signaling networks in human platelets. *Blood,* 119**,** e22-34.

BRAHMER, A., NEUBERGER, E., ESCH-HEISSER, L., HALLER, N., JORGENSEN, M. M., BAEK, R., MÖBIUS, W., SIMON, P. & KRÄMER-ALBERS, E.-M. 2019. Platelets, endothelial cells and leukocytes contribute to the exercise-triggered release of extracellular vesicles into the circulation. *Journal of Extracellular Vesicles,* 8**,** 1615820.

BREIJYEH, Z. & KARAMAN, R. 2020. Comprehensive Review on Alzheimer's Disease: Causes and Treatment. *Molecules,* 25.

BRENNAN, K., MARTIN, K., FITZGERALD, S. P., O'SULLIVAN, J., WU, Y., BLANCO, A., RICHARDSON, C. & MC GEE, M. M. 2020. A comparison of methods for the isolation and separation of extracellular vesicles from protein and lipid particles in human serum. *Scientific Reports,* 10.

BURBIDGE, K., ZWIKELMAIER, V., COOK, B., LONG, M. M., BALVA, B., LONIGRO, M., ISPAS, G., RADEMACHER, D. J. & CAMPBELL, E. M. 2020. Cargo and cell-specific differences in extracellular vesicle populations identified by multiplexed immunofluorescent analysis. *Journal of Extracellular Vesicles,* 9**,** 1789326.

BURNUM-JOHNSON, K. E., CONRADS, T. P., DRAKE, R. R., HERR, A. E., IYENGAR, R., KELLY, R. T., LUNDBERG, E., MACCOSS, M. J., NABA, A., NOLAN, G. P., PEVZNER, P. A., RODLAND, K. D., SECHI, S., SLAVOV, N., SPRAGGINS, J. M., VAN EYK, J. E., VIDAL, M., VOGEL, C., WALT, D. R. & KELLEHER, N. L. 2022. New Views of Old Proteins: Clarifying the Enigmatic Proteome. *Molecular & Cellular Proteomics,* 21**,** 100254.

CAI, T., ZHANG, Q., WU, B., WANG, J., LI, N., ZHANG, T., WANG, Z., LUO, J., GUO, X., DING, X., XIE, Z., NIU, L., NING, W., FAN, Z., CHEN, X., GUO, X., CHEN, R., ZHANG, H. & YANG, F. 2021. LncRNA-encoded microproteins: A new form of cargo in cell culture-derived and circulating extracellular vesicles. *Journal of Extracellular Vesicles,* 10**,** e12123.

CARRERO, D., SORIA-VALLES, C. & LÓPEZ-OTÍN, C. 2016. Hallmarks of progeroid syndromes: lessons from mice and reprogrammed cells. Dis Model Mech, 9, 719-35.

CHEN H, LI Y, TOLLEFSBOL TO. Cell senescence culturing methods. Methods of Molecular Biology. 2013;1048:1-10. doi: 10.1007/978-1-62703-556-9_1.

CHEN, H., CHEN, C., SPANOS, M., LI, G., LU, R., BEI, Y. & XIAO, J. 2022. Exercise training maintains cardiovascular health: signaling pathways involved and potential therapeutics. *Signal Transduction and Targeted Therapy,* 7**,** 306.

CHOUDHURY, A., CHUNG, I., BLANN, A. D. & LIP, G. Y. 2007. Platelet surface CD62P and CD63, mean platelet volume, and soluble/platelet P-selectin as indexes of platelet function in atrial fibrillation: a comparison of "healthy control subjects" and "disease control subjects" in sinus rhythm. *Journal of the American College of Cardiology,* 49**,** 1957-64.

COLY, P.-M. & BOULANGER, C. M. 2022. Role of extracellular vesicles in atherosclerosis: An update. *Journal of Leukocyte Biology,* 111**,** 51-62.

COPPÉ, J. P., DESPREZ, P. Y., KRTOLICA, A. & CAMPISI, J. 2010. The senescence-associated secretory phenotype: the dark side of tumor suppression. *Annual Review of Pathology: Mechanisms of Disease,* 5**,** 99-118.

COSSARIZZA, A., CHANG, H.-D., RADBRUCH, A., ABRIGNANI, S., ADDO, R., AKDIS, M., ANDRÄ, I., ANDREATA, F., ANNUNZIATO, F., ARRANZ, E., BACHER, P., BARI, S., BARNABA, V., BARROS-MARTINS, J., BAUMJOHANN, D., BECCARIA, C. G., BERNARDO, D., BOARDMAN, D. A., BORGER, J., BÖTTCHER, C., BROCKMANN, L., BURNS, M., BUSCH, D. H., CAMERON, G., CAMMARATA, I., CASSOTTA, A., CHANG, Y., CHIRDO, F. G., CHRISTAKOU, E., ČIČIN-ŠAIN, L., COOK, L., CORBETT, A. J., CORNELIS, R., COSMI, L., DAVEY, M. S., DE BIASI, S., DE SIMONE, G., DEL ZOTTO, G., DELACHER, M., DI ROSA, F., DI SANTO, J., DIEFENBACH, A., DONG, J., DÖRNER, T., DRESS, R. J., DUTERTRE, C.-A., ECKLE, S. B. G., EEDE, P., EVRARD, M., FALK, C. S., FEUERER, M., FILLATREAU, S., FIZ-LOPEZ, A., FOLLO, M., FOULDS, G. A., FRÖBEL, J., GAGLIANI, N., GALLETTI, G., GANGAEV, A., GARBI, N., GARROTE, J. A., GEGINAT, J., GHERARDIN, N. A., GIBELLINI, L., GINHOUX, F., GODFREY, D. I., GRUARIN, P., HAFTMANN, C., HANSMANN, L., HARPUR, C. M., HAYDAY, A. C., HEINE, G., HERNÁNDEZ, D. C., HERRMANN, M., HOELSKEN, O., HUANG, Q., HUBER, S., HUBER, J. E., HUEHN, J., HUNDEMER, M., HWANG, W. Y. K., IANNACONE, M., IVISON, S. M., JÄCK, H.-M., JANI, P. K., KELLER, B., KESSLER, N., KETELAARS, S., KNOP, L., KNOPF, J., KOAY, H.-F., KOBOW, K., KRIEGSMANN, K., KRISTYANTO, H., KRUEGER, A., KUEHNE, J. F., KUNZE-SCHUMACHER, H., KVISTBORG, P., KWOK, I., LATORRE, D., et al. 2021. Guidelines for the use of flow cytometry and cell sorting in immunological studies (third edition). *European Journal of Immunology,* 51**,** 2708-3145.

COX, J., HEIN, M. Y., LUBER, C. A., PARON, I., NAGARAJ, N. & MANN, M. 2014. Accurate proteome-wide label-free quantification by delayed normalization and maximal peptide ratio extraction, termed MaxLFQ. *Molecular & Cellular Proteomics,* 13**,** 2513-26.

CROSBY, D., BHATIA, S., BRINDLE, K. M., COUSSENS, L. M., DIVE, C., EMBERTON, M., ESENER, S., FITZGERALD, R. C., GAMBHIR, S. S., KUHN, P., REBBECK, T. R. & BALASUBRAMANIAN, S. 2022. Early detection of cancer. *Science,* 375**,** eaay9040.

DALE, G. L., REMENYI, G. & FRIESE, P. 2009. Tetraspanin CD9 is required for microparticle release from coated-platelets. *Platelets,* 20**,** 361-366.

DEMARIA, M., BERTOZZI, B., VERONESE, N., SPELTA, F., CAVA, E., TOSTI, V., PICCIO, L., EARLY, D. S. & FONTANA, L. 2023. Long-term intensive endurance exercise training is associated to reduced markers of cellular senescence in the colon mucosa of older adults. *npj Aging,* 9**,** 3.

DONOVAN, T., BAIN, A. L., TU, W., PYNE, D. B. & RAO, S. 2021. Influence of Exercise on Exhausted and Senescent T Cells: A Systematic Review. *Frontiers in Physiology,* 12.

DOMEN, A., DEBEN, C., VERSWYVELl, J., FLIESWASSER, T., PRENAN, H., PEETERS, M., LARDON, F., WOUTERS., A. Cellular senescence in cancer: clinical detection and prognostic implications. *J Exp Clin Cancer Res* **41**, 360 (2022). https://doi.org/10.1186/s13046-022-02555-3

EITAN, E., GREEN, J., BODOGAI, M., MODE, N. A., BÆK, R., JØRGENSEN, M. M., FREEMAN, D. W., WITWER, K. W., ZONDERMAN, A. B., BIRAGYN, A., MATTSON, M. P., NOREN HOOTEN, N. & EVANS, M. K. 2017. Age-Related Changes in Plasma Extracellular Vesicle Characteristics and Internalization by Leukocytes. *Scientific Reports,* 7**,** 1342.

ENGLUND, D. A., SAKAMOTO, A. E., FRITSCHE, C. M., HEEREN, A. A., ZHANG, X., KOTAJARVI, B. R., LECY, D. R., YOUSEFZADEH, M. J., SCHAFER, M. J., WHITE, T. A., ATKINSON, E. J. & LEBRASSEUR, N. K. 2021. Exercise reduces circulating biomarkers of cellular senescence in humans. *Aging Cell,* 20**,** e13415.

ENJETI, A. K., ARIYARAJAH, A., D'CRUS, A., SELDON, M. & LINCZ, L. F. 2017. Circulating microvesicle number, function and small RNA content vary with age, gender, smoking status, lipid and hormone profiles. *Thrombrosis Research,* 156**,** 65-72.

FENG, Z., HANSON, R. W., BERGER, N. A. & TRUBITSYN, A. 2016. Reprogramming of energy metabolism as a driver of aging. *Oncotarget,* 7**,** 15410-20.

FOX, Z. R., BARKAI, E. & KRAPF, D. 2021. Aging power spectrum of membrane protein transport and other subordinated random walks. *Nature Communications,* 12**,** 6162.

FRÜHBEIS, C., HELMIG, S., TUG, S., SIMON, P. & KRÄMER-ALBERS, E.-M. 2015. Physical exercise induces rapid release of small extracellular vesicles into the circulation. *Journal of Extracellular Vesicles,* 4**,** 28239.

FULZELE, S., MENDHE, B., KHAYRULLIN, A., JOHNSON, M., KAISER, H., LIU, Y., ISALES, C. M. & HAMRICK, M. W. 2019. Muscle-derived miR-34a increases with age in circulating extracellular vesicles and induces senescence of bone marrow stem cells. *Aging (Albany NY),* 11**,** 1791-1803.

GARCIA-MARTIN, R., BRANDAO, B. B., THOMOU, T., ALTINDIS, E. & KAHN, C. R. 2022. Tissue differences in the exosomal/small extracellular vesicle proteome and their potential as indicators of altered tissue metabolism. *Cell Reports,* 38**,** 110277.

GE, S. X., JUNG, D. & YAO, R. 2019. ShinyGO: a graphical gene-set enrichment tool for animals and plants. *Bioinformatics,* 36**,** 2628-2629.

GHASEMZADEH, M., AHMADI, J. & HOSSEINI, E. 2022. Platelet-leukocyte crosstalk in COVID-19: How might the reciprocal links between thrombotic events and inflammatory state affect treatment strategies and disease prognosis? Thromb Res, 213, 179-194.

GILL, S., CATCHPOLE, R. & FORTERRE, P. 2019. Extracellular membrane vesicles in the three domains of life and beyond. *FEMS Microbiology Reviews,* 43**,** 273-303.

GONG, L., ZHONG, M., GONG, K., WANG, Z., ZHONG, Y., JIN, Y., CHEN, H., TAI, P., CHEN, X., CHEN, A. & CAO, K. 2023. Multi-Omics Analysis and Verification of the Oncogenic Value of CCT8 in Pan-Cancers. J Inflamm Res, 16, 2297-2315.

GUESCINI, M., CANONICO, B., LUCERTINI, F., MAGGIO, S., ANNIBALINI, G., BARBIERI, E., LUCHETTI, F., PAPA, S. & STOCCHI, V. 2015. Muscle Releases Alpha-Sarcoglycan Positive Extracellular Vesicles Carrying miRNAs in the Bloodstream. *PLoS One,* 10**,** e0125094.

HAN, Q.-F., LI, W.-J., HU, K.-S., GAO, J., ZHAI, W.-L., YANG, J.-H. & ZHANG, S.-J. 2022. Exosome biogenesis: machinery, regulation, and therapeutic implications in cancer. *Molecular Cancer,* 21**,** 207.

HARI, P., MILLAR, F. R., TARRATS, N., BIRCH, J., QUINTANILLA, A., RINK, C. J., FERNÁNDEZ-DURAN, I., MUIR, M., FINCH, A. J., BRUNTON, V. G., PASSOS, J. F., MORTON, J. P., BOULTER, L. & ACOSTA, J. C. 2019. The innate immune sensor Toll-like receptor 2 controls the senescence-associated secretory phenotype. *Science Advances,* 5**,** eaaw0254.

HEBER, S. & VOLF, I. 2015. Effects of Physical (In)activity on Platelet Function. *Biomedical Research International,* 2015**,** 165078.

HELMIG, S., FRÜHBEIS, C., KRÄMER-ALBERS, E.-M., SIMON, P. & TUG, S. 2015. Release of bulk cell free DNA during physical exercise occurs independent of extracellular vesicles. *European Journal of Applied Physiology,* 115**,** 2271-2280.

HUET, E., GABISON, E., VALLEE, B., MOUGENOT, N., LINGUET, G., RIOU, B., JAROSZ, C., MENASHI, S. & BESSE, S. 2015. Deletion of extracellular matrix metalloproteinase inducer/CD147 induces altered cardiac extracellular matrix remodeling in aging mice. J Physiol Pharmacol, 66, 355-66.

HORBAY, R., HAMRAGHANI, A., ERMINI, L., HOLCIK, S., BEUG, S. T. & YEGANEH, B. 2022. Role of Ceramides and Lysosomes in Extracellular Vesicle Biogenesis, Cargo Sorting and Release. *International Journal of Molecular Sciences,* 23.

ISRAELS, S. J. & MCMILLAN-WARD, E. M. 2005. CD63 modulates spreading and tyrosine phosphorylation of platelets on immobilized fibrinogen. *Thrombosis and Haemostasis,* 93**,** 311-8.

JAMIN, A. & WIEBE, M. S. 2015. Barrier to Autointegration Factor (BANF1): interwoven roles in nuclear structure, genome integrity, innate immunity, stress responses and progeria. Curr Opin Cell Biol, 34, 61-8.

JOHNSON, A. A. & STOLZING, A. 2019. The role of lipid metabolism in aging, lifespan regulation, and age-related disease. *Aging Cell,* 18**,** e13048.

JONES, C. I. 2016. Platelet function and ageing. *Mammalian Genome,* 27**,** 358-366.

JURGIELEWICZ, B. J., YAO, Y. & STICE, S. L. 2020. Kinetics and Specificity of HEK293T Extracellular Vesicle Uptake using Imaging Flow Cytometry. *Nanoscale Research Letters,* 15**,** 170.

JUST, J., YAN, Y., FARUP, J., SIELJACKS, P., SLOTH, M., VENØ, M., GU, T., DE PAOLI, F. V., NYENGAARD, J. R., BÆK, R., JØRGENSEN, M. M., KJEMS, J., VISSING, K. & DRASBEK, K. R. 2020. Blood flow-restricted resistance exercise alters the surface profile, miRNA cargo and functional impact of circulating extracellular vesicles. *Scientific Reports,* 10**,** 5835.

KALLURI, R. & LEBLEU, V. S. 2020. The biology, function, and biomedical applications of exosomes. *Science,* 367.

KAMTEKAR, S., KENNEDY, W. D., WANG, J., STATHOPOULOS, C., SÖLL, D. & STEITZ, T. A. 2003. The structural basis of cysteine aminoacylation of tRNAPro by prolyl-tRNA synthetases. *Proceedings of the National Academy of Sciences of the United States of America,* 100**,** 1673-8.

KAPAŁCZYŃSKA, M., KOLENDA, T., PRZYBYŁA, W., ZAJĄCZKOWSKA, M., TERESIAK, A., FILAS, V., IBBS, M., BLIŹNIAK, R., ŁUCZEWSKI, Ł. & LAMPERSKA, K. 2018. 2D and 3D cell cultures - a comparison of different types of cancer cell cultures. *Archives of Medical Science,* 14**,** 910-919.

KHAN, N. Z., CAO, T., HE, J., RITZEL, R. M., LI, Y., HENRY, R. J., COLSON, C., STOICA, B. A., FADEN, A. I. & WU, J. 2021. Spinal cord injury alters microRNA and CD81+ exosome levels in plasma extracellular nanoparticles with neuroinflammatory potential. *Brain, Behavior, and Immunity,* 92**,** 165-183.

KIM, H.-S., KIM, H. J., LEE, M. R. & HAN, I. 2021. EMMPRIN expression is associated with metastatic progression in osteosarcoma. BMC Cancer, 21, 1059.

KIM, Y. J., CHO, M. J., YU, W. D., KIM, M. J., KIM, S. Y. & LEE, J. H. 2022. Links of Cytoskeletal Integrity with Disease and Aging. *Cells,* 11.

KOBAYASHI , Y., EGUCHI, A., TAMAI, Y., FUKUDA, S., TEMPAKU, M., IZUOKA, K., IWASA, M., TAKEI, Y. & TOGASHI, K. 2021. Protein Composition of Circulating Extracellular Vesicles Immediately Changed by Particular Short Time of High-Intensity Interval Training Exercise. *Frontiers in Physiology,* 12.

KRYLOVA, S. V. & FENG, D. 2023. The Machinery of Exosomes: Biogenesis, Release, and Uptake. *International Journal of Molecular Medicine,* 24.

KUEHNEMANN, C., HU, K.-Q., BUTERA, K., PATEL, S. K., BONS, J., SCHILLING, B., AGUAYO-MAZZUCATO, C. & WILEY, C. D. 2022. Extracellular Nicotinamide Phosphoribosyltransferase Is a Component of the Senescence-Associated Secretory Phenotype. *Frontiers in Endocrinology,* 13.

KUGERATSKI, F. G., HODGE, K., LILLA, S., MCANDREWS, K. M., ZHOU, X., HWANG, R. F., ZANIVAN, S. & KALLURI, R. 2021. Quantitative proteomics identifies the core proteome of exosomes with syntenin-1 as the highest abundant protein and a putative universal biomarker. *Nature Cell Biology,* 23**,** 631-641.

LARIOS, J., MERCIER, V., ROUX, A. & GRUENBERG, J. 2020. ALIX- and ESCRT-III-dependent sorting of tetraspanins to exosomes. *Journal of Cell Biology,* 219.

LAZARETH, H., HENIQUE, C., LENOIR, O., PUELLES, V. G., FLAMANT, M., BOLLÉE, G., FLIGNY, C., CAMUS, M., GUYONNET, L., MILLIEN, C., GAILLARD, F., CHIPONT, A., ROBIN, B., FABREGA, S., DHAUN, N., CAMERER, E., KRETZ, O., GRAHAMMER, F., BRAUN, F., HUBER, T. B., NOCHY, D., MANDET, C., BRUNEVAL, P., MESNARD, L., THERVET, E., KARRAS, A., LE NAOUR, F., RUBINSTEIN, E., BOUCHEIX, C., ALEXANDROU, A., MOELLER, M. J., BOUZIGUES, C. & THARAUX, P.-L. 2019. The tetraspanin CD9 controls migration and proliferation of parietal epithelial cells and glomerular disease progression. *Nature Communications,* 10**,** 3303.

LEHALLIER, B., GATE, D., SCHAUM, N., NANASI, T., LEE, S. E., YOUSEF, H., MORAN LOSADA, P., BERDNIK, D., KELLER, A., VERGHESE, J., SATHYAN, S., FRANCESCHI, C., MILMAN, S., BARZILAI, N. & WYSS-CORAY, T. 2019. Undulating changes in human plasma proteome profiles across the lifespan. *Nature Medicine,* 25**,** 1843-1850.

LEHMANN, B. D., PAINE, M. S., BROOKS, A. M., MCCUBREY, J. A., RENEGAR, R. H., WANG, R. & TERRIAN, D. M. 2008. Senescence-associated exosome release from human prostate cancer cells. *Cancer Res,* 68**,** 7864-71.

LESTER, M., SHEFFIELD, L. T., TRAMMELL, P. & REEVES, T. J. 1968. The effect of age and athletic training on the maximal heart rate during muscular exercise. *American Heart Journal,* 76**,** 370-376.

LIAO, Q., REN, Y., YANG, Y., ZHU, X., ZHI, Y., ZHANG, Y., CHEN, Y., DING, Y. & ZHAO, L. 2021. CCT8 recovers WTp53-suppressed cell cycle evolution and EMT to promote colorectal cancer progression. Oncogenesis, 10, 84.

LIBERTI, M. V. & LOCASALE, J. W. 2016. The Warburg Effect: How Does it Benefit Cancer Cells? *Trends in Biochemical Sciences,* 41**,** 211-218.

LU, L., MAO, L., FENG, Y., AINSWORTH, B. E., LIU, Y. & CHEN, N. 2021. Effects of different exercise training modes on muscle strength and physical performance in older people with sarcopenia: a systematic review and meta-analysis. *BMC Geriatr,* 21**,** 708.

LU, Y., THAVARAJAH, T., GU, W., CAI, J. & XU, Q. 2018. Impact of miRNA in Atherosclerosis. *Arteriosclerosis, Thrombosis, and Vascular Biology,* 38**,** e159-e170.

MALKIN, E. Z. & BRATMAN, S. V. 2020. Bioactive DNA from extracellular vesicles and particles. *Cell Death Discovery,* 11**,** 584.

MANNI, G., BURATTA, S., PALLOTTA, M. T., CHIASSERINI, D., DI MICHELE, A., EMILIANI, C., GIOVAGNOLI, S., PASCUCCI, L., ROMANI, R., BELLEZZA, I., URBANELLI, L. & FALLARINO, F. 2023. Extracellular Vesicles in Aging: An Emerging Hallmark? *Cells,* 12**,** 527.

MARCOZZI, S., BIGOSSI, G., GIULIANI, M. E., GIACCONI, R., PIACENZA, F., CARDELLI, M., BRUNETTI, D., SEGALA, A., VALERIO, A., NISOLI, E., LATTANZIO, F., PROVINCIALI, M. & MALAVOLTA, M. 2023. Cellular senescence and frailty: a comprehensive insight into the causal links. *Geroscience,* 45**,** 3267-3305.

MAS-BARGUES, C. & ALIQUE, M. 2023. Extracellular Vesicles as "Very Important Particles" (VIPs) in Aging. *International Journal of Molecular Sciences,* 24.

MATO-BASALO, R., LUCIO-GALLEGO, S., ALARCÓN-VELEIRO, C., SACRISTÁN-SANTOS, M., QUINTANA, M., MORENTE-LÓPEZ, M., DE TORO, F. J., SILVA-FERNÁNDEZ, L., GONZÁLEZ-RODRÍGUEZ, A., ARUFE, M. C. & LABORA, J. A. F. 2022. Action Mechanisms of Small Extracellular Vesicles in Inflammaging. *Life (Basel),* 12.

MAUGERI, N., DE LORENZO, R., CLEMENTI, N., ANTONIA DIOTTI, R., CRISCUOLO, E., GODINO, C., TRESOLDI, C., ANGELS FOR COVID-BIO, B. S. G. B., BONINI, C., CLEMENTI, M., MANCINI, N., CICERI, F., ROVERE-QUERINI, P. & MANFREDI, A. A. 2022. Unconventional CD147-dependent platelet activation elicited by SARS-CoV-2 in COVID-19. J Thromb Haemost, 20, 434-448.

MCILVENNA, L. C., PARKER, H.-J., SEABRIGHT, A. P., SALE, B., ANGHILERI, G., WEAVER, S. R. C., LUCAS, S. J. E. & WHITHAM, M. 2023. Single vesicle analysis reveals the release of tetraspanin positive extracellular vesicles into circulation with high intensity intermittent exercise. *The Journal of Physiology.*

MELO, S. A., LUECKE, L. B., KAHLERT, C., FERNANDEZ, A. F., GAMMON, S. T., KAYE, J., LEBLEU, V. S., MITTENDORF, E. A., WEITZ, J., RAHBARI, N., REISSFELDER, C., PILARSKY, C., FRAGA, M. F., PIWNICA-WORMS, D. & KALLURI, R. 2015. Glypican-1 identifies cancer exosomes and detects early pancreatic cancer. *Nature,* 523**,** 177-82.

MENON, D., INNES, A., OAKLEY, A. J., DAHLSTROM, J. E., JENSEN, L. M., BRÜSTLE, A., TUMMALA, P., ROOKE, M., CASAROTTO, M. G., BAELL, J. B., NGUYEN, N., XIE, Y., CUELLAR, M., STRASSER, J., DAHLIN, J. L., WALTERS, M. A., BURGIO, G., O'NEILL, L. A. J. & BOARD, P. G. 2017. GSTO1-1 plays a pro-inflammatory role in models of inflammation, colitis and obesity. *Scientific Reports,* 7**,** 17832.

MERIGHI, A., GIONCHIGLIA, N., GRANATO, A. & LOSSI, L. 2021. The Phosphorylated Form of the Histone H2AX (γH2AX) in the Brain from Embryonic Life to Old Age. *Molecules,* 26.

MEWES, M., NEDELE, J., SCHELLECKES, K., BONDAREVA, O., LENDERS, M., KUSCHE-VIHROG, K., SCHNITTLER, H.-J., BRAND, S.-M., SCHMITZ, B. & BRAND, E. 2017. Salt-induced Na+/K+-ATPase-α/β expression involves soluble adenylyl cyclase in endothelial cells. Pflügers Archiv - European Journal of Physiology, 469, 1401-1412.

MIKAWA, T., SHIBATA, E., SHIMADA, M., ITO, K., ITO, T., KANDA, H., TAKUBO, K., LLEONART, M. E., INAGAKI, N., YOKODE, M. & KONDOH, H. 2020. Phosphoglycerate Mutase Cooperates with Chk1 Kinase to Regulate Glycolysis. *iScience,* 23**,** 101306.

MITCHELL, E. & WALKER, R. 2020. Global ageing: successes, challenges and opportunities. *British Journal of Hospital Medicine,* 81**,** 1-9.

MORRIS, O., DENG, H., TAM, C. & JASPER, H. 2020. Warburg-like Metabolic Reprogramming in Aging Intestinal Stem Cells Contributes to Tissue Hyperplasia. *Cell Reports,* 33**,** 108423.

MULVEY, C., THUR, B., CRAWFORD, M. & GODOVAC-ZIMMERMANN, J. 2010. How Many proteins are Missed in Quantitative proteomics Based on Ms/Ms sequencing Methods? *Proteomics Insights,* 3**,** 61-66.

MUÑOZ-ESPÍN, D., CAÑAMERO, M., MARAVER, A., GÓMEZ-LÓPEZ, G., CONTRERAS, J., MURILLO-CUESTA, S., RODRÍGUEZ-BAEZA, A., VARELA-NIETO, I., RUBERTE, J., COLLADO, M. & SERRANO, M. 2013. Programmed cell senescence during mammalian embryonic development. *Cell,* 155**,** 1104-18.

MURAO, N., YOKOI, N., TAKAHASHI, H., HAYAMI, T., MINAMI, Y. & SEINO, S. 2022. Increased glycolysis affects β-cell function and identity in aging and diabetes. *Molecular Metabolism,* 55**,** 101414.

NAKAHARA A, NAIR S, ORMAZABAL V, ELFEKY O, GARVEY CE, LONGO S, SALOMON C. Circulating Placental Extracellular Vesicles and Their Potential Roles During Pregnancy. Ochsner J. 2020 Winter;20(4):439-445. doi: 10.31486/toj.20.0049. PMID: 33408584; PMCID: PMC7755551.

NIGRI, J., LECA, J., TUBIANA, S.-S., FINETTI, P., GUILLAUMOND, F., MARTINEZ, S., LAC, S., IOVANNA, J. L., AUDEBERT, S., CAMOIN, L., VASSEUR, S., BERTUCCI, F. & TOMASINI, R. 2022. CD9 mediates the uptake of extracellular vesicles from cancer-associated fibroblasts that promote pancreatic cancer cell aggressiveness. *Science Signaling,* 15**,** eabg8191.

NOORMOHAMMADI, A., KHODAKARAMI, A., GUTIERREZ-GARCIA, R., LEE, H. J., KOYUNCU, S., KÖNIG, T., SCHINDLER, C., SAEZ, I., FATIMA, A., DIETERICH, C. & VILCHEZ, D. 2016. Somatic increase of CCT8 mimics proteostasis of human pluripotent stem cells and extends C. elegans lifespan. Nat Commun, 7, 13649.

O'BRIEN, K., BREYNE, K., UGHETTO, S., LAURENT, L. C. & BREAKEFIELD, X. O. 2020. RNA delivery by extracellular vesicles in mammalian cells and its applications. *Nature Reviews Molecular Cell Biology,* 21**,** 585-606.

OEYEN, E. V. M., KURT ; BAGGERMAN, GEERT ; WILLEMS, HANNY; BOONEN, KURT; ROLFO, CHRISTIAN; PAUWELS, PATRICK; JACOBS, AN; SCHILDERMANS, KARIN; CHO, WILLIAM C; MERTENSA, INGE 2018. Ultrafiltration and size exclusion chromatography combined with asymmetrical-flow field-flow fractionation for the isolation and characterisation of extracellular vesicles from urine. *Journal of Extracellular Vesicles,* 7.

OFTEDAL, B. E., MAIO, S., HANDEL, A. E., WHITE, M. P. J., HOWIE, D., DAVIS, S., PREVOT, N., ROTA, I. A., DEADMAN, M. E., KESSLER, B. M., FISCHER, R., TREDE, N. S., SEZGIN, E., MAIZELS, R. M. & HOLLÄNDER, G. A. 2021. The chaperonin CCT8 controls proteostasis essential for T cell maturation, selection, and function. Communications Biology, 4, 681.

OKUDA, J., NIIZUMA, S., SHIOI, T., KATO, T., INUZUKA, Y., KAWASHIMA, T., TAMAKI, Y., KAWAMOTO, A., TANADA, Y., IWANAGA, Y., NARAZAKI, M., MATSUDA, T., ADACHI, S., SOGA, T., TAKEMURA, G., KONDOH, H., KITA, T. & KIMURA, T. 2013. Persistent overexpression of phosphoglycerate mutase, a glycolytic enzyme, modifies energy metabolism and reduces stress resistance of heart in mice. *PLoS One,* 8**,** e72173.

ONO, K., EGUCHI, T., SOGAWA, C., CALDERWOOD, S. K., FUTAGAWA, J., KASAI, T., SENO, M., OKAMOTO, K., SASAKI, A. & KOZAKI, K.-I. 2018. HSP-enriched properties of extracellular vesicles involve survival of metastatic oral cancer cells. *Journal of Cellular Biochemistry,* 119**,** 7350-7362.

PAQUET, N., BOX, J. K., ASHTON, N. W., SURAWEERA, A., CROFT, L. V., URQUHART, A. J., BOLDERSON, E., ZHANG, S.-D., O'BYRNE, K. J. & RICHARD, D. J. 2014. Néstor-Guillermo Progeria Syndrome: a biochemical insight into Barrier-to-Autointegration Factor 1, alanine 12 threonine mutation. BMC Molecular Biology, 15, 27.

PATHAN, M., FONSEKA, P., CHITTI, S. V., KANG, T., SANWLANI, R., VAN DEUN, J., HENDRIX, A. & MATHIVANAN, S. 2019. Vesiclepedia 2019: a compendium of RNA, proteins, lipids and metabolites in extracellular vesicles. *Nucleic Acids Research,* 47**,** D516-d519.

PATRIZZ, A., DORAN, S. J., CHAUHAN, A., AHNSTEDT, H., ROY-O'REILLY, M., LAI, Y. J., WESTON, G., TARABISHY, S., PATEL, A. R., VERMA, R., STAFF, I., KOFLER, J. K., LI, J., LIU, F., RITZEL, R. M. & MCCULLOUGH, L. D. 2020. EMMPRIN/CD147 plays a detrimental role in clinical and experimental ischemic stroke. Aging (Albany NY), 12, 5121-5139.

PENNINGS, G. J., YONG, A. S. & KRITHARIDES, L. 2010. Expression of EMMPRIN (CD147) on circulating platelets in vivo. J Thromb Haemost, 8, 472-81.

PEREZ-RIVEROL, Y., BAI, J., BANDLA, C., GARCÍA-SEISDEDOS, D., HEWAPATHIRANA, S., KAMATCHINATHAN, S., KUNDU, DEEPTI J., PRAKASH, A., FRERICKS-ZIPPER, A., EISENACHER, M., WALZER, M., WANG, S., BRAZMA, A. & VIZCAÍNO, JUAN A. 2021. The PRIDE database resources in 2022: a hub for mass spectrometry-based proteomics evidences. *Nucleic Acids Research,* 50**,** D543-D552.

PERRIN, P., JANSSEN, L., JANSSEN, H., VAN DEN BROEK, B., VOORTMAN, L. M., VAN ELSLAND, D., BERLIN, I. & NEEFJES, J. 2021. Retrofusion of intralumenal MVB membranes parallels viral infection and coexists with exosome release. *Current Biology,* 31**,** 3884-3893.e4.

PIETROWSKA, M., WLOSOWICZ, A., GAWIN, M. & WIDLAK, P. 2019. MS-Based Proteomic Analysis of Serum and Plasma: Problem of High Abundant Components and Lights and Shadows of Albumin Removal. *Advances in Experimental Medicine and Biology,* 1073**,** 57-76.

PRATTICHIZZO, F., MATACCHIONE, G., GIULIANI, A., SABBATINELLI, J., OLIVIERI, F., DE CANDIA, P., DE NIGRIS, V. & CERIELLO, A. 2021. Extracellular vesicle-shuttled miRNAs: a critical appraisal of their potential as nano-diagnostics and nano-therapeutics in type 2 diabetes mellitus and its cardiovascular complications. *Theranostics,* 11**,** 1031-1045.

QIAO, Z., ZHANG, Y., GE, M., LIU, S., JIANG, X., SHANG, Z., LIU, H., CAO, C. & XIAO, H. 2019. Cancer Cell Derived Small Extracellular Vesicles Contribute to Recipient Cell Metastasis Through Promoting HGF/c-Met Pathway. *Molecular & Cellular Proteomics,* 18**,** 1619-1629.

RANI, A., O'SHEA, A., IANOV, L., COHEN, R. A., WOODS, A. J. & FOSTER, T. C. 2017. miRNA in Circulating Microvesicles as Biomarkers for Age-Related Cognitive Decline. *Frontiers in Aging Neuroscience,* 9**,** 323.

RAPOSO, G. & STOORVOGEL, W. 2013. Extracellular vesicles: exosomes, microvesicles, and friends. *Journal of Cell Biology,* 200**,** 373-83.

RAPPSILBER, J., MANN, M. & ISHIHAMA, Y. 2007. Protocol for micro-purification, enrichment, pre-fractionation and storage of peptides for proteomics using StageTips. *Nature Protocols,* 2**,** 1896-1906.

RASMUSSEN, J. & LANGERMAN, H. 2019. Alzheimer's Disease - Why We Need Early Diagnosis. *Degenerative Neurological and Neuromuscular Disease,* 9**,** 123-130.

RAYESS, H., WANG, M. B. & SRIVATSAN, E. S. 2012. Cellular senescence and tumor suppressor gene p16. *International Journal of Cancer,* 130**,** 1715-25.

RHIM, W.-K., KIM, J. Y., LEE, S. Y., CHA, S.-G., PARK, J. M., PARK, H. J., PARK, C. G. & HAN, D. K. 2023. Recent advances in extracellular vesicle engineering and its applications to regenerative medicine. *Biomaterials Research,* 27**,** 130.

RICHES, A., CAMPBELL, E., BORGER, E. & POWIS, S. 2014. Regulation of exosome release from mammary epithelial and breast cancer cells - a new regulatory pathway. *European Journal of Cancer,* 50**,** 1025-34.

RIECKMANN, J. C., GEIGER, R., HORNBURG, D., WOLF, T., KVELER, K., JARROSSAY, D., SALLUSTO, F., SHEN-ORR, S. S., LANZAVECCHIA, A., MANN, M. & MEISSNER, F. 2017. Social network architecture of human immune cells unveiled by quantitative proteomics. *Nature Immunology,* 18**,** 583-593.

ROME S, TACCONI S. High-fat diets: You are what you eat….your extracellular vesicles too! J Extracell Vesicles. 2024 Jan;13(1):e12382. doi: 10.1002/jev2.12382.

SABATH, N., LEVY-ADAM, F., YOUNIS, A., ROZALES, K., MELLER, A., HADAR, S., SOUEID-BAUMGARTEN, S. & SHALGI, R. 2020. Cellular proteostasis decline in human senescence. Proc Natl Acad Sci U S A, 117, 31902-31913.

SANZ-ROS, J., ROMERO-GARCÍA, N., MAS-BARGUES, C., MONLEÓN, D., GORDEVICIUS, J., BROOKE, R. T., DROMANT, M., DÍAZ, A., DEREVYANKO, A., GUÍO-CARRIÓN, A., ROMÁN-DOMÍNGUEZ, A., INGLÉS, M., BLASCO, M. A., HORVATH, S., VIÑA, J. & BORRÁS, C. 2022. Small extracellular vesicles from young adipose-derived stem cells prevent frailty, improve health span, and decrease epigenetic age in old mice. *Science Advances,* 8**,** eabq2226.

SAPOŃ, K., MAŃKA, R., JANAS, T. & JANAS, T. 2023. The role of lipid rafts in vesicle formation. *Journal of Cell Science,* 136.

SCHAUM, N., LEHALLIER, B., HAHN, O., PÁLOVICS, R., HOSSEINZADEH, S., LEE, S. E., SIT, R., LEE, D. P., LOSADA, P. M., ZARDENETA, M. E., FEHLMANN, T., WEBBER, J. T., MCGEEVER, A., CALCUTTAWALA, K., ZHANG, H., BERDNIK, D., MATHUR, V., TAN, W., ZEE, A., TAN, M., ALMANZAR, N., ANTONY, J., BAGHEL, A. S., BAKERMAN, I., BANSAL, I., BARRES, B. A., BEACHY, P. A., BERDNIK, D., BILEN, B., BROWNFIELD, D., CAIN, C., CHAN, C. K. F., CHEN, M. B., CLARKE, M. F., CONLEY, S. D., DARMANIS, S., DEMERS, A., DEMIR, K., DE MORREE, A., DIVITA, T., DU BOIS, H., EBADI, H., ESPINOZA, F. H., FISH, M., GAN, Q., GEORGE, B. M., GILLICH, A., GÒMEZ-SJÖBERG, R., GREEN, F., GENETIANO, G., GU, X., GULATI, G. S., HAHN, O., HANEY, M. S., HANG, Y., HARRIS, L., HE, M., HOSSEINZADEH, S., HUANG, A., HUANG, K. C., IRAM, T., ISOBE, T., IVES, F., JONES, R., KAO, K. S., KARKANIAS, J., KARNAM, G., KELLER, A., KERSHNER, A. M., KHOURY, N., KIM, S. K., KISS, B. M., KONG, W., KRASNOW, M. A., KUMAR, M. E., KUO, C. S., Y. LAM, J., LEE, D. P., LEE, S. E., LEHALLIER, B., LEVENTHAL, O., LI, G., LI, Q., LIU, L., LO, A., LU, W.-J., LUGO-FAGUNDO, M. F., MANJUNATH, A., MAY, A. P., MAYNARD, A., MCGEEVER, A., MCKAY, M., MCNERNEY, M. W., MERRILL, B., METZGER, R. J., MIGNARDI, M., MIN, D., NABHAN, A. N., NEFF, N. F., NG, K. M., et al. 2020. Ageing hallmarks exhibit organ-specific temporal signatures. *Nature,* 583**,** 596-602.

SCHIOPPO, T., UBIALI, T., INGEGNOLI, F., BOLLATI, V. & CAPORALI, R. 2021. The role of extracellular vesicles in rheumatoid arthritis: a systematic review. *Clinical Rheumatology,* 40**,** 3481-3497.

SCHOTTE, R., VILLAUDY, J., DE JONG, G., NEVIANI, V., POS, W., LEVIE, S. E., GO, D. M., YASUDA, E., FRANKIN, E., CERCEL, M., VAN HAL-VAN VEEN, S. E., VAN DE BERG, D., SZABÓ, A., FATMAWATI, C., KEDDE, M., CLAASSEN, Y., HORBACH, S., RIJNEVELD, A. W., GROS, P., SPITS, H., HAZENBERG, M. D. & VAN EENENNAAM, H. 2020. Preclinical Development of AT1412, a Patient Derived CD9 Antibody That Does Not Induce Thrombosis for Treatment of B ALL. *Blood,* 136**,** 41-42.

SHOCK, N. W. 1967. Physical activity and the "rate of ageing". *Cancer Medical Association Journal,* 96**,** 836-42.

SIDHOM, K., OBI, P. O. & SALEEM, A. 2020. A Review of Exosomal Isolation Methods: Is Size Exclusion Chromatography the Best Option? *International Journal of Molecular Sciences,* 21.

SILVA, C. I. D., GONÇALVES-DE-ALBUQUERQUE, C. F., MORAES, B. P. T. D., GARCIA, D. G. & BURTH, P. 2021. Na/K-ATPase: Their role in cell adhesion and migration in cancer. Biochimie, 185, 1-8.

SINITCYN, P., RICHARDS, A. L., WEATHERITT, R. J., BRADEMAN, D. R., MARX, H., SHISHKOVA, E., MEYER, J. G., HEBERT, A. S., WESTPHALL, M. S., BLENCOWE, B. J., COX, J. & COON, J. J. 2023. Global detection of human variants and isoforms by deep proteome sequencing. *Nature Biotechnology*.

SUNG, Y., YOON, I., HAN, J. M. & KIM, S. 2022. Functional and pathologic association of aminoacyl-tRNA synthetases with cancer. *Experimental & Molecular Medicine,* 54**,** 553-566.

TERMINI, C. M. & GILLETTE, J. M. 2017. Tetraspanins Function as Regulators of Cellular Signaling. *Frontiers in Cell and Developmental Biology,* 5.

THÉRY, C., WITWER, K. W., AIKAWA, E., ALCARAZ, M. J., ANDERSON, J. D., ANDRIANTSITOHAINA, R., ANTONIOU, A., ARAB, T., ARCHER, F., ATKIN-SMITH, G. K., AYRE, D. C., BACH, J.-M., BACHURSKI, D., BAHARVAND, H., BALAJ, L., BALDACCHINO, S., BAUER, N. N., BAXTER, A. A., BEBAWY, M., BECKHAM, C., BEDINA ZAVEC, A., BENMOUSSA, A., BERARDI, A. C., BERGESE, P., BIELSKA, E., BLENKIRON, C., BOBIS-WOZOWICZ, S., BOILARD, E., BOIREAU, W., BONGIOVANNI, A., BORRÀS, F. E., BOSCH, S., BOULANGER, C. M., BREAKEFIELD, X., BREGLIO, A. M., BRENNAN, M. Á., BRIGSTOCK, D. R., BRISSON, A., BROEKMAN, M. L., BROMBERG, J. F., BRYL-GÓRECKA, P., BUCH, S., BUCK, A. H., BURGER, D., BUSATTO, S., BUSCHMANN, D., BUSSOLATI, B., BUZÁS, E. I., BYRD, J. B., CAMUSSI, G., CARTER, D. R., CARUSO, S., CHAMLEY, L. W., CHANG, Y.-T., CHEN, C., CHEN, S., CHENG, L., CHIN, A. R., CLAYTON, A., CLERICI, S. P., COCKS, A., COCUCCI, E., COFFEY, R. J., CORDEIRO-DA-SILVA, A., COUCH, Y., COUMANS, F. A., COYLE, B., CRESCITELLI, R., CRIADO, M. F., D'SOUZA-

SCHOREY, C., DAS, S., DATTA CHAUDHURI, A., DE CANDIA, P., DE SANTANA, E. F., DE WEVER, O., DEL PORTILLO, H. A., DEMARET, T., DEVILLE, S., DEVITT, A., DHONDT, B., DI VIZIO, D., DIETERICH, L. C., DOLO, V., DOMINGUEZ RUBIO, A. P., DOMINICI, M., DOURADO, M. R., DRIEDONKS, T. A., DUARTE, F. V., DUNCAN, H. M., EICHENBERGER, R. M., EKSTRÖM, K., EL ANDALOUSSI, S., ELIE-CAILLE, C., ERDBRÜGGER, U., FALCÓN-PÉREZ, J. M., FATIMA, F., FISH, J. E., FLORES-BELLVER, M., FÖRSÖNITS, A., FRELET-BARRAND, A., et al. 2018. Minimal information for studies of extracellular vesicles 2018 (MISEV2018): a position statement of the International Society for Extracellular Vesicles and update of the MISEV2014 guidelines. *Journal of Extracellular Vesicles,* 7**,** 1535750.

TRICARICO, C., CLANCY, J. & D'SOUZA-SCHOREY, C. 2017. Biology and biogenesis of shed microvesicles. *Small GTPases,* 8**,** 220-232.

TUCHER, C., BODE, K., SCHILLER, P., CLAßEN, L., BIRR, C., SOUTO-CARNEIRO, M. M., BLANK, N., LORENZ, H. M. & SCHILLER, M. 2018. Extracellular Vesicle Subtypes Released From Activated or Apoptotic T-Lymphocytes Carry a Specific and Stimulus-Dependent Protein Cargo. *Frontiers in Immunology,* 9**,** 534.

UMLAUF, E., RAPPOLD, E., SCHILLER, B., FUCHS, P., RAINER, M., WOLF, B. & ZELLNER, M. 2016. Careful neuropsychological testing reveals a novel genetic marker, GSTO1*C , linked to the pre-stage of Alzheimer's disease. *Oncotarget,* 7.

UPMEIER, E., LAVONIUS, S., HEINONEN, P., VIITANEN, M., ISOAHO, H., ARVE, S. & LEHTONEN, A. 2011. Longitudinal changes in serum lipids in older people The Turku Elderly Study 1991–2006. *Age and Ageing,* 40**,** 280-283.

VAN DER POL, E., COUMANS, F. A., STURK, A., NIEUWLAND, R. & VAN LEEUWEN, T. G. 2014. Refractive index determination of nanoparticles in suspension using nanoparticle tracking analysis. *Nano Letters,* 14**,** 6195-201.

VAN DEURSEN, J. M. 2014. The role of senescent cells in ageing. *Nature,* 509**,** 439-46.

VAN NIEL, G., CHARRIN, S., SIMOES, S., ROMAO, M., ROCHIN, L., SAFTIG, P., MARKS, M. S., RUBINSTEIN, E. & RAPOSO, G. 2011. The tetraspanin CD63 regulates ESCRT-independent and -dependent endosomal sorting during melanogenesis. *Developmental Cell,* 21**,** 708-21.

VESTAD, B., LLORENTE, A., NEURAUTER, A., PHUYAL, S., KIERULF, B., KIERULF, P., SKOTLAND, T., SANDVIG, K., HAUG, K. B. F. & ØVSTEBØ, R. 2017. Size and concentration analyses of extracellular vesicles by nanoparticle tracking analysis: a variation study. *Journal of Extracellular Vesicles,* 6**,** 1344087.

WANG, L.-X., ZHANG, X., GUAN, L.-J. & PEN, Y. 2023. What role do extracellular vesicles play in developing physical frailty and sarcopenia? *Zeitschrift für Gerontologie und Geriatrie,* 56**,** 697-702.

WANG, Y., ZHAO, M., LIU, S., GUO, J., LU, Y., CHENG, J. & LIU, J. 2020. Macrophage-derived extracellular vesicles: diverse mediators of pathology and therapeutics in multiple diseases. *Cell Death & Disease,* 11**,** 924.

WATSON, S. L., WEEKS, B. K., WEIS, L. J., HARDING, A. T., HORAN, S. A. & BECK, B. R. 2018. High-Intensity Resistance and Impact Training Improves Bone Mineral Density and Physical Function in Postmenopausal Women With Osteopenia and Osteoporosis: The LIFTMOR Randomized Controlled Trial. *Journal of Bone Mineral Research,* 33**,** 211-220.

WHITHAM, M., PARKER, B. L., FRIEDRICHSEN, M., HINGST, J. R., HJORTH, M., HUGHES, W. E., EGAN, C. L., CRON, L., WATT, K. I., KUCHEL, R. P., JAYASOORIAH, N., ESTEVEZ, E., PETZOLD, T., SUTER, C. M., GREGOREVIC, P., KIENS, B., RICHTER, E. A., JAMES, D. E., WOJTASZEWSKI, J. F. P. & FEBBRAIO, M. A. 2018. Extracellular Vesicles Provide a Means for Tissue Crosstalk during Exercise. *Cell Metabolism,* 27**,** 237-251.e4.

WILLMS, E., CABAÑAS, C., MÄGER, I., WOOD, M. J. A. & VADER, P. 2018. Extracellular Vesicle Heterogeneity: Subpopulations, Isolation Techniques, and Diverse Functions in Cancer Progression. *Frontiers in Immunology,* 9.

WOLF, P. 1967. The Nature and Significance of Platelet Products in Human Plasma. *British Journal of Haematology,* 13**,** 269-288.

XU, S., HOU, D., LIU, J. & JI, L. 2018. Age-associated changes in GSH S-transferase gene/proteins in livers of rats. *Redox Report,* 23**,** 213-218.

YÁÑEZ-MÓ, M., SILJANDER, P. R., ANDREU, Z., ZAVEC, A. B., BORRÀS, F. E., BUZAS, E. I., BUZAS, K., CASAL, E., CAPPELLO, F., CARVALHO, J., COLÁS, E., CORDEIRO-DA SILVA, A., FAIS, S., FALCON-PEREZ, J. M., GHOBRIAL, I. M., GIEBEL, B., GIMONA, M., GRANER, M., GURSEL, I., GURSEL, M., HEEGAARD, N. H., HENDRIX, A., KIERULF, P., KOKUBUN, K., KOSANOVIC, M., KRALJ-IGLIC, V., KRÄMER-ALBERS, E. M., LAITINEN, S., LÄSSER, C., LENER, T., LIGETI, E., LINĒ, A., LIPPS, G., LLORENTE, A., LÖTVALL, J., MANČEK-KEBER, M., MARCILLA, A., MITTELBRUNN, M., NAZARENKO, I., NOLTE-'T HOEN, E. N., NYMAN, T. A., O'DRISCOLL, L., OLIVAN, M., OLIVEIRA, C., PÁLLINGER, É., DEL PORTILLO, H. A., REVENTÓS, J., RIGAU, M., ROHDE, E., SAMMAR, M., SÁNCHEZ-MADRID, F., SANTARÉM, N., SCHALLMOSER, K., OSTENFELD, M. S., STOORVOGEL, W., STUKELJ, R., VAN DER GREIN, S. G., VASCONCELOS, M. H., WAUBEN, M. H. & DE

WEVER, O. 2015. Biological properties of extracellular vesicles and their physiological functions. *Journal of Extracellular Vesicles,* 4**,** 27066.

YANG, P., PENG, Y., FENG, Y., XU, Z., FENG, P., CAO, J., CHEN, Y., CHEN, X., CAO, X., YANG, Y. & JIE, J. 2021. Immune Cell-Derived Extracellular Vesicles - New Strategies in Cancer Immunotherapy. *Frontiers in Immunology,* 12**,** 771551.

YOKOI, A. & OCHIYA, T. 2021. Exosomes and extracellular vesicles: Rethinking the essential values in cancer biology. *Seminars in Cancer Biology,* 74**,** 79-91.

YU, X., HARRIS, S. L. & LEVINE, A. J. 2006. The regulation of exosome secretion: a novel function of the p53 protein. *Cancer Research,* 66**,** 4795-801.

ZABOROWSKI, M. P., BALAJ, L., BREAKEFIELD, X. O. & LAI, C. P. 2015. Extracellular Vesicles: Composition, Biological Relevance, and Methods of Study. *Bioscience,* 65**,** 783-797.

ZHANG, B., LEE, D. E., TRAPP, A., TYSHKOVSKIY, A., LU, A. T., BAREJA, A., KEREPESI, C., MCKAY, L. K., SHINDYAPINA, A. V., DMITRIEV, S. E., BAHT, G. S., HORVATH, S., GLADYSHEV, V. N. & WHITE, J. P. 2023. Multi-omic rejuvenation and lifespan extension on exposure to youthful circulation. *Nature Aging,* 3**,** 948-964.

ZHANG, H. & JIN, K. 2020. Peripheral Circulating Exosomal miRNAs Potentially Contribute to the Regulation of Molecular Signaling Networks in Aging. *International Journal of Molecular Sciences,* 21.

ZHANG, M. W., SHEN, Y. J., SHI, J. & YU, J. G. 2020. MiR-223-3p in Cardiovascular Diseases: A Biomarker and Potential Therapeutic Target. *Front Cardiovascular Medicine,* 7**,** 610561.

ZHANG, W., LIN, X. & CHEN, S. 2022. Cysteinyl-tRNA Synthetase 1 Promotes Ferroptosis-Induced Cell Death via Regulating GPX4 Expression. *Journal of Clinical Oncology,* 2022**,** 4849174.

ZHANG, Y., KIM, M. S., JIA, B., YAN, J., ZUNIGA-HERTZ, J. P., HAN, C. & CAI, D. 2017. Hypothalamic stem cells control ageing speed partly through exosomal miRNAs. *Nature,* 548**,** 52-57.

ZOU, Q., ZHANG, M., YUAN, R. *et al.* Small extracellular vesicles derived from dermal fibroblasts promote fibroblast activity and skin development through carrying miR-218 and ITGBL1. *Journal of Nanobiotechnoly* **20**, 296 (2022). https://doi.org/10.1186/s12951-022-01499-2